

# **Modelling of Drug Release from Biodegradable Polymers**

*by*

**Kevser Sevim**



Department of Engineering  
Leicester  
U.K.

Thesis submitted for the degree of  
**Doctor of Philosophy**  
at the University of Leicester

**April 2017**

**ABSTRACT**

## THESIS:

Modelling of drug release from biodegradable polymers

## AUTHOR:

Kevser Sevim

Biodegradable polymers have highly desirable applications in the field of biomedical engineering, such as coronary stents, tissue engineering scaffolds and controlled release formulations. All these applications primarily rely on the fact that the polymers ultimately disappear after providing a desired function. In this respect, the mechanism of their degradation and erosion in aqueous media has attracted great attention. There are several factors affecting the rate of degradation such as composition, molecular weight, crystallinity and sample size. Experimental investigations showed that the type of drug also plays a major role in determining the degradation rate of polymers. However, so far there is no theoretical understanding for the changes in degradation rate during the degradation in the presence of acidic and basic drugs. Moreover, there exists no model to couple the hydrolysis reaction equations with the erosion phenomena for a total understanding of drug release from biodegradable polymers. A solid mathematical framework describing the degradation of bioresorbable polymers has been established through several Ph.D. projects at Leicester. This Ph.D. thesis consists of three parts: the first part reviews the existing literature of biodegradable polymers and drug delivery systems. In the second part, the previous models are refined by considering the presence of acidic and basic drugs. Full interactions between the drug and polyesters are taken into account as well as the further catalyst effect of the species on polymer degradation and the release rates. The third part of this thesis develops a mathematical model combining hydrolytic degradation and erosion in order to fully understand the mechanical behaviour of the biodegradable polymers. The combined model is then applied to several case studies for blank polymers and a drug eluting stent. The study facilitates understanding the various mass loss and drug release trends from the literature and the underlying mechanisms of each study.

## ACKNOWLEDGEMENTS

I would like to start by expressing my sincere gratitude to my supervisor, Prof. Jingzhe Pan, for his continuous support and guidance during my Ph.D. studies. His encouragements, vision and empathy, not only about my academic study but also about academic life, enlightened me and gave me a great motivation for keeping up for the times I stacked. He inspired me in great extent both academically and personally. I could not imagined having a better mentor for my Ph.D. studies. Hopefully, in the future, I would provide the same support and approach to my own students.

I am thankful to my co-supervisor Dr. Csaba Sinka. I am also thankful to Prof. Michel Vert and Prof. Jurgen Siepmann for their guidance in this work. And to Dr. Mesut Erzurumluoglu for valuable advices on my thesis.

I have been continually motivated by my dear family, my parents Fatma and Muzaffer as well as my siblings Esma and Furkan. I am so thankful for my mum's encouraging sentences and all the countless ways she contributed to my emotional and physical wellbeing during this process.

I am extremely grateful for the loving support of my dear friends in Leicester, especially my housemate Turkan Ozket, who suffered with all my mess and cooked for me every single day during the write-up period of this thesis. My wonderful friends Ramy Mesalam and Nawshin Dastagir accompanied me for countless working hours and made my long days and nights full of adventure and laughter. My dear friends Dhuha Abusalih and Amnani Binti Amujiddin supported me emotionally and with their prayers. My officemates, Xinpu Chen, Mazin Al-Isawi, Basam Al Bhadle, Peter Polak, Anas Alshammery and Christopher Campbell made my everyday better. I also thank to Dr. Sivashangari Gnanasambandam, Dr. Ali Tabatabaeian and Maurizio Foresta for their valuable support during my Ph.D. Last but not least, I am grateful to my dear friends Neslihan Suzen, Zahide Yildiz, Nurdan Cabukoglu, Hacer and Ali Yildirim, Burhan Alveroglu, Fatma Altun, Ayse Ulku, Esra Kaya, Tuba Aksu, Asuman Unal, Salih Cihangir, Resul Haser, my lovely aunty Ayse Sevim, and my uncles Dr.

Emin Sevim and Recep Sevim for their support and encouragement during the process. I am truly blessed to have such a strong network of support.

I also acknowledge the financial support given by Republic of Turkey, Ministry of Education (46814609/150.02/142744).

I would like to state that this research used the ALICE High Performance Computing Facility at the University of Leicester.

Kevser SEVIM

## TABLE OF CONTENTS

<b>Part 1 Background information and literature review .....</b>	<b>19</b>
<b>Chapter 1. Introduction to biodegradable-bioerodible polymers and controlled drug release .....</b>	<b>20</b>
1.1 Biodegradable-bioerodible polymers and their applications.....	20
1.2 Controlled drug release .....	24
1.2.1 General concept of controlled drug release .....	24
1.2.2 Controlled drug release using PLA/GA .....	26
1.3 Mechanisms for hydrolytic degradation, erosion and controlled drug release.....	27
1.3.1 Mechanism for hydrolytic degradation .....	27
1.3.2 Mechanism for erosion.....	33
1.3.3 Mechanism for drug release .....	35
1.4 The need for modeling.....	37
<b>Chapter 2. A review of existing mathematical models for polymer degradation and controlled drug release.....</b>	<b>39</b>
2.1 Models for polymer degradation and erosion before the work by Pan and co-workers .....	39
2.1.1 Models for polymer hydrolysis kinetics.....	39
2.1.2 Reaction – diffusion models.....	42
2.1.3 Models for surface erosion.....	43
2.1.4 Monte-Carlo Models.....	43
2.2 Previous work by Pan and co-workers.....	48
2.3 Review of drug release models in the literature .....	56
2.4 Remaining challenges in the literature .....	63
2.5 Research objectives .....	63
2.6 Structure of the thesis.....	64
<b>Part 2 Mathematical models of drug release from PLA/GA polymers .....</b>	<b>67</b>
<b>Chapter 3. A mechanistic model for acidic drug release using microspheres made of PLGA.....</b>	<b>68</b>
3.1 Introduction .....	68
3.2 The mathematical model.....	70
3.2.1 Extension of the autocatalytic term in polymer degradation model to account for acidic drugs.....	71
3.2.2 Diffusion equations of short chains and drug molecules .....	74
3.3 The numerical procedure .....	76

---

3.4	Comparison between model prediction and experimental data obtained in the literature .....	79
3.5	Design of microspheres to achieve desired profile of drug release..	84
3.6	Conclusions .....	88
<b>Chapter 4. A mechanistic model for basic drug release using microspheres made of PLGA .....</b>		<b>90</b>
4.1	Introduction .....	90
4.2	The mathematical model.....	91
4.2.1	Rate of polymer chain scission .....	93
4.2.2	Interaction between drug molecules and carboxylic end groups... ..	94
4.2.3	Diffusion equations of short chains and drug molecules .....	96
4.3	The numerical procedure .....	98
4.4	Validation of the model .....	100
4.4.1	Case Study A .....	100
4.4.2	Case Study B .....	104
4.5	Conclusion .....	110
<b>Part 3 A model by combination of hydrolytic degradation- erosion and its applications .....</b>		<b>112</b>
<b>Chapter 5. Combined hydrolytic degradation and erosion model for drug release .....</b>		<b>113</b>
5.1	Introduction .....	114
5.2	Hypothesis of the model and representation of the polymer matrix	115
5.3	Initializing the computational grid prior to erosion .....	117
5.4	A brief summary of the reaction-diffusion model.....	119
5.5	Surface erosion model.....	120
5.6	Interior erosion model .....	120
5.7	Combined hydrolytic degradation and erosion model .....	121
5.7.1	Rule of interior erosion.....	121
5.7.2	Rule of surface erosion .....	122
5.7.3	Rate equation for oligomer and drug diffusion .....	122
5.8	The numerical procedure .....	123
5.9	Different behaviors of mass loss that can be obtained using the combined model .....	128
5.10	Conclusion .....	134
<b>Chapter 6. Case studies of polymer degradation using combined hydrolytic degradation and erosion model.....</b>		<b>136</b>

---

6.1	Summary of the experimental data by Grizzi <i>et al.</i> (1995) and Lyu <i>et al.</i> (2007).....	136
6.2	Summary of the combined model .....	137
6.3	Summary of the parameters used in the combined model.....	138
6.4	Fittings of the combined model to experimental data.....	140
6.4.1	Case study A.....	140
6.4.2	Case study B.....	147
6.5	Conclusion.....	148
<b>Chapter 7.</b>	<b>Case studies of drug release from stents using the combined hydrolytic degradation and erosion model.....</b>	<b>150</b>
7.1	Introduction.....	150
7.2	Summary of the experimental data by Wang <i>et al.</i> (2006).....	152
7.3	Modification of the combined degradation-erosion model to include drug term .....	153
7.4	Summary of the parameters used in case study.....	155
7.5	Fittings of the modified model with experimental data .....	156
7.6	Conclusion.....	162
<b>Chapter 8.</b>	<b>Major conclusions and future work.....</b>	<b>163</b>
8.1	Major conclusions .....	163
8.2	Future work.....	165
<b>References</b>	<b>.....</b>	<b>166</b>
<b>Appendices</b>	<b>.....</b>	<b>180</b>
<b>Appendix A</b>	<b>.....</b>	<b>181</b>
<b>Appendix B</b>	<b>.....</b>	<b>190</b>
<b>Appendix C</b>	<b>.....</b>	<b>199</b>

## LIST OF FIGURES

Fig. 1.1 Structure of PLA-PGA-PCL .....	23
Fig. 1.2 Drug concentration in plasma ranging from therapeutic level bounded by minimum effective concentration (MEC) and maximum toxic concentration (MTC) (modified from (Ward and Georgiou, 2011)) .....	25
Fig. 1.3 Cumulative drug release for zero order and burst release .....	26
Fig. 1.4 Schematic representation of hydrolytic degradation of polymer .....	28
Fig. 1.5 Acid-catalysed hydrolysis of esters .....	32
Fig. 1.6 Base-catalysed hydrolysis of esters .....	33
Fig. 1.7 Mechanisms of hydrolytic degradation, surface erosion and interior erosion .....	34
Fig. 1.8 Drug release mechanisms from degrading and surface eroding polymeric microspheres.....	37
Fig. 2.1 Configuration of the polymer matrix grid through the device after Monte-Carlo simulations are applied at (a) prior to erosion, (b) 25%, (c) 50% and (d) 75% drug is released. Reproduced from (Zygourakis, 1990) .....	45
Fig. 2.2 Monte-Carlo approach of Siepmann <i>et al.</i> (Siepmann <i>et al.</i> , 2002); the schematic structure of the matrix (a) prior to erosion (b) during the drug release. ....	47
Fig. 2.3 Biodegradation model for thin plate (Wang <i>et al.</i> , 2008) .....	49
Fig. 2.4 Categorization of the mathematical models on drug delivery from polymeric systems.....	57
Fig. 2.5 A literature map showing the state-of-the-art of the current research and the research gap which is the matter of this thesis.....	62
Fig. 3.1 Schematic illustration of drug and oligomer release from a drug-loaded microsphere .....	70
Fig. 3.2 Schematic representation of the possible proton sources .....	72
Fig. 3.3 A schematic illustration of the grid size .....	77
Fig. 3.4 Flow chart for the model in the presence of acidic drugs .....	78
Fig. 3.5 Comparison between model prediction and experimental data for blank particles with different sizes. The dashed and solid lines represent the model predictions for microspheres of the average size of $r = 7.9\mu\text{m}$ , and $55\mu\text{m}$	

---

respectively. The discrete symbols represent the experimental data (Siepmann <i>et al.</i> , 2005).....	80
Fig. 3.6 Comparison between model prediction and experimental data for degradation of blank and ibuprofen-loaded PLGA microspheres. The dashed and solid lines represent model predictions for drug-free and drug-loaded particles respectively. The discrete symbols represent the experimental data (Klose <i>et al.</i> , 2008, Siepmann <i>et al.</i> , 2005).....	81
Fig. 3.7 Independent contributions of drug and oligomers to the proton concentration throughout the degradation process.....	82
Fig. 3.8 Comparison between the model prediction (solid line) and experimental data (Klose <i>et al.</i> , 2008) (discrete symbols) for drug release. The dashed line is model prediction using a constant drug diffusion coefficient. The size of the microsphere is $52\mu\text{m}$ .....	83
Fig. 3.9 Variable diffusivity of ibuprofen calculated using Eq. 18 for micro-particle of $r = 52\mu\text{m}$ .....	83
Fig. 3.10 Schematic representation of the microspheres resulting zero order release profile in the mixture when mixed 1:2 (w/w) ratio of (a) over (b). (a) $75\mu\text{m}$ in radius with drug loading of $400\text{ mol/m}^3$ and a drug free outside layer of $0.2r$ ( $15\mu\text{m}$ ), (b) $150\mu\text{m}$ in radius with a drug loading of $400\text{ mol/m}^3$ and a drug free outside layer of $0.6r$ ( $90\mu\text{m}$ ). .....	85
Fig. 3.11 Calculated profiles of drug release using microspheres of (a) $75\mu\text{m}$ in radius with drug loading of $400\text{ mol/m}^3$ and a drug free outside layer of $0.2r$ , (b) $150\mu\text{m}$ in radius with a drug loading of $400\text{ mol/m}^3$ and a drug free outside layer of $0.6r$ and (c) mixture of (a) and (b) with 1:2 (w/w) ratio of (a) over (b). .....	86
Fig. 3.12 Schematic representation of the microspheres resulting zero order release profile in the mixture when mixed 1:2 (w/w) ratio of (a) over (b). (a) $75\mu\text{m}$ in radius with a uniform drug loading of $400\text{ mol/m}^3$ , (b) $150\mu\text{m}$ in radius with a drug loading of $400\text{ mol/m}^3$ and a drug free outside layer of $0.6r$ ( $90\mu\text{m}$ ). .....	87
Fig. 3.13 Calculated profiles of drug release using microspheres of (a) $75\mu\text{m}$ in radius with a uniform drug loading of $400\text{ mol/m}^3$ , (b) $150\mu\text{m}$ in radius with a drug loading of $400\text{ mol/m}^3$ and a drug free outside layer of $0.6r$ and (c) mixture of (a) and (b) with 1:2 (w/w) ratio of (a) over (b). .....	88

---

Fig. 4.1 Schematic representation of the interaction between basic drugs-oligomers and catalyst effect of the free species.....	93
Fig. 4.2 Flow chart for the model in the presence of basic drugs .....	100
Fig. 4.3 Comparison between the model result and experimental data (Klose <i>et al.</i> , 2008, Siepmann <i>et al.</i> , 2005): a) $M_n$ reduction and b) drug release. Lines represent the model prediction for blank (dashed line) and loaded particles (solid line); discrete symbols represent experimental data for blank (circle) and loaded particles (square, triangle).....	103
Fig. 4.4 Comparison between the model result and experimental data (Dunne <i>et al.</i> , 2000) for blank PLGA microspheres. Lines represent the model prediction for various sizes and discrete symbols represent corresponding experimental data for $r = 20\mu\text{m}$ (solid line, circles) and $50\mu\text{m}$ (dashed line, squares).....	107
Fig. 4.5 Comparison of $M_n$ reduction between model results and experimental data. Solid lines represent the model prediction for microspheres with various levamisole loadings and discrete symbols represent corresponding experimental data (Fitzgerald and Corrigan, 1996) (A) 2.4% w/w (solid line, square) (B) 14.3% w/w (solid line, triangle) and (C) 19.7% w/w (solid line, circle). .....	108
Fig. 4.6 Comparison of drug release between model results and experimental data. Solid lines represent the model prediction for microspheres with various levamisole loadings and discrete symbols represent corresponding experimental data (Fitzgerald and Corrigan, 1996) (A) 2.4% w/w (solid line, square) (B) 14.3% w/w (solid line, triangle) and (C) 19.7% w/w (solid line, circle). .....	108
Fig. 4.7 The effect of partition parameter, $K_p$ , on molecular weight.....	110
Fig. 5.1 The coupling of hydrolytic degradation and erosion .....	117
Fig. 5.2 Schematic illustration of discretised polymer.....	119
Fig. 5.4 Moving boundaries at different times and boundary conditions.....	125
Fig. 5.5 Flow chart of the combined degradation-diffusion and erosion model .....	127
Fig. 5.6 Mass loss due to diffusion of short chains.....	129
Fig. 5.7 Mass loss due to surface erosion.....	130
Fig. 5.8 Mass loss due to interior erosion.....	131
Fig. 5.9 Mass loss due to interior erosion with incubation period of 0.5 weeks .....	132

---

Fig. 5.10 A summary of the mass loss profiles due to individual mechanisms	133
Fig. 5.11 Combined effect of all the mechanisms on mass loss: degradation-diffusion (5.9(a)), surface erosion (5.9(b)), interior erosion with incubation period of 0.5 weeks (5.9(d))	134
Fig. 6.1 Molecular weight distributions of plates at various times during the degradation (a) t= 0 week; (b) t=1 week; (c) t=10 weeks and (d) t=13 weeks.	141
Fig. 6.2 Molecular weight distributions of plates at various times during the degradation (a) t= 0 week; (b) t=1 week; (c) t=10 weeks and (d) t=13 weeks.	142
Fig. 6.3 Comparison of molecular weight change between model prediction and experimental data for samples with thickness of 0.3 mm and 2 mm. The solid and dashed lines represent the model predictions with the discrete symbols representing the experimental data (Grizzi <i>et al.</i> , 1995).	144
Fig. 6.4 Comparison of molecular mass loss between model prediction and experimental data for samples with thickness of 0.3 mm and 2 mm. The solid and dashed lines represent the model predictions with the discrete symbols representing the experimental data (Grizzi <i>et al.</i> , 1995).	144
Fig. 6.5 Hollow structure of PLA37.5GA25 specimen after 10 days of degradation in distilled water (Li <i>et al.</i> , 1990c) with permission via the Copyright Clearance Centre.	146
Fig. 6.6 Temporal evaluation of simulated the polymer matrix	146
Fig. 6.7 Comparison of molecular weight change between model prediction and experimental data. The solid line represents the model prediction with the discrete symbols representing the experimental data (Lyu <i>et al.</i> , 2007)	147
Fig. 6.8 Comparison of mass loss between model prediction and experimental data. The solid line represents the model prediction with the discrete symbols representing the experimental data (Lyu <i>et al.</i> , 2007)	148
Fig. 7.1 Diagrams of the bi-layer and tri-layer polymer films of Wang <i>et al.</i> (Wang <i>et al.</i> , 2006) with the corresponding layer thicknesses (reproduced from relevant study)	153
Fig. 7.2 a) Cross section of an implanted stent in a coronary artery; b) schematic of a single stent strut with drug-loaded polymer matrix; c) schematic of the drug loaded polymer matrix which is modelled in the current chapter.	154

- 
- Fig. 7.3 Comparison of molecular weight decrease of PLGA between model prediction and experimental data. The solid line represents the model predictions with the discrete symbols representing the experimental data (Wang *et al.*, 2006).  
..... 157
- Fig. 7.4 Comparison of mass loss of PLGA between model prediction and experimental data. The solid line represents the model predictions with the discrete symbols representing the experimental data (Wang *et al.*, 2006). .... 158
- Fig. 7.5 Comparison of sirolimus release from PLGA between model prediction and experimental data. The solid line represents the model predictions with the discrete symbols representing the experimental data (Wang *et al.*, 2006). .... 159
- Fig. 7.6 Micrographs of the surface morphology of degrading PLGA 53/47 taken from (Wang *et al.*, 2006) (a) 0 days, (b) 7 days, (c) 14 days and (d) 21 days. 160
- Fig. 7.7 Simulation results for drug loaded polymer matrix at  $t=21$  days. .... 161

**LIST OF TABLES**

Table 3.1 Model parameters used for the predictions .....	80
Table 4.1 Parameters used in the model to fit with experimental data .....	104
Table 4.2 Parameters used in the model to fit with experimental data .....	106
Table 6.1 Parameters used in the fittings.....	139
Table 7.1 Values of the model parameters used in the fittings.....	155

## LIST OF PUBLICATIONS AND CONFERENCE PRESENTATIONS

### Journal Publications

1. SEVIM, K. & PAN, J. 2016. A Mechanistic Model for Acidic Drug Release Using Microspheres Made of PLGA 50: 50. *Molecular Pharmaceutics*, 13, 2729-2735.
2. SEVIM, K. & PAN, J. 2017. A model for hydrolytic degradation and erosion of biodegradable polymers. *Acta Biomaterialia*, In press.
3. SEVIM, K. & PAN, J. 2017. A Mechanistic Model for Release of Basic Drugs Using Microspheres Made of PLGA. Submitted for publication.

### Conference Presentations

1. 2014, A Computer Model for Polymer Degradation in the Presence of Acidic Drug. Poster presentation on 26th Annual Conference of the European Society for Biomaterials (ESB), Liverpool, U.K.
2. 2015, A Mechanistic Model for Drug Release Using Spherical Particles Made of PLGA. Poster presentation at 1st European Conference on Pharmaceutics: Drug Delivery, Reims, France.
3. 2017, A Combined Degradation and Erosion Model for Drug Release from Biodegradable Drug-eluting Stents. Oral presentation in 2<sup>nd</sup> MOM Research Day, Leicester, U.K.
4. 2017, A Combined Degradation and Erosion Model for Biodegradable Polymers. Oral presentation on 28th Annual Conference of the European Society for Biomaterials (ESB), Athens, Greece.
5. 2017, A Mechanistic Model for Release of Basic Drugs Using Microspheres made of PLGA. Oral presentation on 28th Annual Conference of the European Society for Biomaterials (ESB), Athens, Greece.

**LIST OF SYMBOLS**

$A$  : surface area of the samples

$C_d$  : permeability of the polymers

$C_{d,0}$  : initial permeability of the polymers

$C_{drug}$  : mole concentration of drug

$C_{drug,0}$  : initial mole concentration of drug

$C_{drug\_H^+}$  : mole concentration of Drug\_ $H^+$

$C_e$  : mole concentration of ester bonds in the polymer

$C_{e,0}$  : initial mole concentration of ester bonds in the polymer

$C_{H^+}$  : mole concentration of  $H^+$

$C_{H0^+}$  : mole concentration of  $H^+$  donated by the surrounding medium

$C_i$  : mole concentration of species

$C_L$  : drug concentration in the liquid phase

$C_{OH^-}$  : mole concentration of  $OH^-$

$C_{ol}$  : current mole concentration of ester bonds of oligomers

$C_{ol,0}$  : initial mole concentration of oligomers

$C_{R1-COO^-}$  : mole concentration of  $R_1-COO^-$  in the polymer

$C_{R1-COOH}$  : molar concentration of carboxylic end groups in the polymer

$C_{R1-COOH,0}$  : initial mole concentration of  $R_1-COOH$

$C_{R2-COO^-}$  : mole concentration of  $R_2-COO^-$

$C_{R2-COOH}$  : mole concentration of carboxylic acid drug

$C_{sat}$  : saturation concentration of drug in polymer

$C_w$  : mole concentration of water in the polymer

$D_{drug,poly}$  : diffusion coefficient of drug in fresh bulk polymer

- $D_{drug,pore}$  : diffusion coefficient of drug in liquid filled pores
- $D_{drug}$ : effective diffusion coefficient of drug in the polymer
- $D_i$  : effective diffusion coefficient of species in the polymer
- $D_{i,poly}$  : diffusion coefficient of species in fresh bulk polymer
- $D_{ol}$  : effective diffusion coefficient of oligomer in polymer
- $D_{ol,poly}$  : diffusion coefficient of oligomers in fresh bulk polymer
- $D_{ol,pore}$  : diffusion coefficient of oligomers in liquid filled pores
- $D_w$  : diffusion coefficient of water in the polymer
- $E_k$  : activation energy for non-catalytic hydrolysis reaction
- $f$  : geometric and structural properties of the device
- $f_{drug}$  : the volume ratio of drug to the polymer phase
- $J$  : flux of the species
- $k$  : hydrolysis reaction rate constant
- $k_1$  : non-catalytic kinetic constant
- $k_2$  : acid-catalysed kinetic constant
- $k_3$  : base-catalysed kinetic constant
- $K_a$  : acid dissociation constant for oligomers
- $K_{a,drug}$  : acid dissociation constant for drug
- $K_b$  : base dissociation constant for oligomers
- $k_{dis}$  : drug dissolution rate
- $K_p$  : drug-oligomers partition parameter
- $m$  : average degree of polymerization
- $M_b$  : drug release by bulk erosion
- $M_d$  : drug release by diffusion

$M_n$  : number averaged molecular weight of the polymer

$M_{n,critical}$  : critical molecular weight of the polymer

$M_{n,mean}$  : mean value for molecular weight of the polymer

$M_{n,sr\_dev}$  : standart deviation for molecular weight of the polymer

$M_s$  : drug release by surface erosion

$M_t$  : cumulative absolute amount of drug release

$M_t$  : total drug release

$n$  : dissociation parameter

$N_{dp,0}$  : initial degree of polymerisation

$r$  : radius of the polymer samples

$R_{drug}$ : mole concentration of dissolution of drug

$R_{ol}$  : mole concentration of ester bonds of oligomers produced by hydrolysis

$R_s$  : mole concentration of chain scission

$S$  : status of a pixel

$S_m$  : current status of a pixel

$t$  : the degradation time

$T_g$  : glass transition temperature

$T_s$  : reference temperature

$V$ : rate of erosion

$V_{cell}$ : volume of a single pixel

$V_{pore}$  : porosity based on loss of short chains

$V_{pore,drug}$  : porosity due to loss of drug

$V_{pore,ol}$  : porosity due to loss of oligomers

$W_b$  : weight loss of oligomer by bulk erosion

$W_d$  : weight loss of oligomer by diffusion

$W_s$  : weight loss of oligomers by surface erosion

$W_t$  : total weight loss of oligomers

$x_c$  : the degree of crystallinity

$\alpha$  : empirical constant reflecting probability of short chain production due to chain scission

$\beta$  : empirical constant reflecting probability of short chain production due to chain scission

$\varepsilon$  : porosity of the polymer matrix

$\rho$  : polymer density

$\tau$  : tortuosity of polymer matrix

$u$  : the rate of synthesis of oligomers

**LIST OF ABBREVIATIONS**

ASA: acetyl Salicylic Acid (Aspirin)

DCM: Dichloromethane

DMSO: Dimethyl sulfoxide

FESEM: Field Emission Scanning Electron Microscopy

PBS: phosphate buffered saline

PCL: polycaprolactone acid

PDI: polydispersity index

PDLA: poly (D-lactide)

PDLLA: poly (DL-lactide)

PE: polyethylene

PGA: polyglycolic acid

PLA: poly-lactic acid

PLGA: poly(lactic-co-glycolic acid)

PLLA: poly (L-lactide)

PVA: poly(vinyl alcohol)

MARE: mean absolute relative error

## **Part 1**

### **Background information and literature review**

## **Chapter 1. Introduction to biodegradable-bioerodible polymers and controlled drug release**

This chapter provides an overview of the current knowledge on biodegradable polymers including their applications, degradation-erosion mechanisms and principles of controlled drug release. More detailed information is provided at the corresponding introductions of each chapter which is specific to the work presented. Mathematical models describing the degradation is not covered here as it is outside the scope of current chapter and is extensively addressed in Chapter 2.

### **1.1 Biodegradable-bioerodible polymers and their applications**

Biodegradable polymers are largely admitted as the materials that lose their chemical and physical integrity progressively resulting natural by-products. The literature generally uses the expressions bioresorbable, bioabsorbable and bioerodible together with the biodegradable term with no clear distinction between the terms (Vert, 2009). Vert (1992) proposed certain definitions to prevent the confusion on the usage of the terms. From his definitions, first, biodegradable refers to the polymeric systems that undergo the molecular breakdown. Second, bioresorbable term is used for the systems which degrades in biological conditions and further resorbed by the metabolism for a total elimination. Third, bioabsorbable term is used for the devices that can be dissolved in the body fluids without a chain cleavage. Finally, bioerodible term is used for the polymeric systems which is degraded on its material surface (Bosworth and Downes, 2010).

Following the definitions in the literature, degradation refer all the changes in chemical structure and physical properties of the polymer (Pospíšil *et al.*, 1999). According to that description, degradation term includes hydrolytic degradation, enzymatic degradation, thermal degradation, surface erosion and bulk erosion. On the other hand, erosion proceeds only through the morphological changes of the polymer structure (Pillai and Panchagnula, 2001, Ratner *et al.*, 2004). From

the definitions, degradation and erosion refers to different phenomena. However, the difference between polymer degradation and erosion is not clear in many cases in the literature.

Throughout the current thesis, we focus on hydrolytic degradation and erosion of the polymers, and all models are established based on one or two of the mechanisms. In the thesis, the term “hydrolytic degradation” or “hydrolysis” will refer to the processes in which the polymer chains are cleaved to form monomers and oligomers. On the other hand, the term “erosion” will refer to the physical processes through which polymer loses its integrity and eventually fall apart. For an ideal erosion, the material is likely to collapse from the outer shell or from the bulk in which erosion products are transported to the environment through the cavities. The cavities interconnects the inner structure with the surrounding medium. This phenomenon will be discussed in greater detail later in Section 1.3. The definitions used in the current study is consistent with the ones suggested by Gopferich (1996) and Tamada and Langer (1993).

Biodegradable polymers are the key members of the polymer family with the improved mechanical and thermal properties and acceptable shelf life. Furthermore, they are biocompatible, non-toxic and can be easily metabolized in the body leaving no trace (Agrawal and Ray, 2001, Daniels *et al.*, 1990, Middleton and Tipton, 2000). Unlike their non-biodegradable counterparts, they can naturally degrade and disappear from the body over the desired period of time; this avoids the need for surgical treatments to remove the devices after they performed their function (Domb and Kumar, 2011).

Much progress has been done in medical applications in recent years with the exploration of alternative synthetic and naturally occurring polymers (Makadia and Siegel, 2011). In general, synthetic polymers have greater benefits compared to the naturally occurring ones as their required mechanical properties can be easily tailored (Cascone *et al.*, 1995, Domb and Kumar, 2011). Among all biodegradable polymers, aliphatic polyester family in particular polylactic acids (PLAs), polyglycolic acids (PGAs) and polycaprolactone acids (PCLs) (Fig. 1.1) are more commonly used for medical applications. This is because of the

improved mechanical properties as well as the availability of these polymers compared to the other biodegradable polymers (Klose *et al.*, 2008, Saha *et al.*, 2016).

The physical and mechanical properties of the aliphatic polyesters are primarily dependent on the molecular structure and morphology of the polymers. Copolymerization and blending of different polymers also result in a significant change in mechanical strength (Domb and Kumar, 2011). PGA, the simplest aliphatic polyester, is a highly crystalline polymer exhibiting high tensile modules. PLA, has an asymmetric  $\alpha$ -carbon which can be in D or L stereochemical form and exist as three enantiomeric forms as L-PLA (PLLA), D-PLA (PDLA) and D, L-PLA (PDLLA) (Agrawal and Ray, 2001, Makadia and Siegel, 2011). Physical properties of PLA polymers can change from highly crystalline (PLLA) to highly amorphous (PDLA) form depending on the orientation of the polymer chains (Venugopal and Ramakrishna, 2005, Bala *et al.*, 2004, Makadia and Siegel, 2011). PLGA is obtained by copolymerization of PLA and PGA, exhibiting a wide range of mechanical strength depending on the moiety of lactide and glycolide content of the copolymers (Domb and Kumar, 2011). PLGA polymer prepared from L, PLA and PGA are crystalline while those from D, L-PLA are amorphous. As lactic acid is more hydrophobic than glycolic acid, PLGA polymer rich with lactide acids are less hydrophilic and have high mechanical strength (Bala *et al.*, 2004). PCL is a semi-crystalline polymer achieved by copolymerization of PLA, yet have limited applicability in the field as these polymers have high hydrophobic properties. Oligomeric stereo complexes of PLA and PCL blocks also present considerably much more resistant to the degradation compared to homopolymers based on the improved mechanical properties (Huang *et al.*, 2004, Venugopal and Ramakrishna, 2005). Overall, the mechanical strength of the polymers can be significantly controlled dependent on the crystalline and amorphous regions of the polymers which is determined by the composition and stereochemistry (Bala *et al.*, 2004, Ahola *et al.*, 1999).

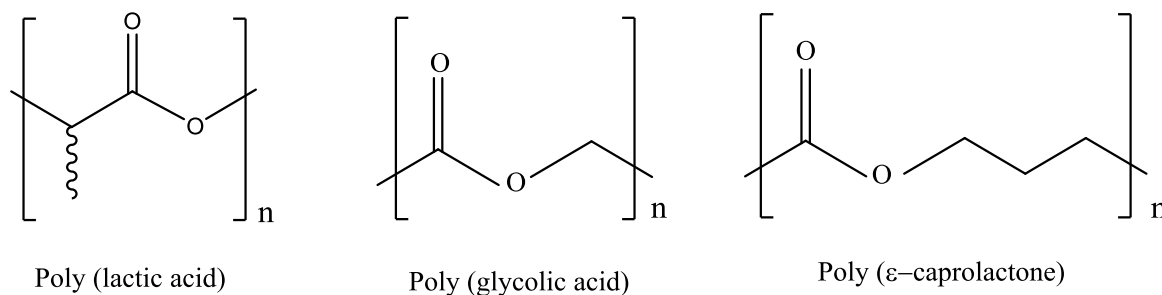


Fig. 1.1 Structure of PLA-PGA-PCL

Several synthetic polyesters have been actively used in environmental, agricultural and waste management applications. However, in last few decades, there has been a growing trend towards the use of synthetic polymers in biomedical engineering field including preventive medicine, surgical treatments, and clinical inspections. This includes disposable products (e.g. syringe, blood bag), supporting materials (e.g. sutures, bone plates and sealant), prosthesis for tissue replacements (e.g. dental or breast implant), artificial tissue/organs (e.g. artificial heart, kidney, eyes, teeth and etc.), and engineering products (e.g. tissue engineering products) with an without targeting (Ikada and Tsuji, 2000, Domb and Kumar, 2011, Bastioli, 2005, Rezaie *et al.*, 2015). There are various reasons for the favorable consideration of polyesters in biomedical applications over biostable devices. The major driving force is that these devices would naturally disappear from the tissue by time without the need for any clinical treatment. Moreover, these materials function as long term implants while in contact with the living tissue, without any risk of infection (Ikada and Tsuji, 2000, Rezaie *et al.*, 2015, Nair and Laurencin, 2007). The choice of material for a specific application is primarily dependent on its physicochemical properties like mechanical, chemical and biological functions.

Another common application of biodegradable polymers is as carriers for drugs (e.g. injectable microspheres, drug eluting stents) (Rezaie *et al.*, 2015) from which drug is released at a predetermined rate to the possibly targeted sites. Preferably, homo and copolymers of lactate and glycolide are used for that specific purpose (Philip *et al.*, 2007). The drug is either embedded in a membrane or encapsulated in a matrix releasing the drug by time (Mark, 2004). More

detailed information about the controlled drug delivery systems will be discussed throughout this thesis.

## **1.2 Controlled drug release**

Controlled drug delivery systems are alternative to conventional delivery systems that target to deliver drugs over an extended time or at a specific time in a controlled manner. These systems are comprised of an active agent, drug, and a polymer. Controlled release systems has many advantageous over other release systems providing better management of the drug concentrations, shielding drug to the desired location in action, minimizing side effects and improving patient compliance (Langer, 1980, Mathiowitz *et al.*, 1997, Ford *et al.*, 2011a, Siepmann *et al.*, 2011).

### **1.2.1 General concept of controlled drug release**

Controlled drug release systems are developed for a better administration of the drug in the body enabling a stable concentration over time. Fig. 1.2 illustrates the plasma concentration of drug in the blood. In conventional release systems, single dose (1) leads to a sharp rise and fall in drug amount that might fall out of the range of therapeutic level for certain time intervals. Moreover, the dose repeat (2) might be necessary to extent the concentration of drug in plasma. On the contrary, controlled systems (3) lead to a better regulation of drug concentration by time. Such systems provide a stationary level for drug pharmacokinetics so that drug concentration remains in the therapeutic level eliminating drug to reach to the toxic concentrations (Siepmann *et al.*, 2011).

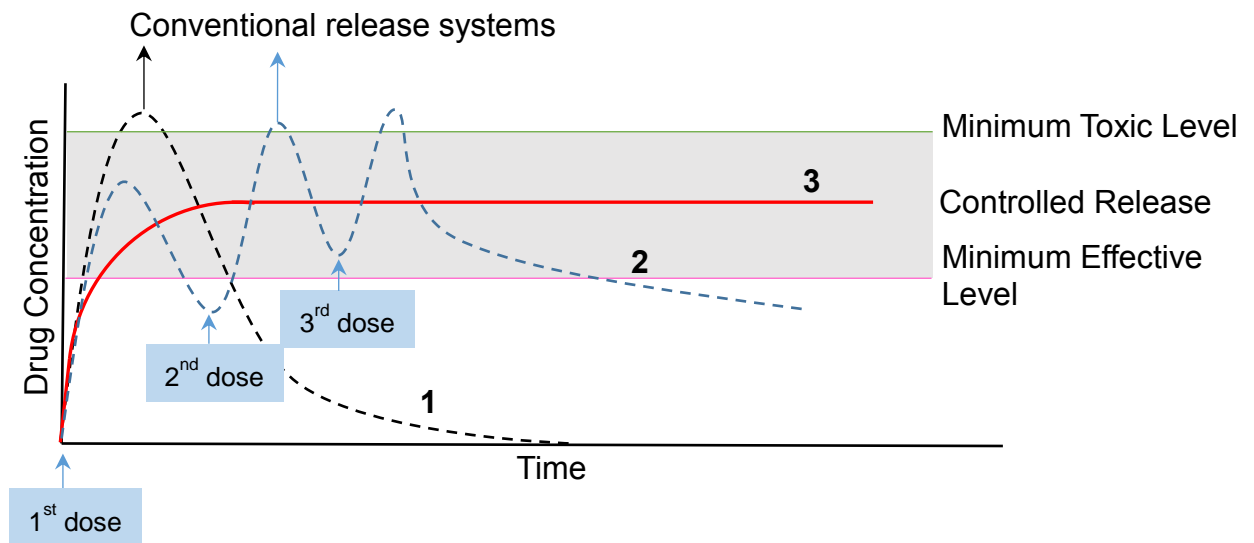


Fig. 1.2 Drug concentration in plasma ranging from therapeutic level bounded by minimum effective concentration (MEC) and maximum toxic concentration (MTC) (modified from (Ward and Georgiou, 2011))

Most of the drug release formulations target a constant release of drug by time (zero order) (see Fig. 1.3). This leads to a better control of drug concentration in plasma. However, in the great extent of controlled release formulations, an initial bolus release occur upon placement into the release medium. This phenomenon has been typically stated to as burst release in the literature (See Fig. 1.3) (Huang and Brazel, 2001). In some particular cases, the initial burst of the drug may be desirable such as the wound treatment and pulsatile release which requires high release rates in the initial stages after the activation (Huang and Brazel, 2001). One of the biggest problems with the burst release is that it is often unpredictable and cannot be remarkably controlled. For a better management, it is important to utilize the burst release as a part of the drug administration. The amount of burst can be significantly controlled depending on the fabrication technique.

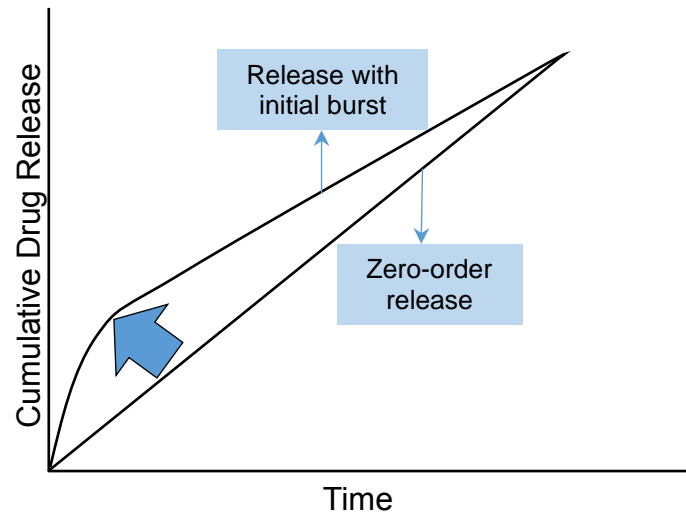


Fig. 1.3 Cumulative drug release for zero order and burst release

### 1.2.2 Controlled drug release using PLA/GA

Polymers made of PLA, PGA and their copolymers mainly tend to undergo degradation. However, the other mechanisms can be also involved in drug release, which occurs concurrently with the degradation. Three theories are generally considered in the literature for drug release from PLA/GA delivery systems: diffusion, degradation, and erosion. At the beginning, the concentration gradient is the main driving force controlling the release from the matrix. At the later stages, hydrolytic degradation of the polymer matrix predominates the release, which facilitates the release rate. After reaching a certain critical molecular weight, the controlling mechanism is switched to be dominated by erosion, which leads to a bolus release of drug in a short period of time (Kamaly *et al.*, 2016). Depending on the combinations of these mechanisms, drug release can follow monophasic, biphasic or triphasic profiles.

The overall drug release process from PLA/GA polymers has been extensively described in the literature. The drug is initially distributed throughout the matrix prior to degradation. Water should ingress into the polymer matrix to hydrolyze the polymer chains. The hydration is a fast process compared to the timescale for degradation and erosion. The water ingresses to the matrix hydrolyzing the polymer chains and break them into smaller fragments. The small oligomers,

which are produced by hydrolyses, are capable of diffusing out of the matrix as a result of a concentration gradient. At the meantime, drug molecules are dissolved and diffuse through the polymeric media (Uhrich *et al.*, 1999, Ford Versypt *et al.*, 2013). Transport of the oligomers and drug take place via the bulk polymer and the pores established during the degradation. Diffusion of the drug can also contribute to the pore volume. Due to the dynamic structure of the polymer matrix, the effective diffusivities of drug and oligomers enhances through the degradation. Both degradation and drug release processes take place in concert during the drug release process. In some cases, polymer matrix loses its integrity after reaching a certain molecular weight which is followed by a sudden erosion. This leads to a bolus release of oligomers and drug in short time. More detail about the mechanism of drug release from PLA/GA polymers is given in Section 1.3.3.

### **1.3 Mechanisms for hydrolytic degradation, erosion and controlled drug release**

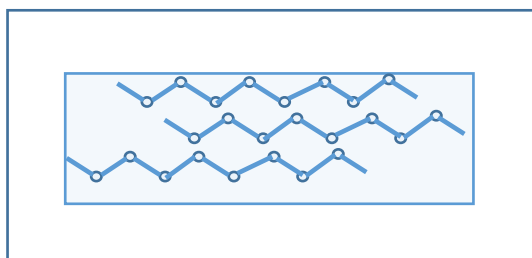
The underlying mechanism of controlled release systems is diverse and complex, and it is essential to comprehend the individual mechanisms involved in the release process.

#### **1.3.1 Mechanism for hydrolytic degradation**

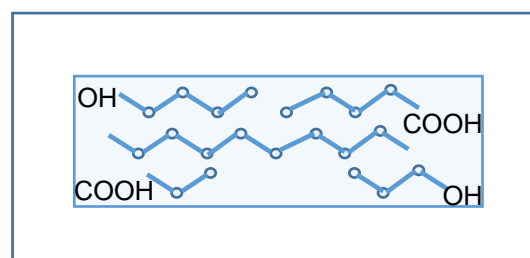
Polymers comprise of long chains made of many identical monomer units. Fig. 1.4 represent a schematic illustration of polymer chains. The blue spheres represent the repeat units (monomers) of a long chain. In the aqueous environment, long chains break into the smaller ester bonds (see Fig. 1.4). This is known as hydrolysis reaction or hydrolytic degradation. Polymer hydrolysis consist of four stages (Scott, 2002). Water uptake is the first stage of the chain cleavage which triggers hydrolysis reaction (stage 1). Since diffusion of water is a rapid process compared to the hydrolysis, one can assume the water molecules to be abundant from the beginning of the reaction. The hydrolysis reaction produces short chains which are known as oligomers. After the cleavage, two

loose ends terminate as alcohol end groups, R-OH and carboxylic acid end groups, R-COOH (Pan, 2014) (stage 2).

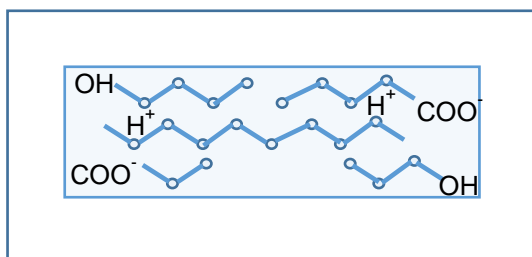
**Stage 1: Water ingress**



**Stage 2: Production of R-COOH and R'-OH**



**Stage 3: Dissociation of short chains**



**Stage 4: Oligomer diffusion**

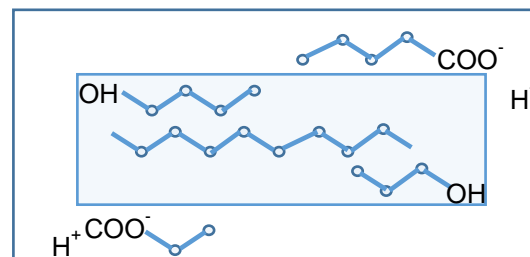


Fig. 1.4 Schematic representation of hydrolytic degradation of polymer

The reaction is known to be autocatalytic which can be catalysed by acids and bases. The acid catalyst can be from an external source such as the acidic medium or an internal source such as carboxylic acids of the polymer chains (Grizzi *et al.*, 1995) (stage 3). The chemical mechanism of acid-catalysed hydrolysis will be explained in detail in the following section.

As the number of chain cleavage increases, more and more carboxylic acid groups are produced which are known to catalyze hydrolysis. The solubilized oligomers are capable of moving out of the matrix leading to a mass loss (stage 4). Depending on the matrix size, monomers and oligomers can be trapped in the device leading to an increase in local acidity. This effect is more predominant for larger devices. Such an accumulation leads to acceleration in degradation rate as well as leading to surface-interior differentiation (Siepmann *et al.*, 2011). Over

time, the autocatalytic effect becomes more predominant, and microspheres forms hollow interiors (Berkland *et al.*, 2003). The experimental studies from the literature have evidences of local acidity increase due to acidic byproducts of the hydrolysis reaction. This provides very strong evidence that coupling between autocatalytic reactions and diffusion of the acidic products is a necessity for the systems made of PLA/GA polymers (Ford *et al.*, 2011a).

It has been reported that there are two types of chain cleavage in a polymer bond: random scission and end scission (Pan, 2014). In random scission, each polymer chain is assumed to have equal chance to be cleaved, while end scission assumes the cleave to happen only at the end of the chain (Gleadall *et al.*, 2014). While the concentration of carboxylic acid groups is low and the total number of ester bonds is high, all ester bonds have same probability to cleavage with random scission. As the concentration of end groups increases, and the autocatalysis become the dominant mechanism, end scission becomes more preferable (van Nostrum *et al.*, 2004, Batycky *et al.*, 1997). Degradation leads to change in polymer microstructure by the formation of pores through which monomers and oligomers are released. As oligomers are released, porosity within the matrix becomes prominent (Gopferich, 1996). Finally, when the internal material is totally transformed to water soluble material hollow structure can be observed in the samples. Therefore, one can claim that the hydrolytic degradation of polymers are heterogeneous depending on the size of the degrading material (stage 4) (Scott, 2002). This leads to an increase in the effective diffusivity of oligomers as microspheres diameter enlarges (Siepmann *et al.*, 2005).

Since the structure of the polymer matrix is dynamic, establishing diffusion-reaction balance is rather difficult. The level of degradation can be monitored by examining the change in molecular weight and mass loss (Gopferich, 1996). The whole process of degradation mechanism is fairly complex and reasonable assumptions should be proposed while developing a mathematical model.

The weaker intermolecular bonds increases the rate of hydrolytic degradation. Several additional factors may also influence on the rate of degradation. In order

to sufficiently design drug delivery devices, it is important to comprehend all these factors affecting the biodegradation of polyesters. As stated before, polymer composition has a significant influence on the rate of degradation. Altering number of units in a homopolymer (polymers with identical monomer units) or proportion of glycolide and lactide units in a copolymer dramatically changes the degradation rate (Park, 1995). Degradation rate is also a function of crystallinity. Literature provides conflicting results about the relationship between degradation rate and crystallinity (Bastioli, 2005). Few groups (Tsuji and Ikada, 2000) state an acceleration of the degradation while others (Li *et al.*, Montaudo and Rizzarelli, 2000, Cai *et al.*, 1996, Li and McCarthy, 1999) propose a decrease in the degradation trend with increasing crystallinity. Both of the results are expected because crystalline regions prevent the water molecules from penetrating into the polymer due to the packing of aligned chains. This causes to resistance to hydrolytic degradation. On the other hand, with increasing crystalline fraction, oligomers accumulate in the amorphous regions. This leads to an increase in oligomer concentration inside the amorphous regions which accelerates the chain scission. The relative influence of these theories determines the rate of chain scission.

The molecular weight and its distribution have a dramatic effect on polymer degradation. This is because of the fact that the physical properties of the polymer such as  $T_g$ , crystallinity and Young's modulus are directly related to the polymer molecular weight. Basically, polymers having longer polymer chains requires more time to be fully degraded. However, this can be opposite for some cases such as for the case of PLLA due to the increase in crystallinity with increasing chain size (Bastioli, 2005, Park, 1994).

Size and shape of the matrix also affect the biodegradation properties, since higher surface area gives rise to accelerated degradation (Li, 1999). The acidity of the microenvironment, pH, changes the degradation rate; both acidic and basic media can accelerate degradation (Holy *et al.*, 1999).

Drug type is another factor reported to have a significant influence on polymer degradation. However, efforts to relate the drug chemistry to polymer degradation

is very limited and do not yield a strong relationship. Acidic drugs are reported to enhance the polymer degradation rate; whereas there are conflicting results for basic drugs (Siepmann *et al.*, 2005, Makadia and Siegel, 2011, Cha and Pitt, 1989). The effect of drug chemistry on polymer degradation has been discussed in detail through this thesis.

The evidences from the literature show that the factors influencing the degradation rate are very complex and there can be many exceptions which put obstacles to make correlations. Furthermore, a bunch of factors can overlap causing challenges to make generalizations. However, it is still critical to understand the factors affecting the degradation rate in different systems in order to design optimum devices for drug delivery.

#### **1.3.1.1 Hydrolysis of esters**

As mentioned in the previous section, chemical hydrolysis of the polymer ester bonds can be catalysed by acids and bases. In the current section, the catalytic mechanisms of the esters will be explained in detail.

The term acid catalysis generally refers to proton catalysis in the literature. In this sense, acid catalysed hydrolysis begins with protonation of the carbonyl O-atom (stage 1). The main driving force behind the protonation is the susceptibility of carbonyl C atom to nucleophilic attack. After the protonation, the electrophilicity of the carbonyl increases. The first stage is followed by hydration of the carbonium ion to produce a tetrahedral intermediate product (stage 2). In the acidic medium, equilibrium will again be set up within this stage and the proton will be shared by three oxygen atoms. The reaction continues with heterolytic cleavage of the acyl-O bond (stage 3). This stage is followed by an acid-base reaction: deprotonation of the oxygen that comes from the water molecules (stage 4). In the next stage, the neutral methanol group is pushed out by use of the electrons of the adjacent oxygen (stage 5). And finally, the oxonium ion is deprotonated revealing the carbonyl in the carboxylic acid product. Thus, acid catalyst is regenerated. Since the last step includes the loss of proton, the reactions are considered as acid catalysed. All the steps of acid catalyst hydrolysis is reversible. The stages of the acid catalysed hydrolysis is

schematized in Fig. 1.5. The symbol, R, refers to  $-\text{CH}_3$  group, whereas X stands for  $-\text{OCH}_3$  group (Dewick, 2006, Testa and Mayer, 2003).

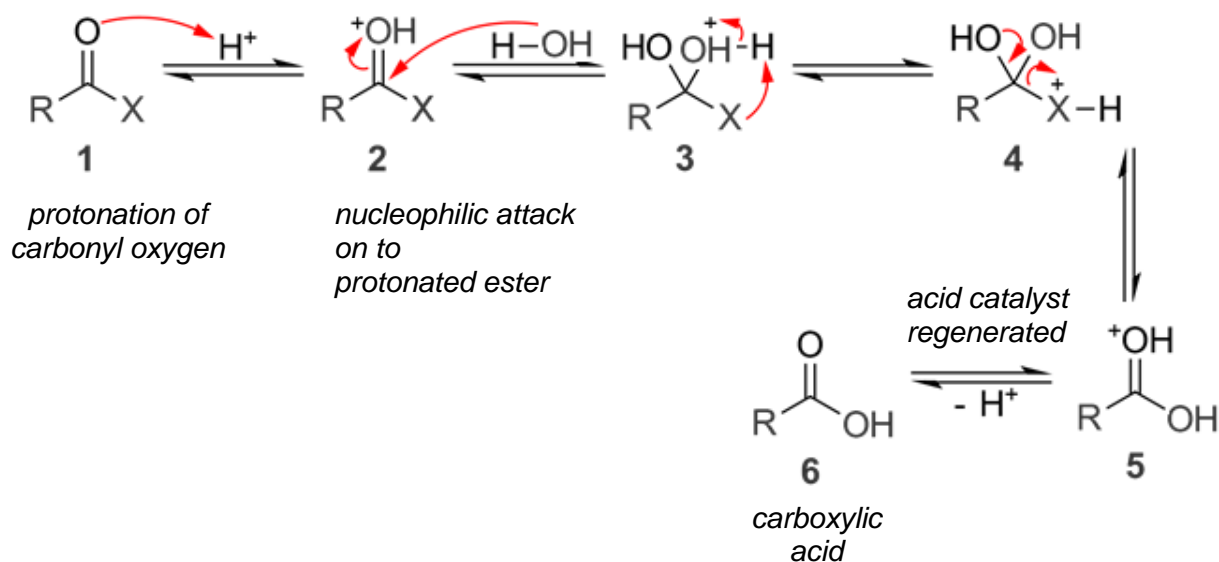


Fig. 1.5 Acid-catalysed hydrolysis of esters

The term base catalysis is generally taken as  $\text{OH}^-$  catalysis. In the base catalysed hydrolysis of esters, the nucleophile which is hydroxide is able to attack to carbonyl. This nucleophilic attack leads formation of a tetrahedral intermediate (stage 1). In the latter stage, intermediate collapses with heterolytic cleavage of the acyl- O bond, which leads to liberation of phenolate anion (represented as X in the figure) (stage 2). This reaction is strongly driven to the right side. The final step is the deprotonation of carboxylic acid (stage 3). The final proton transfer is irreversible. This is why base catalyst hydrolysis is generally schematised with irreversible arrows. The mechanism of base-catalysed ester hydrolysis is presented in Fig. 1.6. The symbol, Nuc refers to the nucleophile which is hydroxide ( $\text{OH}^-$ ) (Testa and Mayer, 2003).

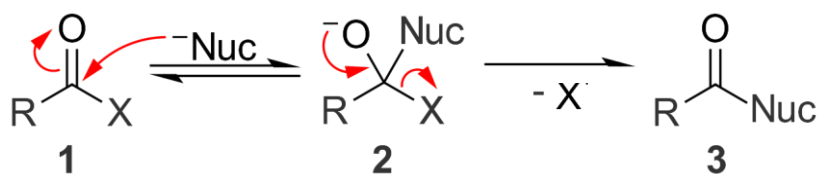


Fig. 1.6 Base-catalysed hydrolysis of esters

As can be seen, both of the acid and base catalysed mechanisms involve a tetrahedral transition state, the protonated ester, which then reacts with water (Clugston and Flemming, 2000). At the end of both reactions, the final product is the carboxylic acids.

### 1.3.2 Mechanism for erosion

The erosion is widely categorised as bulk and surface erosion. Bulk erosion can be further divided into two categories as homogenous and heterogeneous degradation.

Gopferich (1996) describes erosion as a mechanism that can be characterized by the mass loss with the depletion of water-soluble materials. In surface erosion, the hydrolysis rate is much faster than the rate at which water penetrates into the matrix. By contrast, in bulk erosion the rate of hydrolysis is slow compared to the diffusion of water to the device, therefore, a complete polymer matrix is affected by the erosion (Buchanan, 2008).

Unfortunately, a great number of researchers have used the term “bulk erosion” to represent degradation which causes to a big confusion in the literature. In order to eliminate this misconception, “interior erosion” term is used throughout this thesis to represent the bulk erosion. This term has never been used in the literature before and provides a clear distinction between degradation, surface erosion, and bulk erosion. Device dimensions remains constant through the interior erosion. Mass loss also remains very low up to a critical stage of interior erosion, where there is a dramatic mass loss. At that stage, material becomes water soluble and instantly lose all the soluble-material that is trapped in the central regions of the polymer. The soluble materials accumulated inside is

released as soon as interior is connected with the surrounded medium (see Fig. 1.7).

In surface erosion, polymer falls apart with a constant speed starting from the matrix surface, slowly decreasing the size and shrinking towards its interior as illustrated in Fig. 1.7. For an ideal surface erosion, erosion rate is constant which is proportional to the external surface area. Molecular weight does not change significantly during the erosion process.

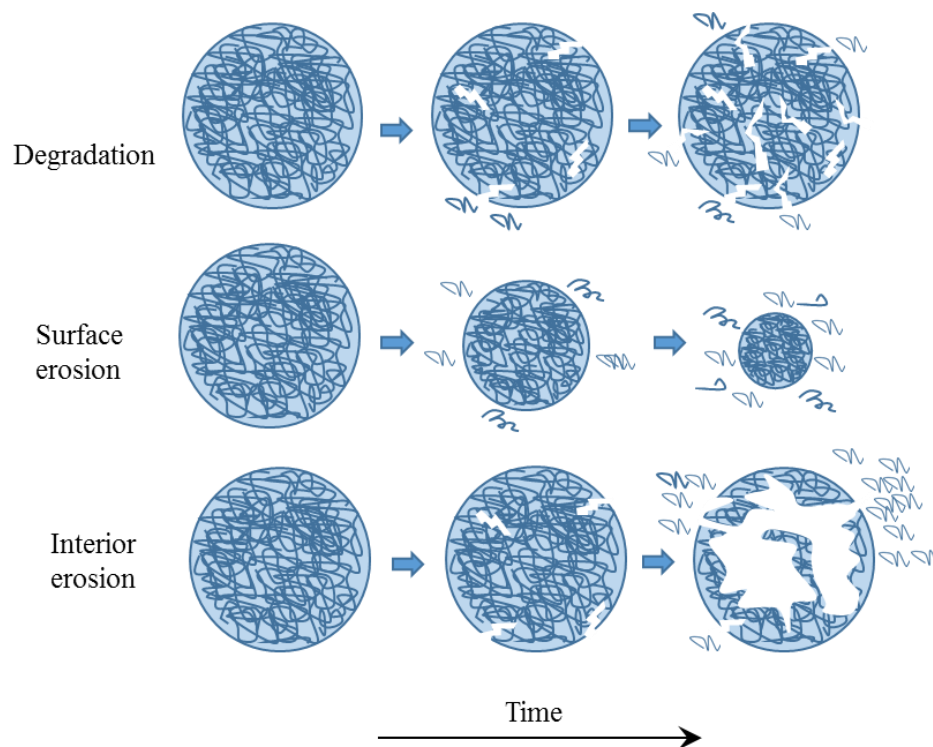


Fig. 1.7 Mechanisms of hydrolytic degradation, surface erosion and interior erosion

As a basic rule, the polymers having highly reactive groups tend to undergo erosion, while the ones with less reactive groups undergo degradation. Polyanhydrides, for example, preferably tend to be surface eroding; whereas aliphatic polyesters such as PLA, PGA is more likely to degrade through hydrolytic degradation and interior erosion (Buchanan, 2008). However, it should be bare in mind that such kind of classification is not correct for all the cases

since degradable polymer can erode when the conditions are appropriate (Burkersroda and Goepferich, 1998).

Mass loss profiles can be a simple and effective way to assess the undergoing mechanism of polymers rather being controlled by degradation, surface erosion or interior erosion. Degradation leads to a slow mass loss slightly increasing to the end of the degradation. The observations show that only up to 5-10% mass loss can be achieved with the degradation-diffusion mechanism. Surface erosion leads to a linear mass loss profile through which greater amount of mass can be lost (Engineer *et al.*, 2011). For the case of interior erosion, polymers represent a zero mass loss followed by a spontaneous mass loss after a critical degree (von Burkersroda *et al.*, 2002). Interior erosion leads to a great amount of oligomer release. As can be seen from the definitions, the mechanisms of degradation and erosion are fairly interconnected.

In most of the drug delivery applications, surface erosion is a preferable over the degradation and interior erosion since it is more predictable and easy to control compared to degradation and interior erosion (Kamaly *et al.*, 2016).

### **1.3.3 Mechanism for drug release**

For polymeric drug delivery systems, drug release mechanism generally refers to how drug molecules have been transported from a starting point to the matrix's outer surface and finally released to the surrounding medium; and are classified based on how the drug has been released from the system (Kamaly *et al.*, 2016).

There can be one or more important phenomena controlling drug release from the particles including diffusion, matrix degradation, erosion and swelling (Siepmann *et al.*, 2011, Arifin *et al.*, 2006b). Generally, a combination of different mechanisms is responsible for drug release which depends to the drug and polymer type. In diffusion-controlled systems, drug release is predominantly controlled by a non-degraded polymer, where drug molecules actions upon exposure to a stimulation. Diffusion is caused by Brownian motion that is a random walk of the drug molecules throughout the device. The prime modes of degradation controlled systems are by the release of drugs throughout the

networks generated during the chain cleavage reactions (see Fig. 1.8). In an erosion-controlled system, the drug has been released by the loss of matrix starting from the surface or the interior (see Fig. 1.8). More detailed information about the mechanisms of polymer degradation and erosion is the subject of Section 1.3.1 and 1.3.2, therefore, will not be discussed in further detail in the current section. In swelling controlled systems the drug is released from hydrophilic polymers as swelling front moves into the matrix. In such systems, the release rate is determined by the transport of the solvent into the matrix (Siepmann and Siepmann, 2012, Ranga Rao and Padmalatha Devi, 1988, Heller, 1987).

Here, a brief introduction of the mechanisms for drug release is provided for several drug delivery systems. However, it is a challenge to discuss these processes independently. For an instance, in the case of swelling controlled systems, the diffusion rate of water would be a key issue for the control. Likewise, degradation and erosion mechanism are interlinked with each other as explained in Section 1.3.

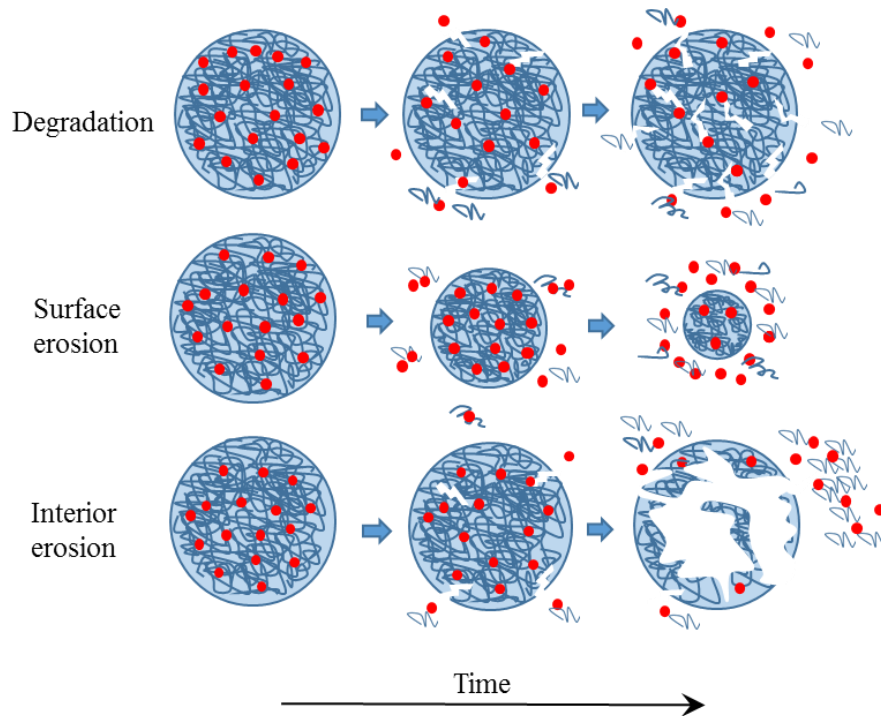


Fig. 1.8 Drug release mechanisms from degrading and surface eroding polymeric microspheres

## 1.4 The need for modeling

The mechanisms of polymer degradation, erosion, and drug release are fairly interconnected. This dependency makes it challenging to evaluate the mechanisms independently. In order to quantify the drug release from biodegradable and bioerodible polymers, one should consider all the mechanisms including autocatalytic hydrolysis, diffusion, pore formation, erosion and the acidic-basic character of the drugs as well as drug-polymer interactions. The complicated and interlinked character of the polymer degradation makes it difficult to optimize the design of the drug delivery systems.

Development of the polymeric devices made of biodegradable and bioerodible polymers are currently based on trial and error experiments. The experimental studies are far from focusing the primary mechanisms of the degradation and

erosion processes. Moreover, the experimental approach has many limitations including requirement of excess amount of time and money.

Modeling approaches help to understand the experimental data revealing underlying mechanisms of drug release. This information in turn helps optimization of release kinetics and tablet design. Mathematical models can enlighten the effect of several parameters, including composition of polymers, size, shape, drug content on polymer degradation and corresponding drug release. Moreover, systemic use of the mathematical models in drug delivery field significantly reduces the cost and the experimentation time. In terms of a better design of biodegradable devices used in drug delivery field, mathematical models have been proved to be effective and extend our knowledge of understanding the biodegradable devices used for controlled drug delivery. Therefore, creating advanced models would be able to meet the criteria needed for the market such as being cost effective, applicable and efficient.

Many mathematical models have been developed to predict the polymer degradation and erosion as well as the corresponding drug release from biodegradable polymers. These models can be either empirical, semi empirical, mechanistic or probabilistic. Mechanistic models are known to reflect real physics behind the drug diffusion, degradation and erosion (Kamaly *et al.*, 2016). In most of the mechanistic models, the diffusivity of the species are reflected by Fick's laws of diffusion. A comprehensive review of the previous degradation and drug release models are provided in Chapter 2.

The existing models form a solid baseline for the mathematical models developed throughout the thesis. Taking these models as a basis, several mathematical models will be developed to enlighten the underlying mechanism of drug release from biodegradable polymers. This includes: *i*) the mechanistic models presenting the effects of the acidic and basic drugs on the hydrolytic degradation rate; *ii*) combined modelling of hydrolytic degradation and erosion; and *iii*) the applications of proposed models on several case studies from the literature.

## Chapter 2. A review of existing mathematical models for polymer degradation and controlled drug release

In order to obtain the precise quantification of polymer degradation, erosion, and drug release, modeling is extremely important. Mathematical/computational models have some preferable properties over experimental studies such as avoiding excessive experiments, allowing precise prediction of design parameters (size, shape, geometry etc.) and accurately determination of degradation and release profiles (Shaikh *et al.*, 2015). Models for drug delivery systems also helps to provide transfer mechanisms based on scientific knowledge which facilitates the development of novel pharmaceutical products.

This chapter presents a brief review of the previous models in the literature for the polymer degradation, erosion, and drug release. Degradation and erosion models have been divided into the subsections such as the studies proposed before Pan and co-workers (Section 2.1) and by Pan and co-workers (Section 2.2). Drug release models have been detailed in Section 2.3. This chapter also gives details about the gaps in the literature as well as overall aims, objectives, and structure of the thesis.

### 2.1 Models for polymer degradation and erosion before the work by Pan and co-workers

#### 2.1.1 Models for polymer hydrolysis kinetics

The simplest model for polymer hydrolysis has been proposed by Pitt and Gu (1987) assuming that the rate of hydrolysis is only dependent on ester and water concentrations

$$\frac{dC_{R_1-COOH}}{dt} = kC_wC_e \quad (2.1)$$

where  $k$  is the rate constant,  $C_e$ ,  $C_w$  and  $C_{R_1-COOH}$  are the mole concentrations of the ester bonds, water and carboxylic end groups of oligomers, respectively and

$t$ , the time. The model proposed lacks considering the catalyst effect of the acidic groups. Pitt and Gu then correlated the reaction rate to include catalytic impact of the carboxylic groups such as

$$\frac{dC_{R_1-COOH}}{dt} = kC_w C_e C_{R_1-COOH} \quad (2.2)$$

Due to accounting the acid concentration, Eq. 2.2 has been referred as the autocatalytic hydrolysis reaction. In their model, Pitt and Gu assumed that reaction kinetics is proportional to the concentration of carboxylic acid end groups. Siparsky *et al.* (1998) made a clear distinction between the acid catalyst concentration,  $C_{H^+}$ , and acid product concentration,  $C_{R_1-COOH}$ , and updated the hydrolysis rate equation to include autocatalytic terms. They considered the dissociation of carboxylic acids which leads to generation of  $H^+$  and that has been reckon as the main source of autocatalysis reaction. The equilibrium constant of the oligomer dissociation reaction,  $K_a$ , is

$$K_a = \frac{C_{R_1-COOH}}{(C_{H^+} C_{R_1-COO^-})} \quad (2.3)$$

Since  $C_{H^+} = C_{R_1-COO^-}$ , Eq. 2.2 can be rearranged as  $C_{H^+} = [K_a C_{R_1-COOH}]^{1/2}$  which is used to represent the acid catalyst concentration. Then the rate equation can be updated as

$$\frac{dC_{R_1-COOH}}{dt} = kC_w C_e [C_{R_1-COOH} K_a]^{0.5} \quad (2.4)$$

The reaction rate proposed by Siparsky *et al.* (1998) can be fitted with most of the experimental data in the literature. The concentration of the chain ends is usually very low to be measured. Therefore, instead of  $C_{R_1-COOH}$ , it is convenient to characterize the polymer degradation with the number average molecular weight,  $M_n$ . Basically, concentration of the carboxylic end groups are reciprocal to the number average molecular weight of the polymers. Lyu and Untereker (2009) proposed the following equation to link these two such as

$$M_n = \frac{\rho}{C_{R_1-COOH}}. \quad (2.5)$$

Integrating Eq. 2.4 yields to

$$C_{R_1-COOH} - C_{R_1-COOH,0} = kC_wC_e t \quad (2.6)$$

where  $C_{R_1-COOH,0}$  is the initial mole concentration of acid end groups. By using Eqs. (2.5) and (2.6), we have

$$\frac{1}{M_n} = \frac{1}{M_{n,0}} + \frac{1}{M_{unit}} kC_wC_e t. \quad (2.7)$$

Here,  $M_{unit}$  is the molecular weight of a polymer unit. Some published data uses weight average molecular weight,  $M_w$  or viscosity averaged molecular weight,  $M_v$ , to show reaction kinetics, which is not accurate. However, since these are proportional to  $M_n$  values, similar trend can be observed (Buchanan, 2008).

All the mentioned models above assume that the water concentration is a limiting factor for the reaction kinetics, however, one can simply assume that water is abundant during the physicochemical reactions. This assumption is acceptable since the water ingress rate is much faster than hydrolysis reaction rate.

Arrhenius analyzed the effect of temperature on the reaction rate; proposed a temperature dependent kinetic constant such as

$$k = k_0 e^{-E_k/RT} \quad (2.8)$$

in which  $E_k$  is the activation energy for the reaction;  $k_0$ , a constant. Arrhenius equation has some limitations above and below glass transition temperature,  $T_g$ . Lyu *et al.* (2007) proposed an alternative equation to Arrhenius equation which can be used below and under the  $T_g$  such as

$$k = k_0 e^{-(E_k/R(T-T_s))}. \quad (2.9)$$

This equation is called as Vogel-Tammann-Fulcher equation. Here,  $T_s$  is a reference temperature. Eq. (2.9) can be effectively used below and under  $T_g$ .

### 2.1.2 Reaction – diffusion models

Thombre and Himmelstein (1985) and Joshi and Himmelstein (1991) developed a comprehensive approach for drug release taking into account autocatalytic effect of degradation products. In their model, water ingress into the matrix, hydrolyzing the acid generator such as an acid anhydride, and the generated acid is assumed to catalyze the chain cleavage. The chemical reactions then linked with the diffusion controlled mass transfer equations. They used the following equation to introduce diffusion component to the reaction equations such as

$$\frac{dC_i}{dt} = \frac{\partial}{\partial x} \left( D_i(x, t) \frac{\partial C_i}{\partial x} \right) + v_i \quad (2.10)$$

in which  $C_i$  and  $D_i$  represents the concentration and effective diffusion coefficient of the oligomers, respectively;  $x$  the position and  $v_i$ , the rate of oligomer production. Here, diffusion is assumed to be only in one direction. To introduce the changing permeability of the system,  $C_d$ , they applied the following equation

$$D_i = D_{i,poly} \exp \left[ \frac{\mu (C_{d,0} - C_d)}{C_{d,0}} \right]. \quad (2.11)$$

Here,  $D_{i,poly}$  is the diffusivity of the oligomers at fresh bulk polymer;  $C_{d,0}$ , the initial permeability of the polymer and  $\mu$ , the constant.

Their model was solved numerically and tested over experimental data to prove the effectiveness of the model. The model is fairly effective to predict the mass loss and drug release behavior of the polymers loaded with drugs. The method also effectively involves the dependency of the diffusion coefficients to the dynamics of the matrix system. Zilberman and Malka (2009) has proposed an alternative time-dependent diffusion coefficient, altering based on polymer's mass loss and degree of crystallinity such as

$$D_i(t) = D_{i,poly} + (D_w - D_{i,poly}) * W(t) * (100\% - x_c(t)) \quad (2.12)$$

in which  $D_i$  is the effective diffusion coefficient of the species,  $D_{i,poly}$ , the diffusion coefficient of the species at fresh bulk polymer,  $D_w$ , the diffusion coefficient of

particles in water,  $W$  is the mass loss (%),  $x_c$ , the degree of crystallinity. Compared to the polymer crystallinity, degradation rate of polymer was proved to have a greater effect on the effective diffusivity of the species. Zhao *et al.* (2010) considered the generation of pores during the chain scission reactions and they linked the degradation kinetics to the pore radius which is a function of time. The diffusion component of the models proposed in this thesis considers Fick's law of diffusion similar with the model proposed by Thombre and Himmelstein (1985), Joshi and Himmelstein (1991).

### 2.1.3 Models for surface erosion

As stated at the beginning of Section 1.3, erosion refers to the physical processes leading to a mass loss in the polymer. By virtue of this definition, surface erosion models would be considered in the current section.

There is a large volume of published studies describing surface and interior erosion behavior of polymers. Hopfenberg proposed a constant release of incorporated agent for the case of the constant surface area (Paul and Harris, 1976). Similarly, Lee (2001) proposed moving boundaries for erodible devices which consist of a moving diffusion front and a moving erosion front. Surface erosion is characterized by a zero order rate constant. Thombre and Himmelstein (1984) coupled the moving diffusion front with the moving erosion front to represent the surface erosion. The speed of the moving boundary is given by

$$\frac{dV(t)}{dt} = -B. \quad (2.13)$$

in which  $\frac{dV(t)}{dt}$  represents the volume of material lost per unit surface area per unit time, and  $B$  is a material constant. The rate equation proposed by Thombre and Himmelstein is a simple way of representing the mathematics of surface erosion and will be used in our model presented in Chapter 5.

### 2.1.4 Monte-Carlo Models

In the previous section, existing phenomenological models capturing surface erosion behavior have been presented. In addition to the phenomenological

models, a considerable amount of literature has been published on Monte-Carlo based models for the simulation of polymer degradation and drug release. From our knowledge, one of the very first Monte-Carlo based model is proposed by Zygourakis (1990), in order to simulate the polymer degradation and drug release from surface eroding polymer samples. Cellular automata and discrete iterations are used in the simulations. The method is based on the generation of regular grids of cells. The status of each cell is defined by the status of current cell as well as the states of the neighbouring cell. The rules are being applied to the whole grid. The method has been applied to a surface eroding polymer by initially representing the matrix consisting of 2-dimensional grids. Each pixel is assumed to represent one of drug, polymer, filler and pore. A life expectancy was defined for individual pixels. When the pixels are in contact with the aqueous medium, their life expectancy starts to decrease. As soon as the life expectancy of the pixels are expired, they assumed to dissolve instantaneously. The Fig. 2.1 shows the initial configuration of their cellular array modelling as well as the grid after 25%, 50% and 75% drug is released.

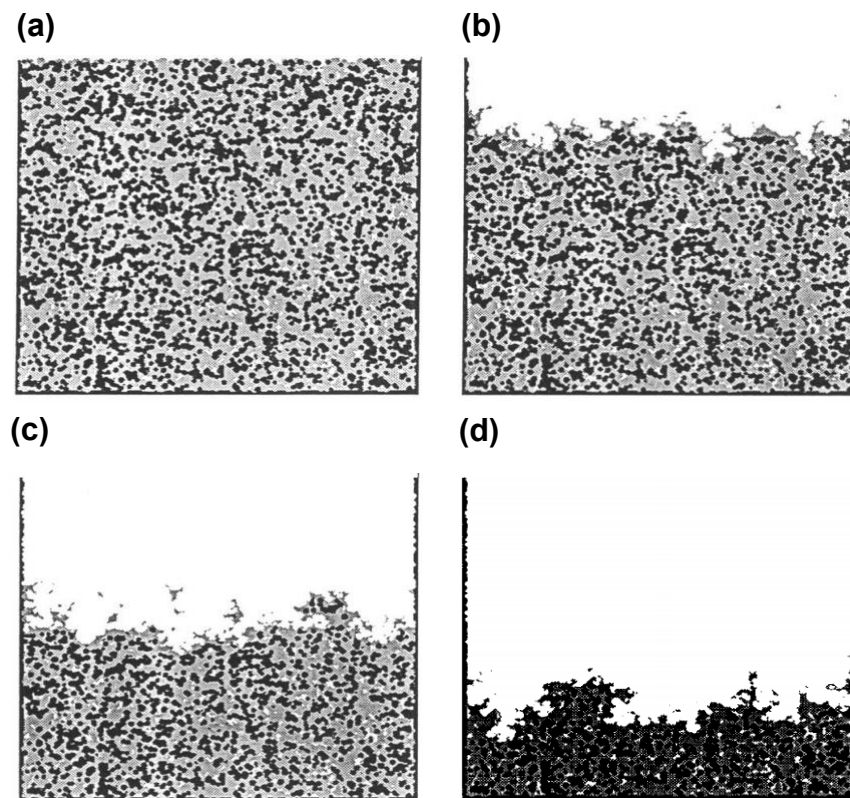


Fig. 2.1 Configuration of the polymer matrix grid through the device after Monte-Carlo simulations are applied at (a) prior to erosion, (b) 25%, (c) 50% and (d) 75% drug is released. Reproduced from (Zygourakis, 1990)

Only the top boundary is assumed to be exposed to the aqueous medium. Fig. 2.1 represents the move of the erosion front from top to bottom. Model is shown to be pioneering to apply the Cellular automata and discrete iterations for an eroding polymer. However, the main weakness of the model is that the erosion is not linked with the degradation of the polymer matrix. Moreover, diffusion of the species such as drug and oligomers are not considered in the study.

Gopferich and Langer (1993) used a similar approach in their model, by simplifying the design of the structural changes. Instead of describing the whole matrix as a grid of pixels, Gopferich and Langer focused on the representative part of the polymer matrix. The main target with their approach was to significantly reduce the number of big calculations. The periodic boundary conditions are used to account the new condition of the matrix. The life expectancies of each pixel is randomly distributed according to first order Erlang distribution, which is a known

to be a specific Monte-Carlo method. The grids are initially categorised as crystalline and amorphous phases. The matrix is assumed to be eroded only if it contact with an eroded neighbour, at which the life expectation initiates to count down. Another critical issue introduced with the study is that, Gopferich and Langer assigned different life expectancy for crystalline and amorphous pixels. This approach leads the simulations to converge to the real physics. The time series of their representative polymer matrix was presented. The model becomes a useful tool to understand the behaviour of surface erosion, however, the simulations are restricted to surface erosion only.

Siepmann *et al.* (2002) took the application of Monte –Carlo studies on a degrading polymer one step further. This has been accomplished by considering the bulk erosion of the polymers as well the surface erosion. Likewise in the previous Monte-Carlo models, a lifetime was individually assigned for all the pixels. The lifetime of individual pixels as a function of the random variable “ $R_{ran}$ ” is shown as

$$t_{lifetime} = t_{average} + \frac{(-1)^{R_{ran}}}{\lambda} \ln\left(1 - \frac{R_{ran}}{100}\right). \quad (2.14)$$

where  $t_{average}$  is the average lifetime of the pixels and  $\lambda$  is a constant which is characteristic for specific polymer. This equation is similar with the one used by Gopferich. The polymer pixel was counted as eroded as soon as the lifetime expired. By knowing the status of each pixel at any time and location, the time dependent porosities,  $\varepsilon$ , in radial and axial directions was calculated

$$\varepsilon(r, t) = 1 - \frac{1}{n_z} \sum_{j=1}^{j=n_z} S(i, j, t). \quad (2.15)$$

$$\varepsilon(z, t) = 1 - \frac{1}{n_r} \sum_{j=1}^{j=n_r} S(i, j, t). \quad (2.16)$$

The other main novelty with Siepmann’s model is to involve drug release by considering drug dissolution and diffusion with effective diffusivities. The diffusional mass transfer has been introduced by use of Fick’s second law for

spherical particles. Effective diffusivities,  $D$ , are dependent to the porosities for axial and radial directions such that

$$D(r, t) = D_{crt} \varepsilon(r, t). \quad (2.17)$$

$$D(z, t) = D_{crt} \varepsilon(z, t). \quad (2.18)$$

in which  $D_{crt}$  represents a critical diffusion coefficient which is characteristic for a specific drug-polymer combination. The principle of their Monte-Carlo approach is represented in Fig. 2.2 prior to erosion and during the drug release. In the figure, grey, dotted and white pixels show the non-degraded polymer, drug and pores, respectively. The results obtained with the model proposed, showed a good agreement with the experimental studies and provide further insight on the underlying mechanisms of polymer erosion and drug release. In contrast with the previous Monte-Carlo models, all phases of drug release including burst and zero order release could be obtained. However, the one major limitation of their model was to neglect the autocatalysis effects which is a product of polymer degradation.

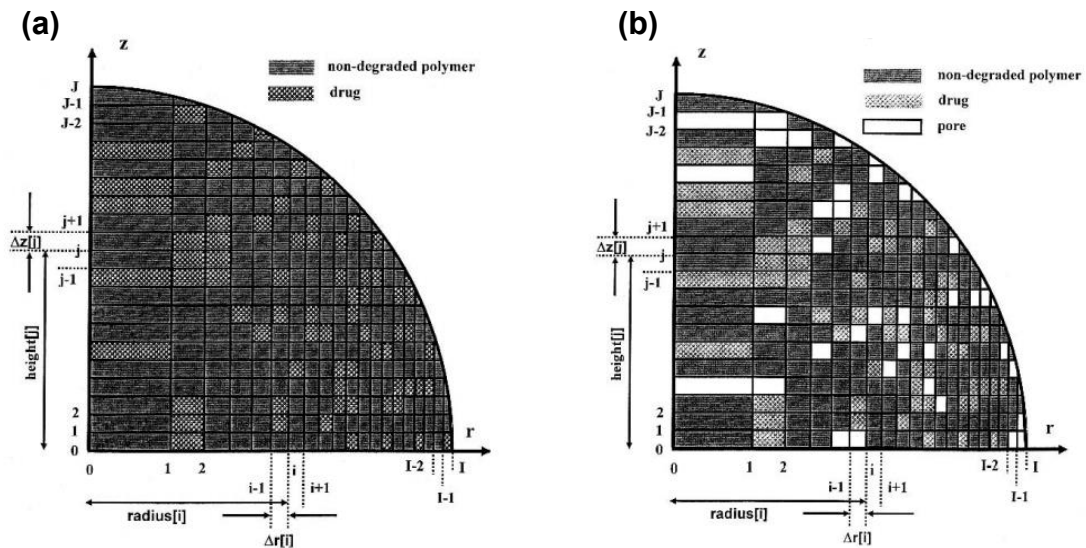


Fig. 2.2 Monte-Carlo approach of Siepmann *et al.* (Siepmann *et al.*, 2002); the schematic structure of the matrix (a) prior to erosion (b) during the drug release.

Collectively, the phenomenological and Monte-Carlo based models provide important insights into the hydrolysis and erosion mechanisms of the polymer devices. However, the studies reviewed here, remain insufficient to interlink the all possible mechanisms such as autocatalytic hydrolysis, erosion, drug release and far from calculating the effective diffusivities dependent on the heterogeneous structure of the polymer matrix. However, the evidences from the experimental studies give the hint of more than one mechanism is involved in the process.

## 2.2 Previous work by Pan and co-workers

**Ying Wang (2009):** In his Ph.D thesis, Ying Wang developed a phenomenological model for hydrolytic degradation of polymers using reaction-diffusion equations. The equations include non-catalysed and acid-catalysed terms. Monomers and oligomers were considered as the diffusing species and their diffusivities are reflected by an effective diffusion coefficient. A concept of biodegradation map is demonstrated to reveal the conditions leading to different behaviours. The map has two limitations such as fast and slow diffusion limit of oligomers. For the case of former, autocatalysis mechanism can be ignored in the hydrolysis reaction since the reaction products quickly walk away from the matrix. The thickness of the material becomes unimportant for this limit. For the case of later, the short chains are caged in the matrix leading to domination of autocatalysis on hydrolysis. This has been represented with four different zones on the map on Fig. 2.3 marked as zones A, B, C and D. Zone B is the fast diffusion zone, in which polymer is entirely controlled by non-catalysed hydrolysis. Zone C represents the slow diffusion zone where degradation is entirely controlled by autocatalysis. Zone D represents fast non-catalysed hydrolysis zone. In zone A, all the kinetics are in the issue and has an effect on the degradation rate. The degradation map provided is proved to be useful to tool for design of biodegradable fixation devices.

Wang suggested the presence of a critical diffusion coefficient below which degradation is independent of the material thickness. Taken together, these

theories are demonstrated in the biodegradation map for different degradation mechanisms to provide a guide for the design of biodegradable devices.

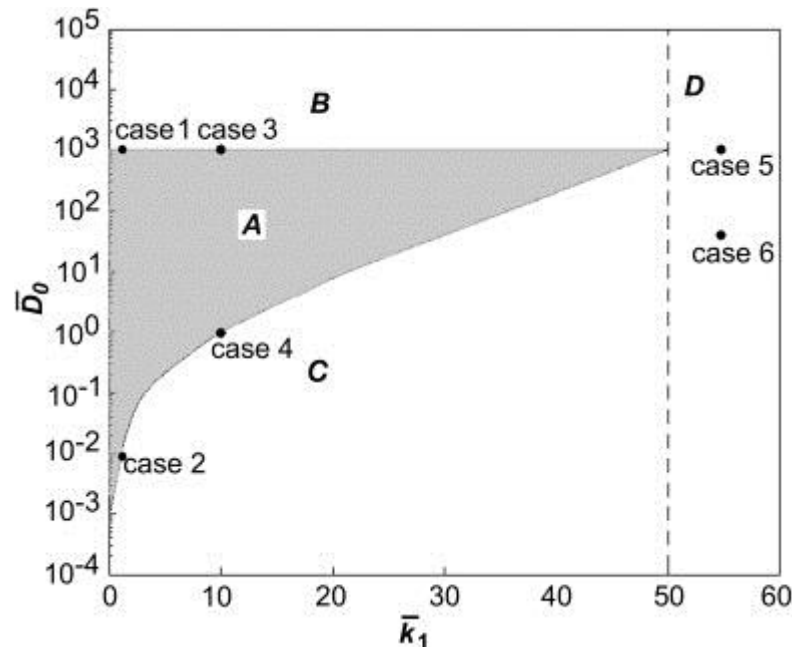


Fig. 2.3 Biodegradation model for thin plate (Wang *et al.*, 2008)

Wang also suggested to link Young's modulus to the molecular weight in a Monte Carlo simulation to investigate the polymer behavior. The linked model is based on entropy spring theory that calculates Young's modulus linearly dependent on the number of polymer chains. The combined model allows the spatiotemporal evaluation of Young's modulus. For the crystalline polymers, the composite theory is also included into the model to be able to predict Young's modulus (Wang, 2009).

**Xiaoxiao Han (2011):** In her Ph.D thesis, Xiaoxiao Han analyzed the interaction between the polymer degradation and crystallization by drawing on the concept of Wang. She modified Avrami's theory which predicts the degree of crystallinity and linked the theory with the mole concentrations in the amorphous phase. Thus, chain scission equations were improved to involve crystallinity term. The degradation model is then improved to predict the effect of elevated temperature

on degradation rate. This has been accomplished by integrating Arrhenius Equation with chain scission equations. The model then compared with the literature data to investigate whether models predict the experimental data. It is concluded that the Arrhenius equation is only valid until a certain temperature. In her thesis, Han also presented a model which couples chain scission equations to the dissolution of tricalcium phosphate (TCP) and the related buffering reactions. The biodegradation map provided by Ying Wang was modified to incorporate the TCP which decelerates the degradation rate with the buffering reactions. The updated map provides a deep understanding of the saturation behavior of TCP, incorporated in the polyesters. TCP model is proved to be valid for early stages of degradation before a certain critical molecular weight is reached. The method used in the thesis provides a methodological approach for the design of biomaterials and is applicable to other composites with a buffering agent. In addition to focusing polymer degradation, a preliminary phase field model capturing drug release from swellable polymers was presented. The swelling of the tablet was separated into three phases: the thickness of gel phase, drug dissolved phase, and drug dispersed phase. It was shown that drug release is highly sensitive to the free volume of the matrix generated during the swelling of polymer (Han, 2011).

**Andrew Colin Gleadall (2015):** In his Ph.D thesis, Andrew C. Gleadall significantly simplified the chain scission equations proposed by Wang and Han and provided a clear picture of in what extent the end scission and random scission affect the polymer degradation. A significant analysis and discussion on the effect of factors including autocatalytic and non-catalytic degradation; initial molecular weight and residual monomer are presented. Gleadall also had an attempt to develop a new atomic finite element analysis technique that translates interatomic energy functions into linear functions. The technique uses the existing MD coordinate input files and force fields. All atomic interactions were represented in the linear elastic finite elements. This method has been applied to further analyze the effect of mechanical properties on degradation rate. Moreover, the atomic finite element analyses are combined with the degradation

model to present a complete set of the equations for molecular weight, crystallinity and Young's modulus (Gleadall, 2015).

**Hassan Samami (2016):** In his Ph.D thesis, Hassan Samami used the existing mathematical models proposed by Pan and co-workers and analysed the effect of size and geometry on the degradation of polymeric scaffolds. A great deal of his studies was focused on presenting constitutive laws to determine the changes in mechanical properties such as elastic modulus, tensile strength and Poisson's ratio for semi-crystalline and amorphous polymers. Furthermore, he applied the damage detection method into coronary stents to detect the distribution of degradation within the device. Both analytical and computational models were used to detect the degradation in the degrading samples. His results showed that the analytical displacement mode shapes lack to detect the degradation within the beam since the method fails to identify the correct location of the damage. On the other hand, analytical and FE curvature mode shapes were successful in detecting the degradation during all the phases of polymer (Samami, 2016).

**The hydrolytic degradation equations by Pan and co-workers (2014):**

Pan and his co-workers provided a constitutive reaction-diffusion model for hydrolytic degradation of polymers. This equations forms a solid basis for the models developed during the current thesis. Therefore, it is convenient to clearly and precisely describe their reaction-diffusion equations first.

As stated in the previous chapter, polyesters consist of long polymer chains. In the presence of water, the long chains reduce their length and produce short chain. The hydrolytic degradation of ester bonds leads the cleavage of the polymer chains. After the cleavage two chain ends, one is with carboxylic group,  $R_1\text{-COOH}$  and one is with alcohol group,  $R'\text{-OH}$  are produced. The degradation rate resorbable polymers is known to be accelerated by the acidic products. The groups with carboxylic acids, indeed, have a high degree of acid dissociation, which catalyse the reaction. Thus, the degradation of polyesters are autocatalytic.

The hydrolysis reaction of most poly- $\alpha$ -hydroxy acids, such as PLA, PGA and their co-polymers can be schematically written as



The polymer degradation is known to be catalysed by the acid end groups. Since the acid groups of polymer degradation Pan *et al.* used the following rate equation for polymer chain scission:

$$\frac{dR_s}{dt} = k_1 C_e + k_2 C_e C_{H^+}. \quad (2.19)$$

Here,  $R_s$ ,  $C_e$ , and  $C_{H^+}$  represent the mole concentrations of chain scission, ester bonds, and acid respectively. The first term on the right-hand side reflects the non-catalytic part, whereas the second term reflects the autocatalytic part of the hydrolysis reaction;  $k_1$  and  $k_2$  represent the kinetic rate constants for non-catalytic and autocatalytic hydrolysis reactions, respectively. The hydration is relatively fast compared to the time scale for polymer chain scission- on the order of few hours compared to months. Since the hydration is a fast process, water concentration is assumed to be abundant inside the polymer, therefore, it does not appear in the rate equation.

As polymer chains are cleaved by the hydrolysis reaction, more and more short chains (oligomers) are produced. According to few study in the literature (Kulkarni *et al.*, 2007, van Nostrum *et al.*, 2004, Zhao *et al.*, 2010), oligomers having less than 10 monomer units are water soluble. Besides, Batycky *et al.* (1997) and Zhao *et al.* (2010) reported that only the oligomers up to and including nonamers (chains with 9 monomer units) are water soluble and they used that information in their simulations. However, Pan *et al.* (2014) assumed that oligomers up to and including 4 monomer units are water soluble. This assumption led to good fittings with the experimental data. By considering this, Pan *et al.* (2014) then separated the short chains from long chains in the sense that the short chains can diffuse out of the polymer while long chains cannot. Following Pan *et al.* the short chain production due to chain scission can be calculated as

$$R_{ol} = \alpha C_{e,0} \left( \frac{R_s}{C_{e,0}} \right)^\beta \quad (2.20)$$

in which  $R_{ol}$  represents the mole concentration of ester bonds of short chains produced by hydrolysis. The ester bond concentration of the long chains,  $C_e$ , is consumed by the production of short chains and can be expressed as

$$C_e = C_{e,0} - R_{ol} = C_{e,0} - \alpha C_{e,0} \left( \frac{R_s}{C_{e,0}} \right)^\beta. \quad (2.21)$$

Here,  $C_{e,0}$  represents the initial concentration of ester bonds and  $\alpha$  and  $\beta$  are empirical constants reflecting the probability of short chain production due to chain scissions.

Substituting (2.21) into (2.19) gives a final expression for chain scission rate equation:

$$\frac{dR_s}{dt} = C_{e,0} \left[ 1 - \alpha \left( \frac{R_s}{C_{e,0}} \right) \right] (k_1 + k_2 C_{H^+}). \quad (2.22)$$

Once an ester bond is broken, carboxylic and alcoholic end groups are formed. The carboxylic groups have a high degree of acid dissociation; their equilibrium reaction can be expressed as



in which  $R_1\text{-COOH}$  represents short chains with carboxylic ends. The acid dissociation constant for short chains,  $K_a$ , can be expressed by

$$K_a = \frac{C_{H^+} C_{R_1\text{-COO}^-}}{C_{R_1\text{-COOH}}}. \quad (2.23)$$

Here,  $C_{R_1\text{-COOH}}$  and  $C_{R_1\text{-COO}^-}$  represent the concentrations of  $R_1\text{-COOH}$  and  $R_1\text{-COO}^-$  respectively. The charge balance requires  $C_{H^+} = C_{R_1\text{-COO}^-}$  and Eq. (2.23) can be rearranged as

$$C_{H^+} = [K_a C_{R_1\text{-COOH}}]^{0.5}. \quad (2.24)$$

Eq. (2.24) can be substituted into Eq. (2.21) which gives

$$\frac{dR_s}{dt} = C_{e,0} \left[ 1 - \alpha \left( \frac{R_s}{C_{e,0}} \right) \right] \left( k_1 + k_2 [K_a C_{R_1-COOH}]^{0.5} \right). \quad (2.25)$$

Using  $C_{ol}$  to represent the current concentration of the short chains and  $m$ , the average number of carboxylic end groups on the short chains is given by

$$C_{R_1-COOH} = \frac{C_{ol}}{m}. \quad (2.26)$$

Wang *et al.* (2008) and Han and Pan (2009) then introduced the diffusion equations into the degradation model. They considered an extremely large plate; only left and right surfaces are exposed to the aqueous environment. Because of the symmetry, the diffusion occurs only in the  $x$  direction. As chains scission proceeds, the short chains generated diffuse into the aqueous media. The molar flux due to diffusion,  $J$ , is proportional to the concentration gradient per unit area per time. Fick's first law relates the diffusive flux to the concentration under the assumption of steady state which is governed by

$$J = -D_{ol} \frac{dC_{ol}}{dx}. \quad (2.27)$$

in which  $D_{ol}$  is the effective diffusion coefficient of oligomers. Fick's law is the simplistic way of describing the diffusion, and is capable of capturing the experimental data.

The concentration of oligomers is contributed by two factors: (i) production of short chains at that location, (ii) removal of the short chains by diffusion. First can be calculated by differentiating (2.20) which leads to

$$\frac{dR_{ol}}{dt} = \alpha \beta \left( \frac{R_s}{C_{e,0}} \right)^{\beta-1} \frac{dR_s}{dt}. \quad (2.28)$$

For a very small  $\Delta x$ , the matter conversation gives the changing rate of the concentration such as

$$\frac{dC_{ol}}{dt} = -\frac{dJ}{dx} \quad (2.29)$$

The change in concentration is given by the summation of these two factors such as

$$\frac{dC_{ol}}{dt} = \frac{dR_{ol}}{dt} - \frac{dJ}{dx} \quad (2.30)$$

Substituting Eqs. (2.27) and (2.28) into Eq. (2.29) gives a final expression for the change in the concentration of the short chains by the time such as

$$\frac{dC_{ol}}{dt} = \alpha\beta \left(\frac{R_s}{C_{e,0}}\right)^{\beta-1} \frac{dR_s}{dt} + \frac{d}{dx} \left(D_{ol} \frac{dC_{ol}}{dx}\right) \quad (2.31)$$

Eq. 2.31 is a general equation for plates in which diffusion route is in the  $x$  direction. This equation can be expanded to represent other coordinates and geometries.

The model proposed is referred as reaction-diffusion model in the literature. The governing equations can be solved numerically by applying related initial and boundary conditions.

Pan and co-workers, moreover, considered the degrading polymer consisting of two phase: a polymer phase and a porous phase. They used a diffusion coefficient based on the related porosity  $V_{pore}$  through (Jiang *et al.*, 2008)

$$D_{ol} = D_{ol,poly} + (1.3V_{pore}^2 - 0.3V_{pore}^3)(D_{ol,pore} - D_{ol,poly}) \quad (2.32)$$

Here,  $D_{ol,poly}$  is the diffusion coefficient of short chains in bulk polymer and  $D_{ol,pore}$ , the diffusion coefficient of short chain in liquid filled pores. The porosity based on the loss of short chains is

$$V_{pore} = \frac{R_{ol} - (C_{ol} - C_{ol,0})}{C_{e,0}} = \alpha \left(\frac{R_s}{C_{e,0}}\right)^\beta - \frac{C_{ol} - C_{ol,0}}{C_{e,0}} \quad (2.33)$$

The average molecular weight is calculated as a function of chain scission rate as follows

$$M_n = M_{n,0} \frac{1 - \alpha \left( \frac{R_s}{C_{e,0}} \right)^\beta}{1 + N_{dp,0} \left( \frac{R_s}{C_{e,0}} - \frac{\alpha}{m} \left( \frac{R_s}{C_{e,0}} \right)^\beta \right)} \quad (2.34)$$

where  $M_{n,0}$  is the initial molecular weight of the polymer and  $N_{dp,0}$ , the initial degree of polymerisation.  $N_{dp,0}$  can be defined as average number of ester units per polymer chains.

The studies of the Pan and co-workers reviewed so far tends to fill gaps in the literature by providing a clear picture of polymer degradation and considers the autocatalytic effect arising from dissociation of carboxylic ends. Further, the group used the established phenomenological model to explain the behavior of various physical systems including beams, stents and scaffolds. However, use of degradation equations to explain drug release from biodegradable polymers are missing.

### 2.3 Review of drug release models in the literature

The mathematical models on polymeric drug delivery can be categorised based on their release mechanisms i.e. diffusion controlled systems (diffusion from non-degraded polymers), swelling controlled systems and degradation controlled systems (release as a result of hydrolytic degradation, enzymatic degradation and erosion) (Ford Versypt *et al.*, 2013). These mechanisms are summarized in Fig. 2.4 for the sake of clarity. However, for the case of biodegradable polyesters such as PLA, PGA and their copolymers, drug release is mainly controlled by hydrolytic degradation and erosion. Therefore, in the current section, we will be only focusing on mathematical models from degradation-controlled systems.

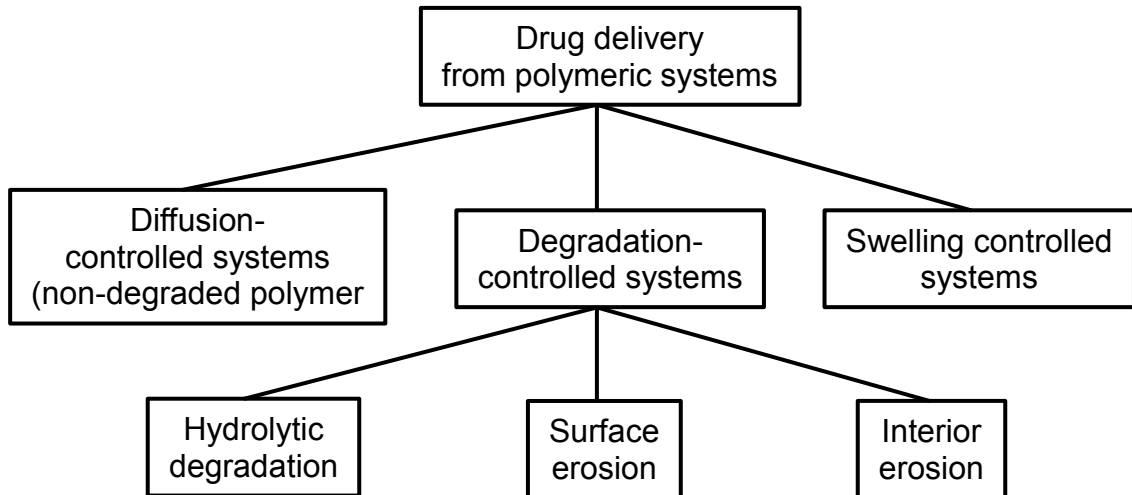


Fig. 2.4 Categorization of the mathematical models on drug delivery from polymeric systems

Degradation controlled systems can be further categorized as reaction-diffusion models and the cellular automata models (Arifin *et al.*, 2006a). The first category considers the combination of chemical reactions and the transport through by use of deterministic equations, whereas the second category treats degradation (hydrolytic degradation and erosion) as random processes by use of Monte-Carlo models. The cellular automata models can be applied to the systems degrading with hydrolytic degradation as well as the surface erosion and interior-erosion.

The most well-known mathematical model describing the drug release is perhaps the Higuchi equation (1961) which is first developed for planar systems and later extended to other geometries (Frenning and Strømme, 2003). The equation neglects the matrix swelling and degradation and assumes a constant diffusivity for drug and water. Drug release is given by the equation

$$\frac{M_t}{M_\infty} = f t^{0.5} \quad (2.35)$$

in which  $f$  is representing the geometric and structural properties of the device,  $M_t$  is the cumulative absolute amount of drug release and  $t$ , the time. This equation assumes drug release is a process which is purely diffusion controlled. A broader model has been adopted by Heller and Baker (1980) who argues that

permeability of the system enhances the drug release from non-degradable polymers such that

$$\frac{dM_t}{dt} = \frac{A}{2} \cdot \sqrt{\frac{2 c_d C_{drug,0}}{t}} \quad (2.36)$$

Here  $c_d$  is the permeability of drug within the matrix,  $A$  is the surface area of the samples and  $C_{drug,0}$ , the initial drug concentration in the matrix. The drug concentration is assumed to be below the solubility limit in the matrix. However, one of the major drawback associated with the proposed equation is that, permeability of the species in a biodegradable matrix is not a constant. Hellen and Baker correlated the drug permeability as a function of time.  $c_{d,0}$ , representing the initial drug permeability, the equation has been modified such as

$$\frac{c_d}{c_{d,0}} = \frac{C_{e,0}}{C_{e,0} - R_s} \quad (2.37)$$

Here the nominator at the right-hand side of the equation represents the initial number of ester bonds while denominator represents the remaining number of ester bonds. They explained the rate of polymer cleavage with first order kinetics such as

$$\frac{dR_s}{dt} = k(C_{e,0} - R_s) \quad (2.38)$$

where  $k$  represents first-order reaction kinetics. The rearrangement of the model leads to the following equation quantifying drug release from an eroding polymer in which drug concentration is above the solubility limit in the matrix

$$\frac{dM_t}{dt} = \frac{A}{2} \sqrt{\frac{2 c_{d,0} \exp(kt) C_{drug,0}}{t}} \quad (2.39)$$

Such modeling efforts, however, have failed to address the autocatalytic character of the biodegradable devices. This is an important underestimation since autocatalysis is one of the main mechanism controlling the degradation rate

of the polymers as stated before. Thombre and Himmelstein (1985), Joshi and Himmelstein (1991) addressed these issues in their models and developed a much comprehensive approach for drug release taking into account autocatalytic effect. In their model, water ingress into the matrix, hydrolyzing the acid generator such as an acid anhydride, and the generated acid is assumed to catalyze the chain cleavage. The chemical reactions then linked with the mass transfer equations. All the four species, water (A), the acid generator (B), acid (C) and drug (D) are considered to diffuse throughout the matrix. They used one single equation to explain diffusion of the four components such as

$$\frac{dC_i}{dt} = \frac{\partial}{\partial x} \left( D_i(x, t) \frac{\partial C_i}{\partial x} \right) + v_i \quad i = A, B, C, D \quad (2.40)$$

in which  $C_i$  and  $D_i$  represents the concentration and diffusion coefficient of each component,  $x$  the position and  $v_i$ , the rate of synthesis and degradation of components. Here, diffusion of the species is assumed to be only in one direction. To introduce the changing permeability of the system, they applied the following equation

$$D_i = D_{i,poly} \exp \left[ \frac{\mu (C_{d0} - C_d)}{C_{d0}} \right] \quad i = A, B, C, D. \quad (2.41)$$

Here,  $D_{i,poly}$  is the diffusivity of the species at fresh bulk polymer at  $t=0$ ; and  $\mu$  is a constant.

Their model was solved numerically and tested over experimental data to prove the effectiveness of the model. The model is fairly powerful to predict the mass loss and drug release behavior of the polymers loaded with the drug. The method also effectively involves the dependency of the diffusion coefficients to the dynamic structure of the polymer matrix. Additionally, some other models have been developed afterwards to link the diffusion coefficient of the species with the degradation kinetics. Couarraze *et al.* (2000) proposed a first order chain cleavage and assumed an exponential increase in the diffusion coefficient by time.

Another study by Zhang *et al.* (2003), characterizes the drug release by combining the drug dissolution, drug diffusion, and the hydrolytic chain cleavage. Degradation kinetics were assumed to follow the linear mode. A recent study by You *et al.* (2016) improved the model by Zhang *et al.* applying the power law and root types model in order to explain the drug release from surface eroding polymers. Their assumptions are: (1) the drug carrier is a microsphere, (2) drug has been uniformly distributed initially and (3) effective diffusion coefficients follows the percolation theory which assumes the effective diffusivity is only a function of changing porosity and diffusivity of the polymer. The governing equation is given by

$$\frac{\partial C_L}{\partial t} = D_{drug} \frac{1}{r^2} \frac{\partial}{\partial r} \left( r^2 \frac{\partial C_L}{\partial r} \right) + k_{dis} (\varepsilon C_{sat} - C_L) \quad (2.42)$$

in which  $C_L$  is the drug concentration in the liquid phase;  $C_{sat}$  is the saturation concentration;  $r$ , the radius,  $\varepsilon$ , the porosity of the polymer,  $k_{dis}$ , the drug dissolution rate,  $D_{drug}$ , the effective diffusivity of drug dependent on the porosity and tortuosity of the matrix which is governed by

$$D_{drug} = D_{drug,poly} \frac{\varepsilon}{\tau}. \quad (2.43)$$

Here,  $D_{drug,poly}$  is the diffusion coefficient of drug in the fresh bulk polymer; and  $\tau$ , the tortuosity of the polymer. The model successfully links the power law mode and root type mode for a better representation of the release behaviour of eroding polymer microspheres. The model is fairly powerful to explain the drug release from surface eroding polymers.

Modelling the hydrolytic degradation as interlinked with erosion is significantly important for a better design of drug delivery devices, since, polyesters are susceptible to erosion as well as the hydrolytic degradation. With such an effort, Zhu and Braatz (2015) coupled degradation, erosion and drug release in a mechanistic approach to describe the drug release from PLGA microspheres. Polymer degradation is reflected as a first order model which is a straightforward way of representing the hydrolytic degradation. Erosion was modelled based on the method of moments, which is a statistical approach on estimation of the

parameters. The model was demonstrated for sirolimus release from stents, which matches well with the experimental studies. Model seemed to be useful to include effective diffusivities, drug hydrophobicity and porosity change successfully, however, one major drawback of this approach is that, hydrolytic degradation and erosion behaviours are represented with analytical equations, which is far from covering the underlying physics.

So far, in the current section, we provided the drug release models considering the real physicochemical phenomena. However, as mentioned at the beginning of the section, the drug release can also be explained by probabilistic degradation models. Monte-Carlo models are known to be most desirable probabilistic approach to quantify the drug release. Most of the Monte-Carlo models quantifying drug release are already discussed in Section 2.1.3. Therefore, they will not be discussed further here. However, it is necessary to assess one of the main limitation of the Monte-Carlo models to be used in drug release systems: the autocatalysis mechanism cannot be accounted for in such models. As the autocatalysis mechanism is significant for PLA/GA systems, this oversimplification makes pure Monte-Carlo models non-justifiable. In order to include this point, Monte-Carlo models are needed to be coupled with autocatalytic reaction-diffusion equations.

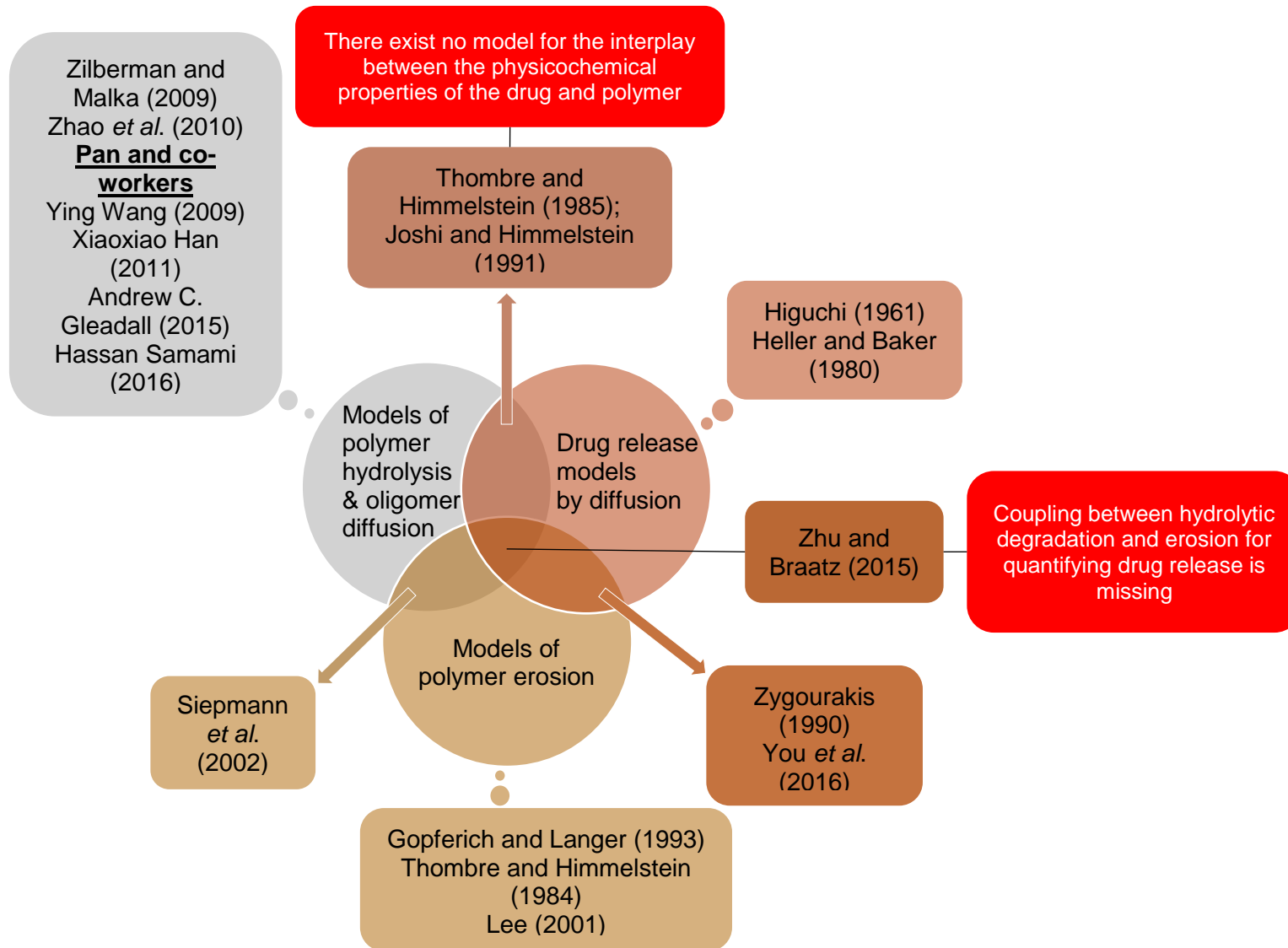


Fig. 2.5 A literature map showing the state-of-the-art of the current research and the research gap which is the matter of this thesis

## 2.4 Remaining challenges in the literature

Mathematical models for polymer degradation have been established in the previous works. However, a major gap is that drug release has not been appropriately embedded into these models. The issues can be summarized as follows:

- The previous work by Pan and co-workers provides a solid foundation for modelling hydrolytic degradation; however, the incorporation of a drug release into the degradation mechanism is missing.
- There exist no model for the interplay between the physicochemical properties of the drug and polymer.
- There is a lack of models and theories describing polymer erosion.
- Coupling between hydrolytic degradation and erosion is missing.
- Current Monte-Carlo models for polymer do not consider autocatalysis.
- There exist no model linking reaction-diffusion equations with statistical erosion models for drug release.
- Current hydrolytic degradation models fail to predict the drug release from drug eluting stents since the drug release follows biphasic or multiphasic trend in these systems.

## 2.5 Research objectives

The overall objective of this thesis is to address the gap highlighted above. The tasks required to achieve the overall objective lead to the formulation of the four specific objectives:

- To develop reaction-diffusion models for drug release considering different type of drug-polymer interaction such as the interaction between acidic drug-polymer and basic drug-polymer.
- To further understand the link between hydrolytic degradation and erosion mechanisms of polymers.
- To develop a combined reaction-diffusion and erosion model and present how each involved mechanism influences the mass loss profiles.

- To modify the combined reaction-diffusion and erosion model to quantify drug release from drug eluting stents.

## 2.6 Structure of the thesis

This thesis contains three main parts. In the first part (i.e. chapters 1 and 2), background information is discussed and the existing literature is reviewed. In the second part (i.e. chapters 3 and 4), mathematical models are developed which quantifies drug release from PLA/GA polymers. These models are then compared with the experimental data from the literature. In the third part (i.e. chapters 5 to 8), a constitutive mathematical model is developed combining hydrolytic degradation with erosion. The model is then further improved for the case drug eluting stents.

Each chapter in this thesis covers different issues highlighted above. Since all these issues cover a wide range of areas, a separate introduction and literature review is also provided at the beginning of each chapter.

Thesis part one; background information and literature review:

**Chapter 1** discusses the existing theory for biodegradable and bioerodible polymers as well as controlled drug release systems. The mechanisms of biodegradation, erosion and controlled drug release systems are also provided in the chapter.

In **Chapter 2**, a review of the previous mathematical models related to the kinetics of hydrolytic degradation, erosion and drug release is presented. Degradation models are categorized as the models before Pan and co-workers and by Pan and co-workers. All hydrolytic degradation equations which form a basis of the models developed in this thesis are provided in Chapter 2.

Thesis part two; mathematical models of drug release from PLA/GA polymers:

**Chapter 3** presents a reaction-diffusion model for polymer degradation which considers the further catalyst influence of acidic drugs on the polymer. The degradation models by Pan and co-workers are enhanced to include an acidic

drug term. The model results are compared with an experimental study from the literature to check the validity of the model. The model is then used to design two microsphere systems such that the drug release profiles follow zero order and burst release.

Similarly, **Chapter 4** provides a degradation model considering the complex interaction between basic drug and polymer. The degradation equations by Pan and co-workers are improved by considering the base catalyst term. The shielding between drug and polymer and the catalyst effects of free acidic and basic species are accounted in the model. Two independent case studies from the literature are reviewed and compared with the model results.

Thesis part three; modelling of hydrolytic degradation–erosion and its applications:

Many polymers undergo erosion after reaching a certain critical molecular weight. However, so far no attempt has been done to link hydrolytic degradation and erosion mechanisms of polymers. **Chapter 5** presents a combined hydrolytic degradation and erosion model to comprehend the two mechanisms together. Both of the interior and surface erosion mechanism are linked with the hydrolytic degradation model. Autocatalysis as a result of carboxylic chain ends of the polymer is also involved successfully into a Monte-Carlo model. The simulation results are further utilized to show the mass loss behaviour from independent mechanisms such as hydrolysis-diffusion, surface erosion and interior erosion.

In **Chapter 6**, the model provided in Chapter 5 is compared with independent case studies from the literature and the underlying mechanisms for each case are determined. The simulation results allow presenting the time dependent evaluation of polymer plates; which is also represented in the chapter.

In **Chapter 7**, the model provided in Chapter 5 is further developed to involve drug term. The simulations are conducted to understand the mechanisms of oligomer and drug release in a polymer. Model results are again compared with a case study from the literature.

**Chapter 8**, discusses the overall achievements and conclusion of the thesis as well as the recommended future work.

## **Part 2**

# **Mathematical models of drug release from PLA/GA polymers**

## Chapter 3. A mechanistic model for acidic drug release using microspheres made of PLGA

In this chapter, the mathematical model developed by Pan and co-workers (see Section 2.2), is extended to include the acidic drugs incorporation. Polymer degradation and drug release is simulated by use of the new model. The autocatalytic term is a function of local acidity gained by oligomer and drug dissociation. It is shown that the model is able to predict both polymer degradation and drug release profile and fits with the experimental data well. Finally, the model is used to design two systems of microspheres such that their drug release follows either a zero order or a burst release profile. By mixing the microspheres with different sizes, the desired release profiles can be achieved. The result of the current chapter has been published in *Molecular Pharmaceutics* (Sevim and Pan, 2016).

### 3.1 Introduction

Poly(lactic acids) (PLAs), poly(glycolic acid) (PGAs) and their copolymers are widely used for drug delivery applications because of their improved biocompatible properties (Klose *et al.*, 2008). For polymer-based delivery systems, there can be one or more important phenomena controlling drug release from the particles including drug diffusion, matrix degradation, swelling, polymer dissolution and erosion (Arifin *et al.*, 2006b). Generally, a combination of the mentioned mechanisms is responsible for drug release depending on drug and polymer type. For biodegradable devices made of PLA, PGA or PLGA, drug release is mainly governed by degradation and diffusion simultaneously.

There are a series of published papers on the degradation rate of polyesters with dispersed drug particles (Klose *et al.*, 2008, Perale *et al.*, 2009, Raman *et al.*, 2005, Siegel *et al.*, 2006). Many of them observe that the acidic-basic character of incorporated drugs can considerably alter the degradation rate. For basic drugs incorporation, there can be two opposing effects: a basic drug can enhance degradation, behaving as a catalyst (Cha and Pitt, 1989) or diminish degradation

as a result of the drug-polymer interaction (Bodmeier and Chen, 1989). The mathematical model for basic drug incorporation is presented in Chapter 4. In the case of acidic drugs incorporation, experimental studies agree on the accelerating influence of drugs on degradation rate. This influence has been monitored either by examining the displays of polymer structure for blank or loaded polymers (Tang and Singh, 2008), or comparing the molecular weight changes between blank and loaded polymers (Klose *et al.*, 2008). However, to date, there has been no mathematical model that considers the catalyst impact of acidic drugs on the rate of degradation. The existing models in the literature are straightforward to capture drug release and changes in polymer properties. However, they do not consider the effect of drug properties on the degradation rate of polyester particles. Therefore, there is a need for a more detailed diffusion reaction models to overcome the limitations of the literature work.

Pan and his coworkers (Han *et al.*, 2010, Wang *et al.*, 2008) proposed a mathematical framework for modeling the degradation rate by considering the effect of autocatalysis on degradation. In this chapter, the mathematical model by Pan *et al.* is extended to the case of acidic drug incorporation to simulate polymer degradation and drug release. Here, the autocatalytic term is a function of local acidity gained by oligomer and drug dissociation. Microspheres were chosen as dosage forms in this study. Such forms are generally used for controlled drug delivery in either local applications such as injection of drugs into some specific sites or oral drug delivery of easily degraded drugs (Ramteke *et al.*, 2012). Ibuprofen-loaded PLGA microspheres can be used in both ways. In the current study, we focus on local applications such as intra-articular administration. Nevertheless, in the case of oral uptake, most absorption occurs in the small intestine because the gastric emptying time is very short in comparison with the drug release time (Wilson and Crowley, 2011). The protons absorbed by the particles in this short period is released quickly by diffusion once they enter the intestine system. Consequently, the low pH in the stomach has little effect on the particle degradation and drug release. It is shown that the model is able to predict the in-vitro data in the literature.

### 3.2 The mathematical model

Fig. 3.1 shows schematically a polyester microsphere loaded with drugs that are considered in the current paper. The degradation behavior of polyester matrix is modeled considering three mechanisms:

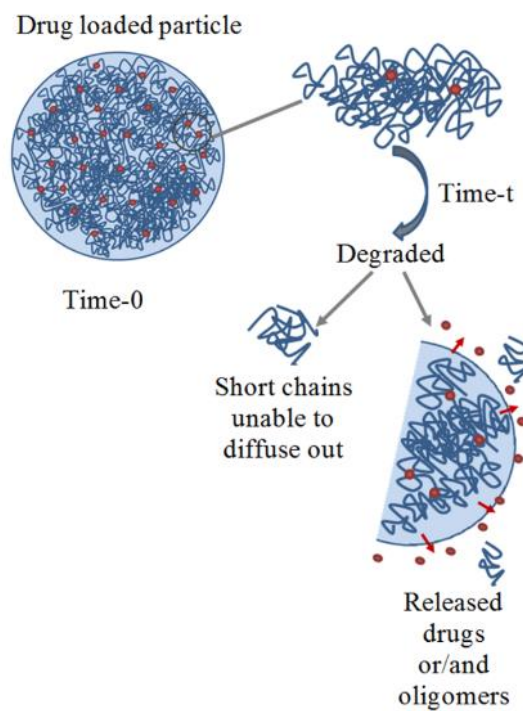


Fig. 3.1 Schematic illustration of drug and oligomer release from a drug-loaded microsphere

- 1) The hydrolysis reaction between ester bonds and penetrated water molecules
- 2) The autocatalytic effect arising from the carboxylic acid end groups of the oligomers
- 3) Further acid catalysis based on drug dissociation.

The hydrolysis reactions take place in the molecular scale whilst the transport process takes place in the device scale. As long polymer chains are broken into short chains, more and more carboxylic and alcoholic end groups are generated. Meanwhile, water dissolves the drug particles. The dissociation reaction of acidic drugs produce more proton, leading to a further increase in acidity. The

solubilized drug diffuses through the polymer matrix accelerating polymer degradation. The previous work by Pan and Chen (2015) demonstrated the autocatalytic effect of short chains on polymer degradation, which proved to be useful for elucidating the degradation mechanism of the blank polymer. For the acidic drug-loaded polymers, the autocatalytic effect is determined by the carboxylic acid groups of the oligomers and acidic drug molecules. The model presented in this chapter considers all these acidic sources which catalyze the hydrolytic degradation of polymers. It is assumed that the acid dissociation of oligomers and drugs are both instantaneous compared to the degradation and transport processes.

### 3.2.1 Extension of the autocatalytic term in polymer degradation model to account for acidic drugs

The phenomenological model presented in Section 2.2 is modified to separate the different acid sources: short chains and drug. Once an ester bond is broken, carboxylic and alcoholic end groups are formed. The carboxylic end groups have a high degree of acid dissociation to generate  $H^+$ ; their equilibrium reaction can be expressed as



in which  $R_1-COOH$  represents the chains with carboxylic ends. The anion formed when the carboxylic acid dissociates is called as carboxylate anion and is represented as  $R_1-COO^-$  in the equilibrium reaction. The acid dissociation constant for carboxylic end groups of polymer,  $K_a$ , can be expressed by

$$K_a = \frac{C_{H^+} C_{R_1-COO^-}}{C_{R_1-COOH}}. \quad (3.1)$$

Here,  $C_{R_1-COOH}$  and  $C_{R_1-COO^-}$  represent the concentrations of  $R_1-COOH$  and  $R_1-COO^-$  respectively. This reaction is fast and reversible and always in equilibrium. As stated before, oligomers are consist of  $m$  monomer units; which is general taken as 4. This has been determined by a widely accepted assumption that this level of short chains becomes water soluble (Gleadall et al., 2014). Using  $C_{ol}$  to

represent the current concentration of the short chains and  $m$  the average degree of polymerization of the short chains, the concentration of short chains as a function of oligomer concentration can be written as

$$C_{R_1-COOH} = \frac{C_{ol}}{m}. \quad (3.2)$$

For aliphatic polyesters, without any further internal or external proton source, the charge balance requires that  $C_{H^+} = C_{R_1-COO^-}$  and the equilibrium expression leads to  $C_{H^+} = (K_a C_{R_1-COOH})^{0.5}$  (Han *et al.*, 2010, Wang *et al.*, 2008). However, this is invalid when other proton sources, such as acidic drugs, are introduced into the polymer.

In a drug-loaded polyester, there are three possible sources of protons that can act as a catalyst for the hydrolysis reaction:

- 1) carboxylic acid end groups of the polymer chains
- 2) dissociation of acidic drug that gives rise to proton generation
- 3) pH of the buffer medium

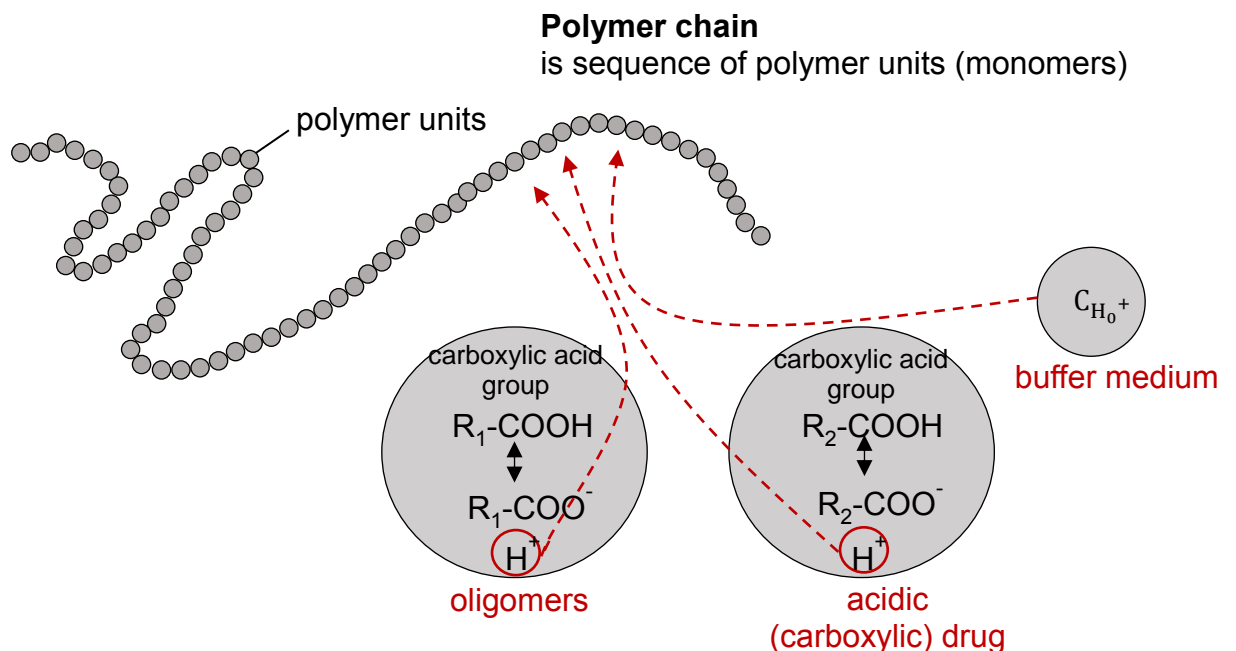


Fig. 3.2 Schematic representation of the possible proton sources

The equilibrium expression for the dissociation of short chains is given above. While carboxylic groups of short chains dissociate, the solid drug particles dissociate in the water concurrently to give an equilibrium solution containing a mixture of unionised molecules: carboxylate ions and  $H^+$ . To eliminate the confusion with the carboxylate ions of short chains, we will call this as anionic drug. The most common functional group conferring acidity to drugs is the carboxylic group (Cairns, 2012). The dissociation reaction for carboxylic drugs can be schematically written as



Here  $R_2-COOH$  is a general representation for carboxylic acid drugs.  $R_2$  can be any functional group including a benzene ring likewise in Ibuprofen or an ester functional group such as in Acetyl Salicylic Acid (ASA, Aspirin). Some other functional groups can also provide an acidic character to the drugs such as phenol groups (Cairns, 2012) and dissociation reaction can be modified to account for these different drugs. The  $H^+$  produced by drug dissociation is available as a further catalyst for the hydrolysis reaction. The acid dissociation constant for drug,  $K_{a,drug}$  can be expressed as

$$K_{a,drug} = \frac{C_{H^+} C_{R_2-COO^-}}{C_{R_2-COOH}}. \quad (3.3)$$

Here,  $C_{R_2-COOH}$  and  $C_{R_2-COO^-}$  represent the concentrations of  $R_2-COOH$  and  $R_2-COO^-$  respectively.

The proton concentration donated by the surrounding medium is referred to as  $C_{H_0^+}$  and the charge conservation requires that

$$C_{H^+} = C_{R_1-COO^-} + C_{R_2-COO^-} + C_{H_0^+}. \quad (3.4)$$

In our calculations,  $C_{H_0^+}$  is calculated assuming that the pH of the medium is 7.4. Arrangement of Eq. 3.1, 3.3 and 3.4, gives a second order quadratic equation. The only unknown of the equation is  $C_{H^+}$ . To be able to solve the quadratic equation, discriminant of the equation is calculated and checked whether it is

zero, positive or negative. Depending on the condition, the root of the quadratic equation was calculated. The root obtained is the local acidity,  $C_{H^+}$ , which is the input for Eq. 2.22. Thus, chains scission rate,  $R_s$ , can be calculated considering the all proton sources affecting the local acidity.

### 3.2.2 Diffusion equations of short chains and drug molecules

Both the short polymer chains and the dissolved drug molecules are capable of diffusion through the polymeric matrix. For the microspheres, these diffusions are spherically symmetric and transportation occurs only in the radial direction  $r$ . It is assumed that the diffusions follow the Fick's law such that

$$\frac{dC_{ol}}{dt} = \frac{dR_{ol}}{dt} + D_{ol} \left( \frac{1}{r^2} \right) \frac{d}{dr} \left( r^2 \frac{dC_{ol}}{dr} \right). \quad (3.5)$$

and

$$\frac{dC_{drug}}{dt} = \frac{dR_{drug}}{dt} + D_{drug} \left( \frac{1}{r^2} \right) \frac{d}{dr} \left( r^2 \frac{dC_{drug}}{dr} \right). \quad (3.6)$$

Here,  $C_{drug}$  ( $= C_{R_2-COOH}$  in Eq. 3.3) represents the current drug concentration,  $t$  the time,  $r$  the radius of the microspheres, and  $D_{ol}$  and  $D_{drug}$  the effective diffusion coefficients for the oligomers and drug molecules. The first term on the right-hand side of Eq. (3.5) represents the production rate of short polymer chains due to chain scission, and that of Eq. (3.6), the rate of drug dissolution. It will be seen in later part of this chapter that the drug release profile can be satisfactorily predicted using Fickian diffusion law.

The loss of short chains and drug molecules generates porosity inside the matrix, which leads to a significant increase in the diffusion coefficients. To reflect the dynamic structure of the polymer matrix, effective diffusion coefficients are used. In a previous study (Wang *et al.*, 2008), this was determined by use of finite element analysis of a representative 3-dimensional cubic material. A randomly distributed second phase is introduced and effective diffusion coefficient of the material was calculated. The details of their numerical approach can be found in the reference study (Wang, 2009). A similar approach is applied when calculating the effective diffusion coefficient of drug. Therefore, variable effective

diffusivities,  $D_{ol}$  and  $D_{drug}$ , are used in the equations based on the diffusion coefficient of in the bulk polymer and the pores as discussed in the work by Pan *et al.* (2014)

$$D_{ol} = D_{ol,poly} + (1.3V_{pore}^2 - 0.3V_{pore}^3)(D_{ol,pore} - D_{ol,poly}). \quad (3.7)$$

and

$$D_{drug} = D_{drug,poly} + (1.3V_{pore}^2 - 0.3V_{pore}^3)(D_{drug,pore} - D_{drug,poly}). \quad (3.8)$$

in which  $D_{ol,poly}$  and  $D_{drug,poly}$  denote the diffusivities of oligomers and drug molecules in the fresh bulk polymer,  $V_{pore}$ , the total porosity, and  $D_{ol,pore}$  and  $D_{drug,pore}$  the diffusion coefficients of oligomers and drugs in liquid-filled pores respectively. In this study  $D_{ol,pore}$  and  $D_{drug,pore}$  are simply taken as 1000 times of their counter parts in the fresh bulk polymer as suggested by Wang *et al.* (2008).

The porosity in the polymer is due to the loss of oligomers and drugs. The volume fraction of pores due to loss of oligomers can be calculated as

$$V_{pore,ol} = \frac{R_{ol}}{C_{e,0}} - \frac{C_{ol}}{C_{e,0}}. \quad (3.9)$$

The volume fraction of pores due to loss of drug can be calculated by the fraction of drug released from the matrix, which is

$$V_{pore,drug} = 1 - \frac{C_{drug}}{C_{drug,0}}. \quad (3.10)$$

The total porosity,  $V_{pore}$ , is contributed by the loss of oligomers and drug and can be calculated using

$$V_{pore} = V_{pore,ol} (1 - f_{drug}) + V_{pore,drug} f_{drug}. \quad (3.11)$$

where  $f_{drug}$  is volume ratio of drug to the polymer phase and  $(1-f_{drug})$ ; the volume ratio of oligomers to the polymer phase.

Finally, the number averaged molecular weight of the polyester at any particular location can be calculated as (Pan, 2014)

$$M_n = M_{n,0} \frac{1 - \alpha \left( \frac{R_s}{C_{e0}} \right)^\beta}{1 + N_{dp0} \left( \frac{R_s}{C_{e,0}} - \frac{a}{m} \left( \frac{R_s}{C_{e,0}} \right)^\beta \right)} \quad (3.12)$$

where  $M_{n,0}$  is the initial molecular weight of the polymer;  $N_{dp,0}$  is the average degree of polymerization.

### 3.3 The numerical procedure

In the current section, boundary conditions and the details of the numerical scheme is provided. The initial conditions of the microsphere are given by

$$\begin{aligned} R_s(r, 0) &= 0 \\ C_{ol}(r, 0) &= C_{ol,0} = 0 \\ C_{drug}(r, 0) &= C_{drug,0}. \end{aligned} \quad (3.13)$$

and the boundary conditions (concentrations at particle surface) are assumed as:

$$\begin{aligned} C_{ol} &= 0. \\ C_{drug} &= 0. \end{aligned} \quad (3.14)$$

For initial drug concentration, two special cases are considered. In the first case, the drug loading is below the solubility limit. An infinite dissolution rate for the drug molecules is assumed and the initial drug concentration is simply taken as the drug loading. This can be schematically represented as

$$\text{If } \frac{V_{drug}}{V_{unit}} < C_s \text{ then } C_{drug,0} = \frac{V_{drug}}{V_{unit}}. \quad (3.15)$$

In the second case, the drug loading is above the solubility limit, the drug dissociation rate becomes a limiting factor (Wise, 2000, Xiang and McHugh,

2011). In this case, the initial drug concentration is taken as the solubility of the drug which can be represented as

$$\text{If } \frac{V_{drug}}{V_{unit}} > C_s \text{ then } C_{drug,0} = C_s. \quad (3.16)$$

It is assumed that drug dissolution is instantaneous and the drug concentration at any  $r$  remains at  $C_s$  until all loaded drug at that location has dissolved.

Equations 2.19 and (3.1-3.16) form the complete mathematical model for polymer degradation and drug release. Applying the initial and boundary conditions, these equations are solved numerically using the central finite difference method (Smith, 1965). The direct Euler scheme was used for the time integration. A particle radius was discretized into 100 finite difference nodes. The grid size (Fig. 3.3) was found to be  $\Delta r=0.000525\text{mm}$ . The time step length was found to be  $\Delta t=2.7\text{s}$ , which ensures convergence both for blank and loaded microspheres. Numerical convergence was ensured by increasing the number of finite difference nodes and reducing the time step length such that no change in the numerical solution can be found. Fig. 3.4 shows the algorithm flow chart for the model developed in this chapter. The computer program is written in FORTRAN 90 (see Appendix A). The computational time for complete solution takes less than 10min on the desktop PC by use of Microsoft Visual Studio 2010 as an integrated development environment (IDE).

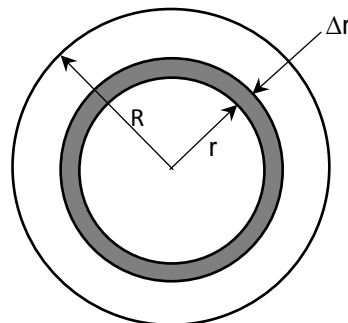


Fig. 3.3 A schematic illustration of the grid size

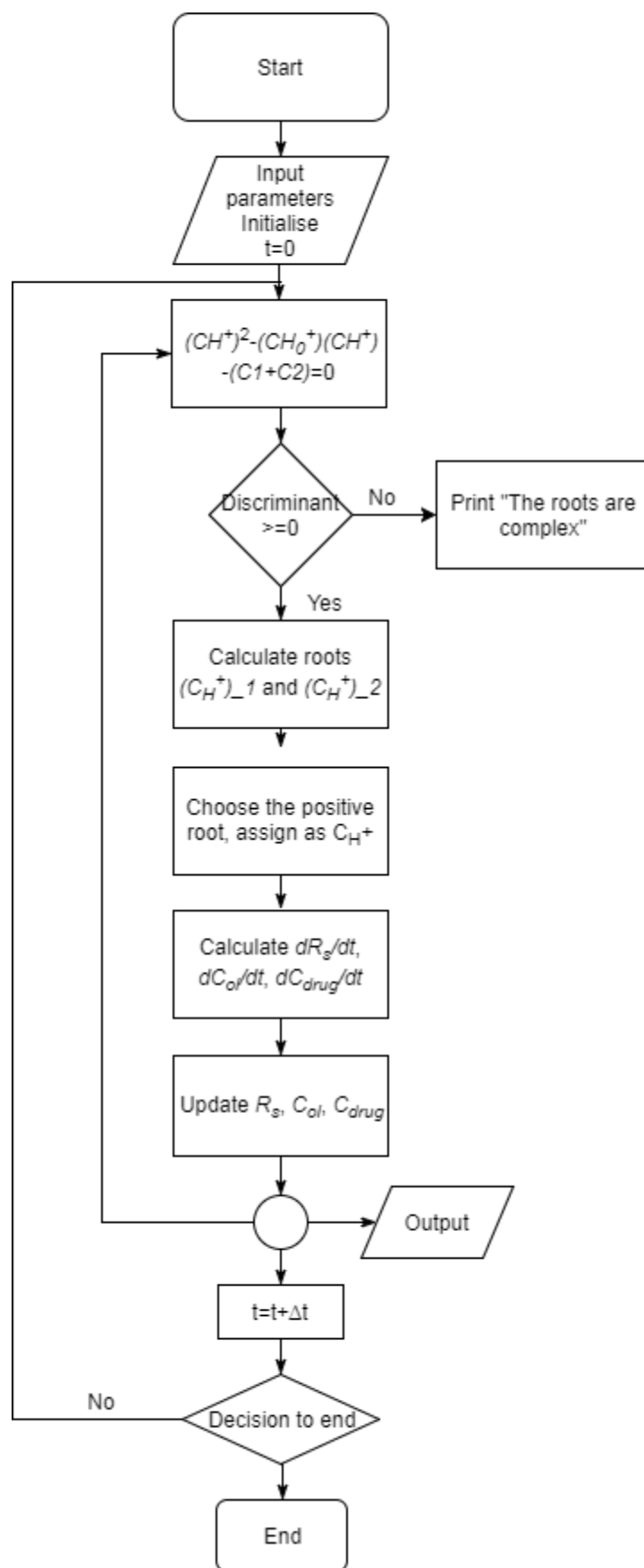


Fig. 3.4 Flow chart for the model in the presence of acidic drugs

### **3.4 Comparison between model prediction and experimental data obtained in the literature**

Siepmann *et al.* (2005) and Klose *et al.* (2008) carried out a set of experiments using microspheres made of PLGA 50:50 in phosphate buffer (pH 7.4) at 37 °C. Here their experimental data are used to test the model presented in Section 3.2. A common set of parameters in the model of polymer degradation is used for both blank and drug-loaded samples. The following experimental data are taken from their papers:

- average molecular weight as a function of time for blank microspheres undergoing autocatalytic degradation (Siepmann *et al.*, 2005)
- average molecular weight as a function of time for the acidic drug (ibuprofen) loaded microspheres undergoing autocatalytic degradation
- ibuprofen release from microspheres (Klose *et al.*, 2008)

Fig. 3.5 presents the comparison between the model prediction and experimental data for average molecular weight changes of blank microspheres. Two different sizes are used in the comparison. The kinetic parameters of the model used in the model prediction are summarized in Table 3.1.

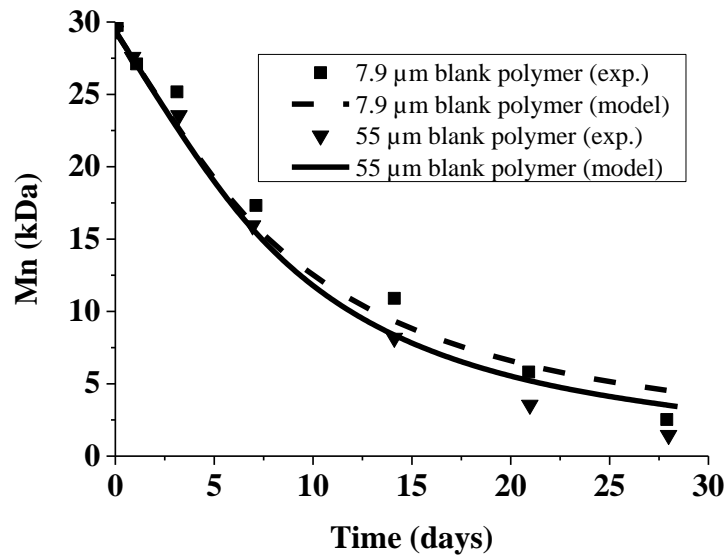


Fig. 3.5 Comparison between model prediction and experimental data for blank particles with different sizes. The dashed and solid lines represent the model predictions for microspheres of the average size of  $r = 7.9\mu\text{m}$ , and  $55\mu\text{m}$  respectively. The discrete symbols represent the experimental data (Siepmann *et al.*, 2005).

Table 3.1 Model parameters used for the predictions

Model parameters (units)	Value
$C_{e,0}$ (mol/m <sup>3</sup> )	20615
$C_{o,0}$ (mol/m <sup>3</sup> )	0
$M_{unit}$ (g/mol)	65 g/mol*
$M_{n0}$ (g/mol)	29000-35000
$m$	4
$\alpha$	0.4
$\beta$	1.0
$K_{a,ol}$	$1.35 \times 10^{-4}$
$D_{ol,poly}$ (m <sup>2</sup> /week)	$1 \times 10^{-12}$
$D_{ol,pore}$ (m <sup>2</sup> /week)	$1000 \times D_{ol,0}$
$k_1$ (1/week)	$8 \times 10^{-4}$
$k_2$ ( $\sqrt{\text{m}^3 / \text{mol} / \text{week}}$ )	$1 \times 10^{-1}$

\*  $M_{unit}$  is the molar mass of PLGA taken as the average of PLA and PGA

Fig. 3.6 shows the comparison between model prediction and experimental data for average molecular weight changes over time. Drug-free and drug-loaded PLGA microspheres are used in the comparison. The following drug-related parameters were used in the predictions:  $K_{a,drug} = 6.3 \times 10^{-6}$ ,  $D_{drug,0} = 1.5 \times 10^{-10}$  m<sup>2</sup>/week, drug loading = 4% w/w and  $D_{drug,pore} = 1000 \times D_{drug,0}$ . This level of drug

loading is below the solubility limit of the drug in the polymer. All the other parameters are common for the blank and loaded microspheres (see Table 3.1).

Compared to the drug free microspheres, ibuprofen loaded PLGA microspheres exhibit significantly faster degradation pattern. In a drug-loaded microsphere, 50% of the initial molecular weight has been reached at 4 days, while it is 7.5 days for drug free microspheres. The enhanced rate of degradation is attributed to the decreased micro pH based on the acidic drug dissociation. The individual contributions of drug and oligomers on the proton concentration are compared in Fig. 3.7 through the degradation process. It can be seen that at the early stage of degradation, most of the proton is dominated by the acidic drugs while the contribution of the short chains are insignificant. As more and more drugs are released and short chains are produced, the order is switched and short chains start to dominate on the proton concentration. It is worth noting that the calculations used the disassociation constants,  $K_{a, drug}$  and  $K_a$ , which are taken from independent literature (Pan *et al.*, 2011, Loftsson and Brewster, 1996).

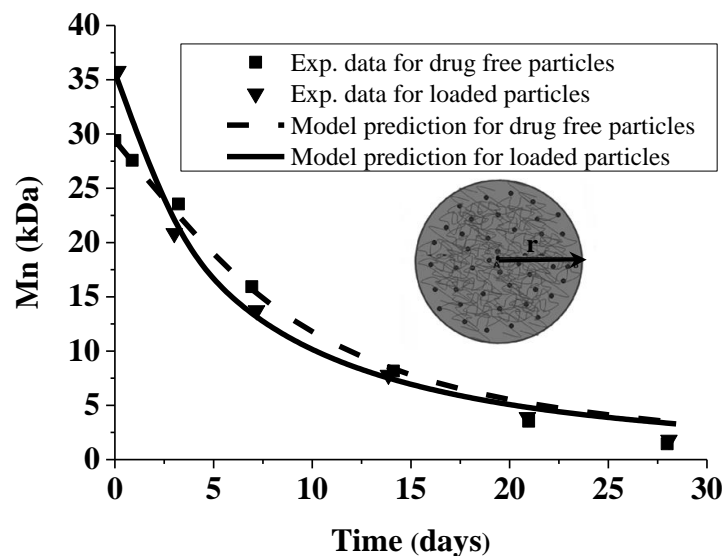


Fig. 3.6 Comparison between model prediction and experimental data for degradation of blank and ibuprofen-loaded PLGA microspheres. The dashed and solid lines represent model predictions for drug-free and drug-loaded particles respectively. The discrete symbols represent the experimental data (Klose *et al.*, 2008, Siepmann *et al.*, 2005).

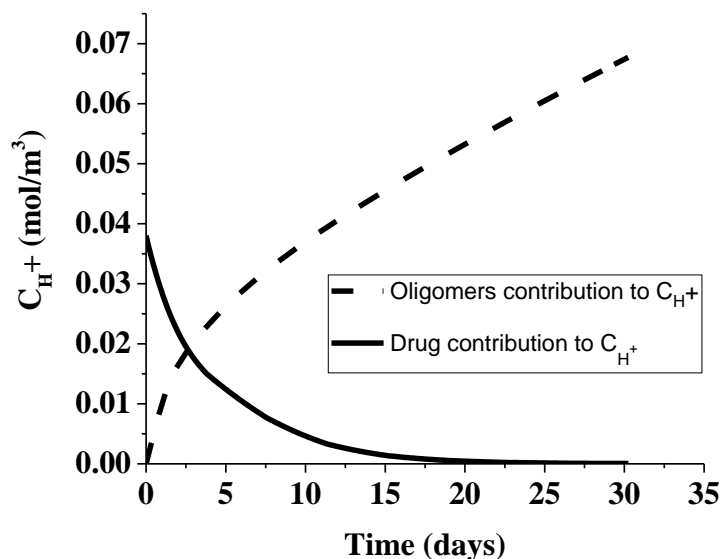


Fig. 3.7 Independent contributions of drug and oligomers to the proton concentration throughout the degradation process.

Fig. 3.8 shows the comparison between the model prediction and experimental data for drug release profile. The drug release from PLGA microspheres is mainly governed by diffusion in the bulk polymer through the generated porous channels which are a product of degradation. It can be observed from the figure that Fickian diffusion is able to predict the drug release profile well. However, the effective diffusivity increased significantly with polymer degradation, as shown in Fig. 3.9, which has to be considered in the model. To demonstrate this key issue, drug release calculated using a constant diffusion coefficient is also presented in Fig. 3.7 for comparison. As seen from Fig. 3.7, using a constant diffusion coefficient would predict 28 days for the complete drug release as opposed to about 10 days when the variable diffusion coefficient is used.

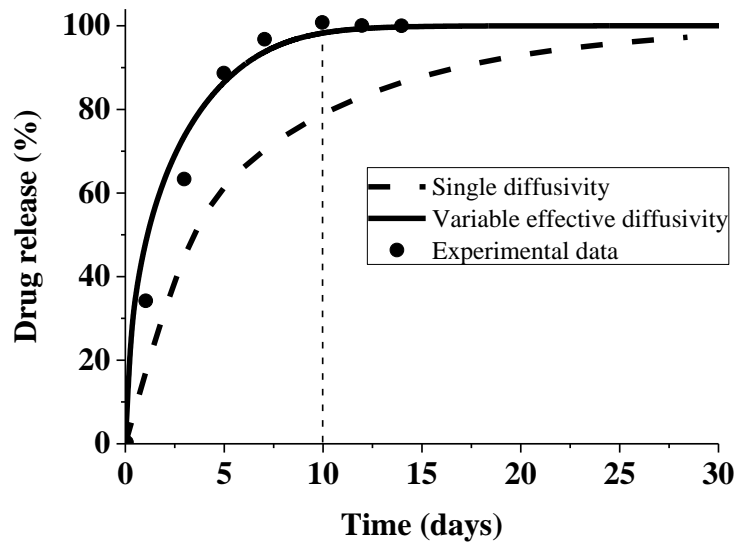


Fig. 3.8 Comparison between the model prediction (solid line) and experimental data (Klose *et al.*, 2008) (discrete symbols) for drug release. The dashed line is model prediction using a constant drug diffusion coefficient. The size of the microsphere is  $52\mu\text{m}$ .

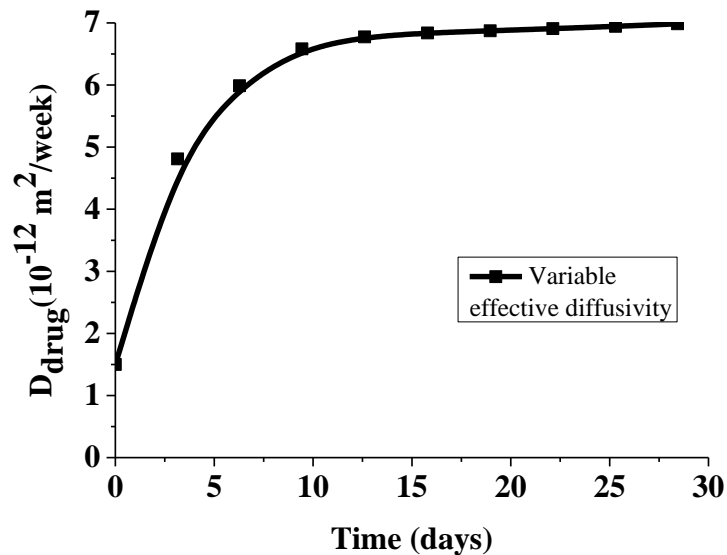


Fig. 3.9 Variable diffusivity of ibuprofen calculated using Eq. 18 for micro-particle of  $r = 52\mu\text{m}$ .

By observing Fig. 3.5, Fig. 3.6 and Fig. 3.8, it can be concluded that the mathematical model presented in the current chapter is able to predict the experimental data both for polymer degradation and drug release. In our calculations, the model parameters were determined by varying them over a range to obtain the best prediction. The hydrolysis rate constants,  $k_1$  and  $k_2$ , in Table 3.1 are determined using the blank polymer data as shown in Fig. 3.5. It is worth highlighting that the model is able to predict the degradation behavior of drug loaded polymers using the rate constants obtained by using the blank polymers.

### **3.5 Design of microspheres to achieve desired profile of drug release**

Over the years, various release systems have been explored both experimentally and computationally to obtain a stable release profile. In many of the controlled release formulations, zero order release profile is desirable in order to maintain a constant drug concentration over time. This is because, the burst effect in ordinary drug delivery systems may result in toxicity and some other side effects (Berkland *et al.*, 2002, Huang and Brazel, 2001). Even if no harm is done during the burst, an excess amount of drug is wasted and this can result in some economic concerns. Drug release from polyester microspheres depends on parameters such as the microsphere diameter and drug loading. Guided by a simple analysis, Berkland *et al.* (2002) showed that a zero order release profile can be achieved by mixing two different microspheres which have concave and convex release profiles respectively. Taking inspiration from the study by Berkland *et al.* (2002) and Narayani and Panduranga Roa (1996) we demonstrate that the mathematical model presented in this chapter can be used to design such systems.

Fig. 3.10 presents the schematic representation of the microspheres resulting zero order release profile when mixed in appropriate portions. Fig. 3.11 shows the drug release from individual microspheres presented in Fig. 3.10, as well as the release when two type of microspheres mixed in 1:2 (w/w) ratio. A convex, concave and nearly zero-order release profiles are obtained, all calculated using

the mathematical model and the parameters that were used in the current chapter. The convex release profile was obtained by using microspheres of  $75\mu\text{m}$  in radius with a drug loading of  $400\text{ mol/m}^3$ . The outer layer of the sphere with a thickness of  $0.2r$  was not loaded with any drug. This outer layer can be considered as a drug-free coating that retards the initial drug release. The concave release profile was obtained by using microspheres of  $150\mu\text{m}$  in radius with the same drug loading. The outer layer of the sphere with a thickness of  $0.6r$  was not loaded with any drug. Such a thick coating prevents drug release in the initial stage and hence produced the convex release profile. The nearly zero release profile was obtained by mixing the two types of spheres with 1:2 (w/w) ratios of the thinly coated microspheres (concave profile) over the thickly coated microspheres (convex profile).

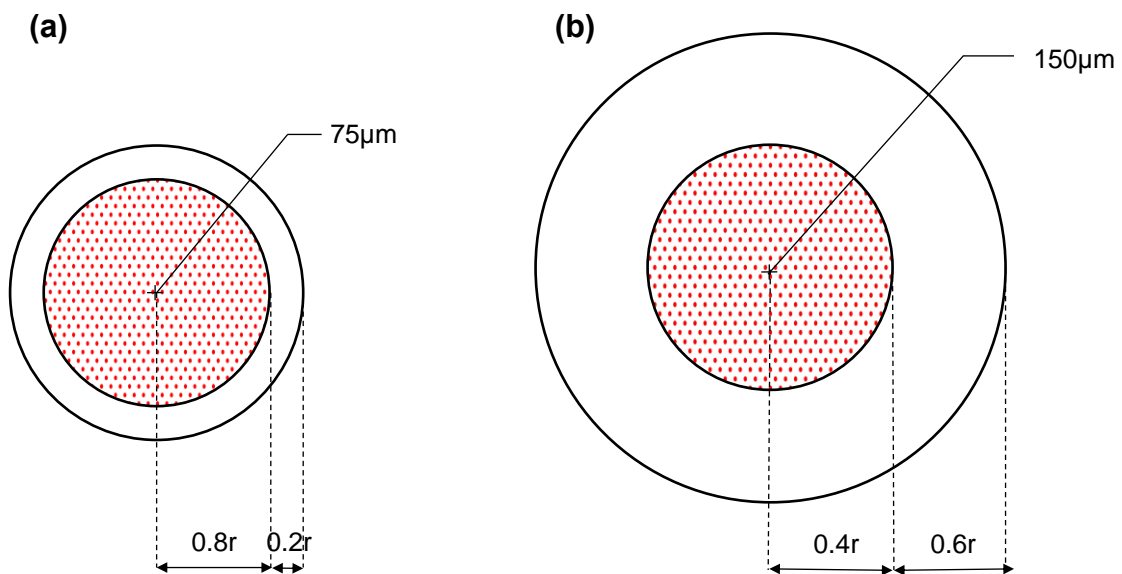


Fig. 3.10 Schematic representation of the microspheres resulting zero order release profile in the mixture when mixed 1:2 (w/w) ratio of (a) over (b). (a)  $75\mu\text{m}$  in radius with drug loading of  $400\text{ mol/m}^3$  and a drug free outside layer of  $0.2r$  ( $15\mu\text{m}$ ), (b)  $150\mu\text{m}$  in radius with a drug loading of  $400\text{ mol/m}^3$  and a drug free outside layer of  $0.6r$  ( $90\mu\text{m}$ ).

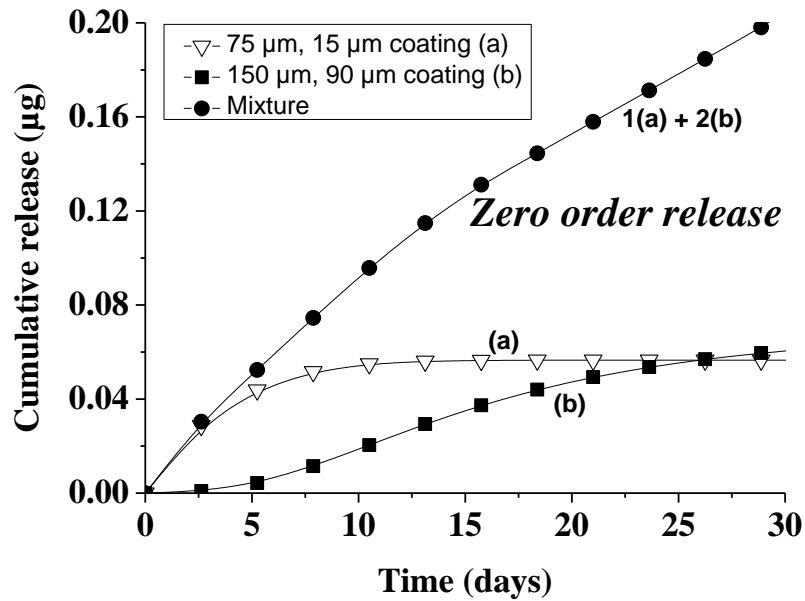


Fig. 3.11 Calculated profiles of drug release using microspheres of (a) 75µm in radius with drug loading of 400 mol/m<sup>3</sup>and a drug free outside layer of 0.2r, (b) 150µm in radius with a drug loading of 400 mol/m<sup>3</sup>and a drug free outside layer of 0.6r and (c) mixture of (a) and (b) with 1:2 (w/w) ratio of (a) over (b).

The long term linear release of drug from particles was crucial in most of the applications. However, in some particular cases, an initial burst release followed by a linear release may be required, likewise in wound treatment. Because of the fact that burst happens in a quite short time compared to the all release process, it cannot be well controlled, and it has been discounted in most of the mathematical models in the literature (Huang and Brazel, 2001). In this study, we proposed a mechanism to control the burst release.

Fig. 3.12 shows the schematic representation of the microspheres resulting a burst release profile when mixed in appropriate portions. Fig. 3.13 presents the drug release from individual microspheres presented in Fig. 3.12, as well as the release when two type of microspheres mixed in 1:2 (w/w) ratio. A convex, concave and burst followed by zero order release profile were obtained, all calculated using the mathematical model. The convex release profile was obtained by using microspheres of 75µm in radius with a uniform drug loading of 400 mol/m<sup>3</sup>. The concave release profile was obtained by using microspheres of

150 $\mu\text{m}$  in radius with the same drug loading. The outer layer of the sphere with a thickness of  $0.6r$  was not loaded with any drug. This is exactly the same as case (b) in Fig. 3.11. The burst followed by nearly zero release profile was obtained by mixing the two types of spheres with 1:2 (w/w) ratios of the uniformly loaded microspheres (concave profile) over the thickly coated microspheres (convex profile).

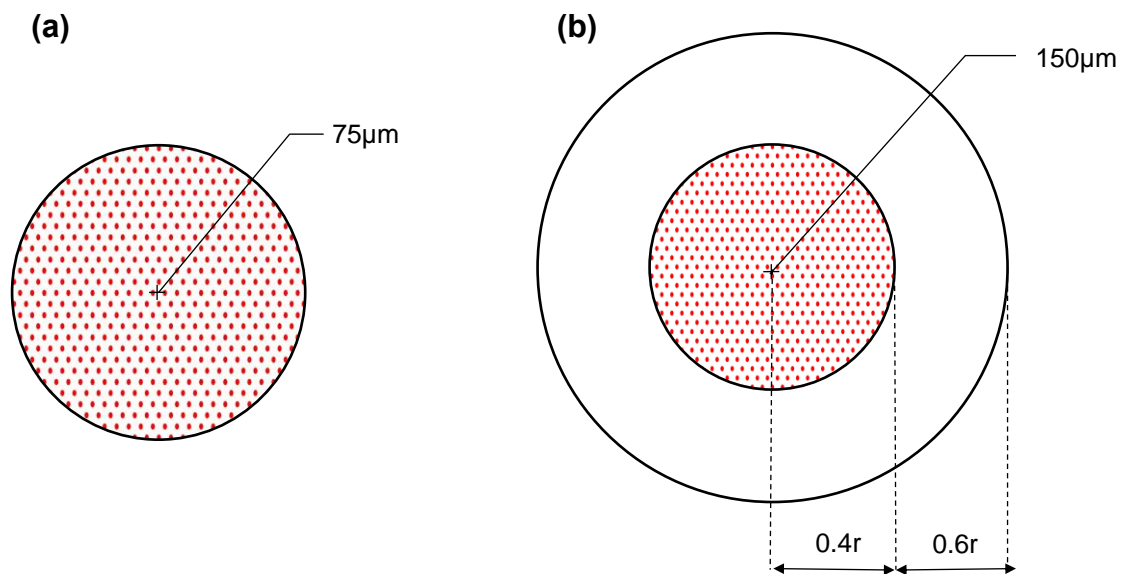


Fig. 3.12 Schematic representation of the microspheres resulting zero order release profile in the mixture when mixed 1:2 (w/w) ratio of (a) over (b). (a)  $75\mu\text{m}$  in radius with a uniform drug loading of  $400\text{ mol/m}^3$ , (b)  $150\mu\text{m}$  in radius with a drug loading of  $400\text{ mol/m}^3$  and a drug free outside layer of  $0.6r$  ( $90\mu\text{m}$ ).

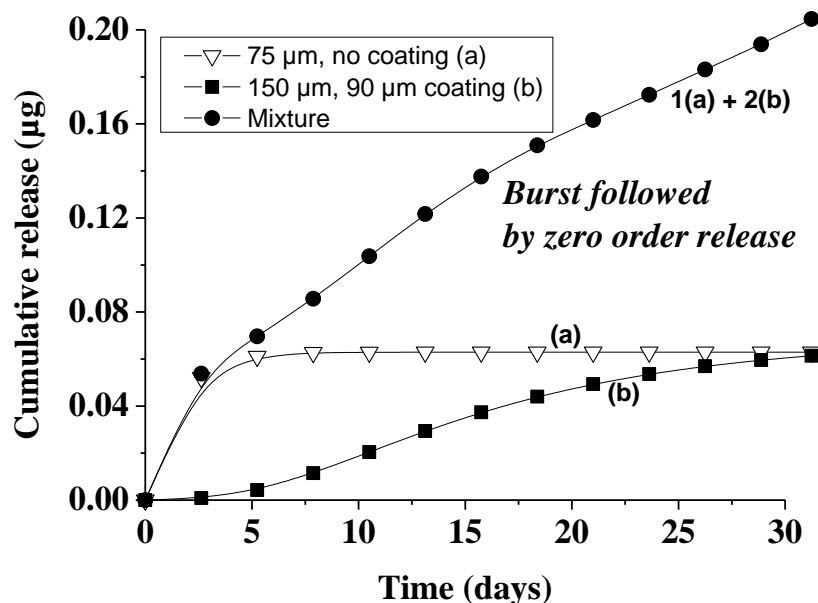


Fig. 3.13 Calculated profiles of drug release using microspheres of (a) 75µm in radius with a uniform drug loading of 400 mol/m<sup>3</sup>, (b) 150µm in radius with a drug loading of 400 mol/m<sup>3</sup> and a drug free outside layer of 0.6r and (c) mixture of (a) and (b) with 1:2 (w/w) ratio of (a) over (b).

### 3.6 Conclusions

A mechanistic-based mathematical model is presented which can be used to calculate the rate of hydrolytic degradation and drug release. The model is generally valid for all the geometries, although, microspheres are used in the chapter as a demonstrating example. The underlying assumptions in the mathematical model were motivated by experimental studies in the literature which demonstrated the influence of the acidic drug on autocatalysis of polyester devices. It is shown that the model can predict polymer degradation and drug release fairly well. Model results clearly indicated that, the presence of acidic drugs significantly accelerates the rate of degradation. A key element of the model is that the drug diffusion coefficient strongly depends on the polymer degradation. This study shows that without considering this interaction between acidic drug and polymer, it is unlikely to capture the observed profile of drug release. It is worth noting that the model is able to predict the degradation behavior of drug-loaded polymers using the kinetic constants for polymer

degradation obtained using blank polymers. Moreover, the model results were successfully implemented on the design of the microspheres to achieve desired profile of drug release. This was achieved by use of appropriate mixtures of uniform microspheres which have concave and convex release profiles. To demonstrate potential applications of the mathematical model, it is shown that the model can be used to design systems of microspheres of different sizes and patterns of drug loading to achieve zero order release or burst followed by zero order release. These systems will have significant practical implications for various applications.

## **Chapter 4. A mechanistic model for basic drug release using microspheres made of PLGA**

This chapter presents a mathematical model predicting the release profiles of basic drugs from biodegradable polyesters. The model calculates drug release and molecular weight reduction as functions of time. The full interactions between drug and polyester are taken into account as well as the effect of polymer degradation on the release rate. These include the attractive ionic interaction between basic drugs and polymer chain ends and the catalytic role played by the free acidic and basic species on the hydrolysis reaction. The model predictions satisfactorily match with different sets of experimental data from the literature, indicating that the model is able to describe the key phenomena governing the release of basic drugs embedded in degradable polymeric devices. The model can be used in the design of microsphere systems for targeted release as well as a tool to gain understanding in the underlying mechanisms responsible for the release of basic drugs. This chapter has been submitted to European Journal of Pharmaceutics and Biopharmaceutics.

### **4.1 Introduction**

The model developed in Chapter 3, based on previous work of Pan and his co-workers, allows investigating the effect of acidic drugs on the degradation rate. It was shown that the protons gained by drug dissociation accelerate the hydrolysis reaction. It is demonstrated that the model is able to fit with the experimental data for the change in the molecular weight, mass loss, and drug release. In this chapter, a mathematical model is presented which can explain the interaction between basic drugs and polymers. The mathematical model is used to relate the degradation behavior of polymers to the basic drug properties.

Unlike acidic drugs, there are contradicting reports in the literature for basic drugs. Several groups (D'Souza *et al.*, 2015, Klose *et al.*, 2008, Fitzgerald and Corrigan, 1996, Cha and Pitt, 1988, Cha and Pitt, 1989) have proposed that the incorporation of basic drugs increases the degradation rate, while others

(Miyajima *et al.*, 1998, Mauduit *et al.*, 1993a) have found a reduction in degradation rate with the incorporation. This divergence can be explained by the fact that basic drugs can act as a catalyst for the hydrolysis reaction, accelerating polymer degradation, and also shield carboxylic end groups, decelerating degradation rate. The relative dominance of one of the two mechanisms determines the observed behavior (Miyajima *et al.*, 1998, Mauduit *et al.*, 1993b, Proikakis *et al.*, 2006).

It has been also reported that, the interaction between the drug and polymer is critical in controlling drug release (Li *et al.*, 1996, Okada *et al.*, 1994). This is again because of the basic drugs ionically interacting with the polymer. Likewise the effects seen in polymer degradation, two opposing results are reported for how the properties of the basic drugs affect their own release rate (Miyajima *et al.*, 1999).

Literature provides a variety of mathematical models (Casalini *et al.*, 2014, Ford *et al.*, 2011b, Siepmann *et al.*, 2002, Thombre and Himmelstein, 1985) simulating the release profiles from a biodegradable matrix. However, the interaction between drugs and polymers has not been considered until our recent work, in which a mathematical model taking into account of the interaction was presented for polyesters loaded with acidic drugs (Sevim and Pan, 2016). In this chapter, the model is further extended for polyesters loaded with basic drugs. The shielding effect of basic drug molecules on the carboxylic end groups of the polymer chains is considered. A partition parameter is introduced to reflect the observed level of attachment of drug molecules to the carboxylic ends. The validity of the model is tested using an experimental data obtained from the literature. Microspheres are chosen as an example in this study but the model is generally valid for any drug-loaded device.

## 4.2 The mathematical model

The microparticles are modelled as microspheres that are spherically symmetric in which basic drug is uniformly distributed. It is assumed that the drug is physically entrapped into the microsphere. Due to symmetry the model only considers a radial coordinate, thus, matter transportation is assumed to occur in

the radial direction,  $r$ . All microspheres are assumed to have the same size. Once the microspheres are placed in a liquid medium, water molecules diffuse into the matrix and break the long polymer chains. Concurrently, water dissolves drug molecules. Drug dissolution is assumed as instantaneous compared to the degradation and the diffusion of oligomer and drugs. Chain scission reaction can be catalysed by both acidic and basic species. A proportion of drug interacts with the carboxyl ends of short chains and neutralizes their acidic effect, whilst the rest stays in free form to catalyse the hydrolysis reaction. On the other side, free short chains are also able to accelerate the hydrolysis reaction. To account for these opposing effects, a partition parameter is introduced in the model such that polymer degradation can either be accelerated or slowed down depending on the partition of drug molecules in free or attached form. The representation of the interaction between drug and polymer as well as the effect of free acidic and basic species on degradation rate is schematised in Fig. 4.1. The model considers transport of oligomers and drug through the polymeric matrix. Drug release is achieved by a combination of (i) diffusion of the drug molecules out of the spheres and (ii) the diffusion of drug molecules that are attached to the ends of the short chains. The water penetration into the polyester devices are rather fast compared to the other kinetic processes such as degradation and drug release. It is therefore assumed that water is always abundant in the polymer particles.

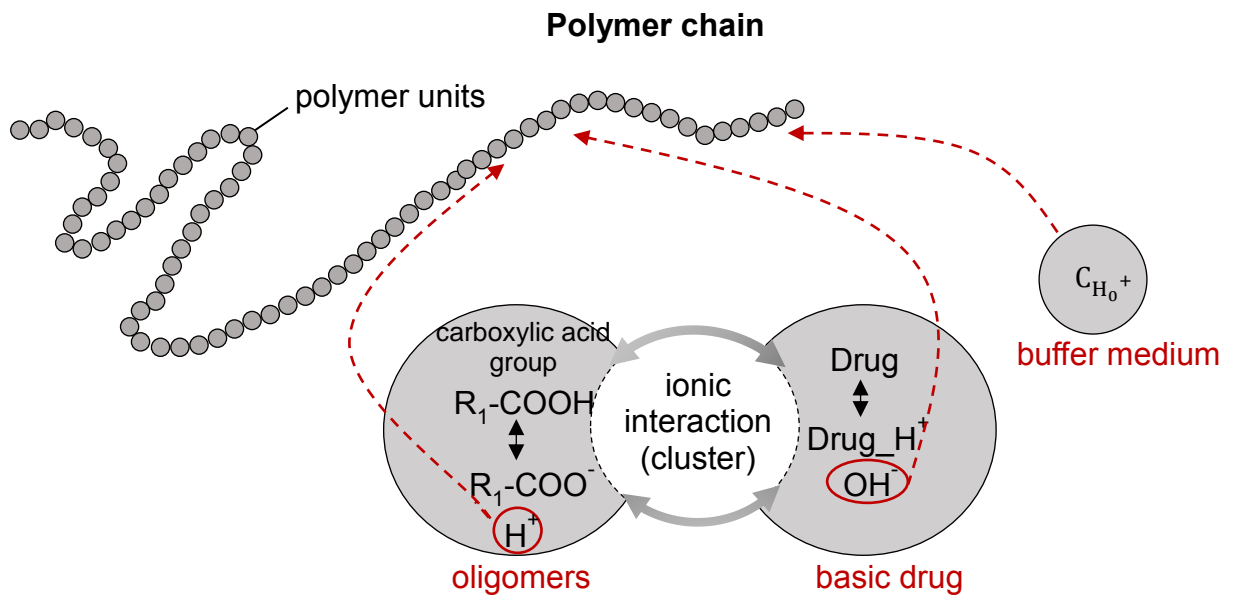


Fig. 4.1 Schematic representation of the interaction between basic drugs-oligomers and catalyst effect of the free species

#### 4.2.1 Rate of polymer chain scission

The phenomenological model by Leicester group, presented in Section 2.2, is modified to include the base catalytic random scission, autocatalytic random scission and non-catalytic scission. The polymer is assumed to consist of amorphous chains, the formation of crystalline phase is again excluded during the model development. It is assumed that water is abundant, therefore, its concentration does not affect the chain scission rate. The rate equation for chain scission in Pan's study (Pan, 2014) is extended such that

$$\frac{dR_s}{dt} = k_1 C_e + k_2 C_e C_{H^+} + k_3 C_e C_{OH^-}. \quad (4.1)$$

Here,  $R_s$ ,  $C_e$ ,  $C_{H^+}$  and  $C_{OH^-}$  represent the molar concentrations of chains scissions, ester bonds,  $H^+$  and  $OH^-$ ;  $k_1$ ,  $k_2$  and  $k_3$ , the non-catalytic, acid-catalyzed and base-catalyzed kinetic constants respectively. The third term on the right-hand side is newly introduced to take into account of catalyst effect of the basic species. Each chain scission generates either a short or long chain. The production rate of short chains and the concentration of ester bond are

provided in Eq. 2.20 and 2.21 in section 2.2, therefore, they will not be mentioned here. By use of Eq. 2.20 and 2.21 in Eq. 4.1, we have

$$\frac{dR_s}{dt} = C_{e,0} \left[ 1 - \alpha \left( \frac{R_s}{C_{e,0}} \right)^\beta \right] (k_1 + k_2 C_{H^+} + k_3 C_{OH^-}). \quad (4.2)$$

Breaking an ester bond results in the formation of a carboxylic and an alcoholic end groups. The dissociation of carboxylic end groups produces  $H^+$  which acts as a catalyst as presented in section 3.2.1. In their studies, Pan and his coworkers (Pan, 2014, Wang *et al.*, 2008) assumed that only the carboxylic end groups of the short chains act as the catalyst for the hydrolysis reaction. They showed that this assumption led to good fitting between the model prediction and the experimental data (Pan, 2014). The mole concentration of acid generated by dissociation of short chains is shown in Eq. 2.24. However, this is not valid in the case of basic drug incorporation because some of the drug molecules can attach to the carboxylic end groups neutralizing the chain ends.

#### 4.2.2 Interaction between drug molecules and carboxylic end groups

As discussed in section 4.1, the following phenomena have to be considered in a degradation model impregnated with basic drugs:

- (i) Basic drug can behave as a catalyst accelerating the cleavage of the polymer chains;
- (ii) The basic drug can shield some of the carboxylic end groups of the short chains diminishing their autocatalytic effect.

In view of the former, dissociation expression for basic drugs can be schematically written as



As with any equilibrium constant for a reversible reaction, the equilibrium expression for this reaction is defined through a base dissociation constant,  $K_b$ , such that

$$K_b = \frac{C_{drug\_H^+} C_{OH^-}}{C_{drug}}. \quad (4.3)$$

Here,  $C_{drug\_H^+}$ ,  $C_{drug}$  and  $C_{OH^-}$  represent the mole concentrations of the cationic drug, drug and  $OH^-$  respectively.  $K_b$  measures the strength of a base and is directly related to the acid dissociation constant,  $K_a$ , by the relationship  $pK_a + pK_b = 14$ . Here,  $pK_a$  and  $pK_b$  are the negative logarithms of  $K_a$  and  $K_b$ , respectively. Therefore, for a known value of  $K_a$ ,  $K_b$  can be easily calculated.

Since the  $Drug\_H^+$  and  $OH^-$  come from the same drug molecules, we then have  $C_{drug\_H^+} = C_{OH^-}$ , the equilibrium expression leads to

$$C_{OH^-} = (K_b C_{drug})^n \quad (4.4)$$

in which  $n$  is generally taken as 0.5.

As stated in many studies (Miyajima *et al.*, 1999, Engineer *et al.*, 2011), the products of the dissociation reaction of drug forms a cluster (shielding) with the products of the dissociation reaction of short chains. The reason is that the polarity increases largely after dissociation of the drug which is a driving force for cationic drug and hydroxyl ions to pull the anionic carboxylic ends and protons (for an example topological polar surface area, tPSA, is 15.6 for  $C_{drug}$  while it is increasing to 18.84 for  $C_{drug\_H^+}$  (Ultra, 2001)). The level of the shielding between the drug and carboxylic ends is dependent on the structure and charge to mass ratio of drug. In this sense, a portion of the drug would be interacted with the carboxylic ends groups while rest would stay in free form. In order to reflect this phenomena, we introduced a partition parameter,  $K_p$ , into the model to reflect the number of drug molecules that are attached to the carboxylic end groups.  $K_p$  varies between 0 and 1.0 with  $K_p = 0$  indicating no attachment and  $K_p = 1.0$  indicating full attachment. Only the drug molecules free from the attachment are available to act as a catalyst, therefore, Eq. (4.4) can be modified as

$$C_{OH^-} = K_b (K_b C_{drug})^{0.5} \quad (4.5)$$

Similarly, only the carboxylic ends free from attachment can act as a catalyst and the concentration of protons in Eq. (4.2) reduces to

$$C_{H^+} = \begin{cases} 0 \text{ or} \\ (K_a C_{R-COOH})^{0.5} - (1 - K_p)(K_b C_{drug})^{0.5} \end{cases} \quad (4.6)$$

Using Eqs. (4.5) and (4.6) in Eq. (4.2) gives the final equation for chain scission rate in the presence of basic drugs

$$\frac{dR_s}{dt} = C_{e,0} \left[ 1 - \alpha \left( \frac{R_s}{C_{e,0}} \right)^\beta \right] \{ k_1 + k_2 C_{H^+} + k_3 K_p (K_b C_{drug})^{0.5} \}. \quad (4.7)$$

Eq. 4.7 forms a final expression for chain scission rate, involving all the interactions between drug and carboxylic ends as well as the catalyst effect of the species free from the attachment. And finally the number average molecular weight of the polyester can be calculated dependent on  $R_s$ , and some other polymer related parameters such as  $\alpha$ ,  $\beta$ ,  $C_{e,0}$ ,  $m$ ,  $N_{dp0}$  and  $M_{n,0}$  as described in Eq. 3.12.

### 4.2.3 Diffusion equations of short chains and drug molecules

Both the short polymer chains and the dissolved drug molecules are capable of diffusion through the polymeric matrix. For the microspheres, diffusion occurs only in the radial direction  $r$ . It is assumed that the diffusions of oligomer and drug follow the Fick's law as stated in Eq. 3.5 and 3.6. The diffusion coefficient is treated as dependent on the porosity of the matrix (see Eqs. 3.7-3.11).

It is fruitful to provide a summary of the equations for completion

$$\frac{dR_s}{dt} = C_{e,0} \left[ 1 - \alpha \left( \frac{R_s}{C_{e,0}} \right)^\beta \right] \{ k_1 + k_2 C_{H^+} + k_3 K_p (K_b C_{drug})^{0.5} \}.$$

$$\frac{dR_{ol}}{dt} = \alpha \beta \left( \frac{R_s}{C_{e,0}} \right)^{\beta-1} \frac{dR_s}{dt}$$

$$\frac{dC_{ol}}{dt} = \frac{dR_{ol}}{dt} + D_{ol} \left( \frac{1}{r^2} \right) \frac{d}{dr} \left( r^2 \frac{dC_{ol}}{dr} \right)$$

$$\frac{dC_{drug}}{dt} = \frac{dR_{drug}}{dt} + D_{drug} \left( \frac{1}{r^2} \right) \frac{d}{dr} \left( r^2 \frac{dC_{drug}}{dr} \right)$$

$$D_{ol} = D_{ol,poly} + (1.3V_{pore}^2 - 0.3V_{pore}^3)(D_{ol,pore} - D_{ol,poly})$$

$$D_{drug} = D_{drug,poly} + (1.3V_{pore}^2 - 0.3V_{pore}^3)(D_{drug,pore} - D_{drug,poly})$$

$$V_{pore} = \frac{R_{ol} - (C_{ol} - C_{ol,0})}{C_{e,0}} = \alpha \left( \frac{R_s}{C_{e,0}} \right)^\beta - \frac{C_{ol} - C_{ol,0}}{C_{e,0}}$$

$$V_{pore,drug} = 1 - \frac{C_{drug}}{C_{drug,0}}$$

$$V_{pore} = V_{pore,ol} (1 - f_{drug}) + V_{pore,drug} f_{drug}$$

$$M_n = M_{n,0} \frac{1 - \alpha \left( \frac{R_s}{C_{e,0}} \right)^\beta}{1 + N_{dp,0} \left( \frac{R_s}{C_{e,0}} - \frac{a}{m} \left( \frac{R_s}{C_{e,0}} \right)^\beta \right)}$$

The definitions of the symbols are provided in the List of Symbols. Here, the chain scission equation reflects all the interactions and the catalyst of the free species. Oligomer production is linked with the rate of chain scission. The effective diffusion coefficients of drug,  $D_{drug}$  and oligomers,  $D_{ol}$  are calculated taking into account the increasing porosity in the matrix. The porosity of the system is calculated considering the oligomers and drug leaving the matrix.

### 4.3 The numerical procedure

The numerical procedure for computation of the model is presented in the current section. The equation summarised forms a complete set of governing equations for  $R_s$ ,  $C_{ol}$  and  $C_{drug}$ . It is assumed that initially there is no oligomer in the matrix, therefore  $C_{ol}(r, 0) = C_{ol,0} = 0$ . Moreover,  $C_{drug}(r, 0) = C_{drug,0}$  and  $R_s(r, 0) = 0$  at  $t=0$ . The perfect sink condition is used that requires  $C_{ol}=0$  and  $C_{drug}=0$  at the particle surface. It is assumed that drug dissolution is instantaneous. For initial drug concentration, we consider two different scenarios. If the drug loading is below the solubility limit, the initial drug concentration is simply taken as the drug loading. If the drug loading is above the solubility limit, the initial drug concentration is taken as the solubility of the drug and the drug concentration at any  $r$  remains at the solubility limit until all loaded drug at that location has dissolved as presented in Section 3.3.

The equations form a complete model for degradation and drug release. Number averaged molecular weight of the polymer can be calculated as Eq. 3.16. The equations are solved numerically using a finite difference method, giving the time evolution and spatial distribution of all the variables from which drug release profile and average molecular weight of the polymers can be calculated. The central finite difference method was used for spatial discretization (Smith, 1965) and the direct Euler scheme was used for the time integration. A particle radius was discretized into 100 finite difference nodes and a very small time step was used. The grid size is set as  $\Delta r = 0.0017 \text{ mm}$ . The schematic illustration of the grid size is represented in Fig. 3.4. The time step length was found to be  $\Delta t = 2.7 \text{ s}$ , which guarantees convergence for all the cases including the blank and loaded microparticles. Numerical convergence was ensured by gradually increasing the number of finite difference nodes and reducing the time step length such that no change in the numerical solution can be found.

The equations developed form the full mathematical model for polymer degradation and drug release. FORTRAN 90 programming language is used for performing the simulations (see Appendix B). The total computation time takes

less than 10min, on the desktop computer. The numerical details are presented in a flow chart in Fig. 4.2.

Finally, the mean absolute relative error (MARE) is used to evaluate the performance of the model which is calculated by the following equation (Malhotra, 2016)

$$MARE = \frac{1}{N} \sum_{i=1}^N \frac{|P_i - A_i|}{A_i} \quad (4.8)$$

in which  $N$  refers to the total number of instances in a data set,  $P_i$  refers to the model results for an instance  $i$  and  $A_i$  refers to the experimental value of an instance  $i$ .

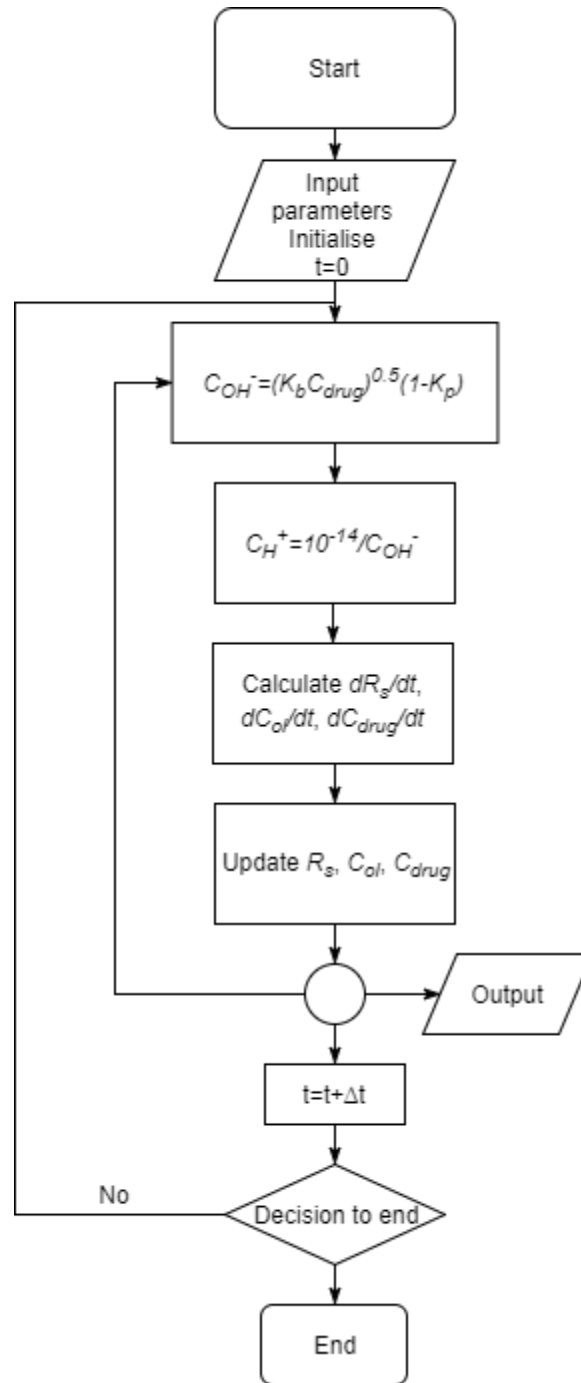


Fig. 4.2 Flow chart for the model in the presence of basic drugs

## 4.4 Validation of the model

### 4.4.1 Case Study A

Siepmann *et al.* (2005) studied the degradation behaviour of drug loaded and drug-free PLGA-based microparticles. Drug free and drug-loaded microparticles

with changing sizes were studied as 7.2 $\mu\text{m}$ , 24 $\mu\text{m}$ , 37 $\mu\text{m}$  and 53 $\mu\text{m}$  for lidocaine loaded microparticles; and 7.9 $\mu\text{m}$ , 26 $\mu\text{m}$ , 38 $\mu\text{m}$  and 55 $\mu\text{m}$  for drug free particles. Accumulation of the short chains resulted an enhanced level of degradation for larger particles. However, varying particle diameter, had no significant effect on the rate of drug release. This was explained with the following phenomena: as diameter of the particle increases, degradation is accelerated, however, diffusion pathways of the drug is increased. This combined effect led to same level of drug release as particle diameter enlarged. A quantitative discussion was made which provided new insights into the importance of the autocatalytic effects in polyester-based microparticles.

Similarly, Klose *et al.* (2008) carried out a set of degradation and drug release experiments using PLGA50:50 microspheres and thin, free films impregnated with lidocaine (free base,  $pK_a$  7.9) and ibuprofen. The initial drug concentrations (4% w/w) were stated to be below the solubility limit in the study (Klose *et al.*, 2008). Molecular weight change for blank and loaded polymers and drug release properties were physicochemically characterized *in vitro* in phosphate buffered solution (pH 7.4) at 37°C. The initial molecular weight,  $M_{n,0}$ , is 29500Da for blank samples and 31000Da for lidocaine loaded microspheres. Their results showed that, the system size strongly affected the release kinetics for thin films. However, for the case of spherical microparticles, the release was almost unaffected by the system size. Ibuprofen release was reported to be much faster than the lidocaine release for all systems geometries and sizes. This is attributed to attractive ionic interaction between the carboxylic end groups of polymer and basic drug, lidocaine.

In the current chapter, the experimental data by Siepmann *et al.* and Klose *et al.* will be used for the fittings. The molecular weight change of blank polymer during degradation is taken from Siepmann *et al.* study, whereas the molecular weight change of the lidocaine loaded microparticles and drug release data is taken from Klose *et al.* study. In order to eliminate the size dependence of degradation and stick on analysing the impact of basic drug incorporation on the degradation rate,

we selected their data for similar particle sizes of 55 $\mu\text{m}$  for blank particles and 48 $\mu\text{m}$  for drug-loaded particles.

The model is first simulated for the case of blank polymer to collect the polymer related parameters. Then the simulations are repeated for the case of loaded microspheres, in order to collect the drug related parameters and the partition parameter,  $K_p$ . Fig. 4.3 shows the comparison between the model results and experimental data. The model results for molecular weight changes are shown in Fig. 4.3a while the release profile is illustrated in Fig. 4.3b. Model parameters used in the simulations are provided in Table 4.1. These parameters are categorized into two groups: Group I consists parameters that were either measured experimentally or cannot be varied artificially to fit a particular set of experimental data.  $M_0$ ,  $M_u$  and  $C_{e0}$  are initial average molecular weight of the polymer, molecular weight of a representing unit and initial ester bond concentration, all of which were taken from Siepmann *et al.* and Klose *et al.*  $m$  is the average number of repeating unit of soluble and short polymer chains, which is taken as 4.  $\alpha$  and  $\beta$  represents the nature of polymer chain cleavage and were taken from Pan *et al.*  $K_a$  and  $K_b$  are equilibrium constants for disassociation of oligomers and drug molecules.  $D_{ol,pore}$  and  $D_{drug,pore}$  are the diffusion coefficients of oligomers and drugs in liquid-filled pores which were just taken as a very large value. Group II consist of parameters that were varied to fit with the experimental data.  $k_1$ ,  $k_2$  and  $k_3$  represent the non-catalytic, acid catalyzed and base catalyzed rate constants for hydrolysis.  $D_{ol,0}$  and  $D_{drug,0}$  are the diffusion coefficients of oligomers and drugs in non-degraded bulk polymer.  $K_p$  is the partition constant indicating percentage of drug molecules shielded by carboxylic ends, which was set 0.75. The value of  $K_p$  implies that 75% of the drug molecules are attached to the carboxylic end groups of the polyester chains whilst the rest remains in free form.

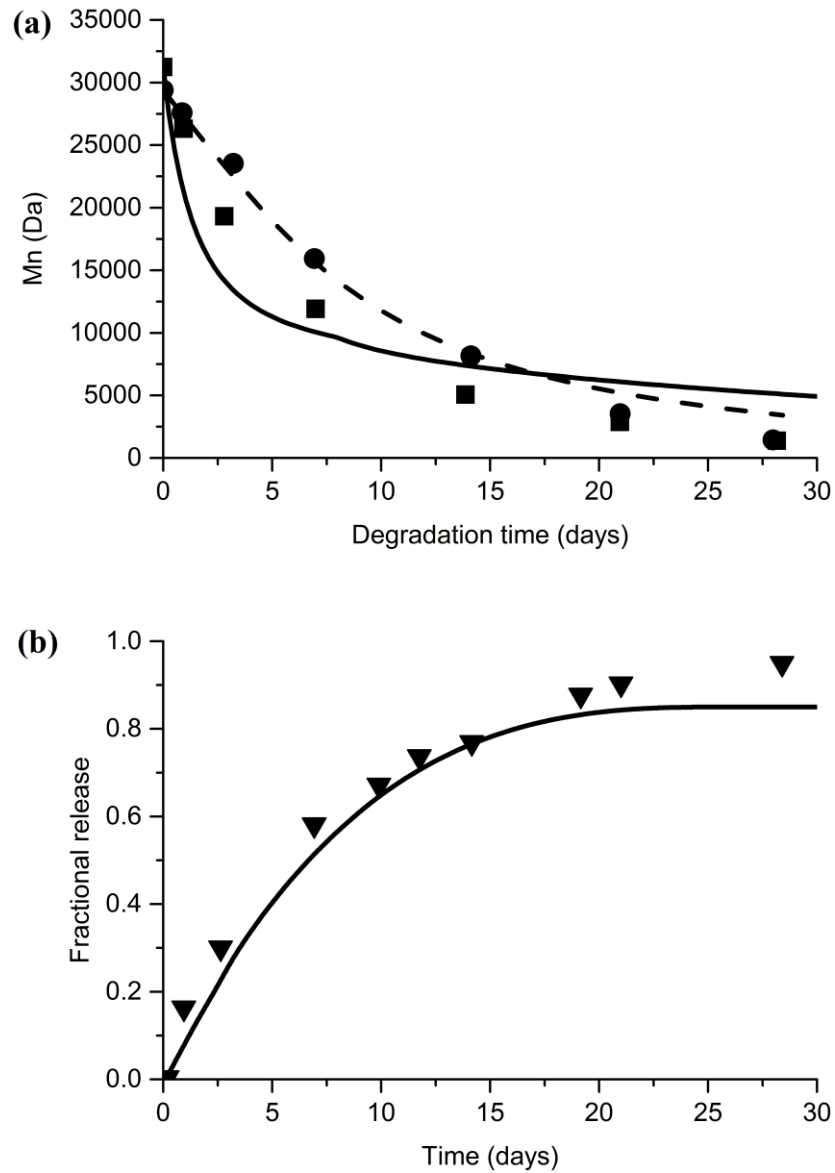


Fig. 4.3 Comparison between the model result and experimental data (Klose *et al.*, 2008, Siepmann *et al.*, 2005): a)  $M_n$  reduction and b) drug release. Lines represent the model prediction for blank (dashed line) and loaded particles (solid line); discrete symbols represent experimental data for blank (circle) and loaded particles (square, triangle).

Table 4.1 Parameters used in the model to fit with experimental data

	<b>Model parameters</b>	<b>Units</b>	<b>Values</b>
Group I	$M_{n0}$	g mol <sup>-1</sup>	2.9-3.5x10 <sup>4</sup>
	$M_{unit}$	g mol <sup>-1</sup>	65
	$m$	no unit	4
	$\alpha$	no unit	0.4
	$\beta$	no unit	1
	$C_{e0}$	mol m <sup>-3</sup>	20615
	$K_a$	no unit	1.35x10 <sup>-4</sup>
	$D_{ol,pore}$	m <sup>2</sup> week <sup>-1</sup>	1.0x10 <sup>-5</sup>
	$D_{drug,pore}$	m <sup>2</sup> week <sup>-1</sup>	1.0x10 <sup>-5</sup>
Group II	$k_1$	week <sup>-1</sup>	8x10 <sup>-4</sup>
	$k_2$	m <sup>3</sup> mol <sup>-1</sup> week <sup>-1</sup>	1x10 <sup>-1</sup>
	$k_3$	m <sup>3</sup> mol <sup>-1</sup> week <sup>-1</sup>	8x10 <sup>1</sup>
	$D_{ol,poly}$	m <sup>2</sup> week <sup>-1</sup>	5.0x10 <sup>-12</sup>
	$D_{drug,poly}$	m <sup>2</sup> week <sup>-1</sup>	6.0x10 <sup>-10</sup>

Compared to the drug-free microspheres, loaded microspheres shows a more rapid decrease in molecular weight, which is attributed to the free acidic and basic species (Fig. 4.3). The increased rate of degradation can be attributed to the dominant impact of basic drug that are free from the attachment. It is also worth highlighting that the base-catalytic coefficient,  $k_3$ , has a major impact on the degradation rate relative to the non-catalytic and autocatalytic constants. The results show that mean absolute relative error is 0.1 and 0.7 for molecular weight reduction of loaded and blank microspheres respectively while is 0.08 for release data.

#### 4.4.2 Case Study B

Dunne *et al.* (2000) carried out a set of experiments to demonstrate the influence of particle size on the molecular weight change of PLGA particles. Moreover, the influence of processing conditions, particle characteristic and the temperature of release media on the degradation of polymers was examined. It was found that the larger particles degrades faster. Moreover, at lower incubation temperatures, PLGA microparticles were reported to show an incubation period which is

followed by degradation. The increasing incubation temperature led to an increase in polymer degradation. The models were then fitted with Prout-Tompkins equations, which are used in the kinetic analysis of solid-state reactions. By use of the kinetic analysis, the activation energy of the hydrolysis reaction was determined.

In connection with the study by Dunne *et al.*, Fitzgerald and Corrigan (1996) examined the degradation behaviour of PLGA microspheres and co-evaporate discs loaded with levamisole drug (free base,  $pK_a$  8). In their study, various drug loadings are compared to capture the impact of drug content on degradation rate. No solid aggregate of the drug has been observed in their analysis; therefore, all these levels of drug loading are assumed to be below the solubility limit (Fitzgerald and Corrigan, 1996). The blank samples have an initial molecular weight of  $M_{n,0} = 40000\text{--}45000\text{Da}$ , with the size range of  $<1\mu\text{m}$  (process A),  $<20\mu\text{m}$  (process B) and  $<50\mu\text{m}$  (process C). Molecular weight varies between  $10000\text{--}13000\text{Da}$  for loaded particles. The sizes of microspheres are defined to be below  $170\mu\text{m}$  in diameter; and constituted as  $170\mu\text{m}$  in the simulations. In addition to the change in molecular weight and mass loss, drug release was monitored from microsphere and disc systems. The analysis showed that the drug content significantly increases the rate of degradation.

Here, the experimental data obtained from Dunne *et al.* (2000) and Fitzgerald and Corrigan (1996) is used for the comparison with the model results. The molecular weight change of blank polymer is obtained from the study by Dunne *et al.* (2000), while molecular weight change of levamisole loaded microspheres is taken from the study by Fitzgerald and Corrigan (1996). Different drug loadings have been compared with the model result in order to comprehend the validity of the model for changing drug loading. Only microspheres are compared with the model results, although the model is valid for all the geometries.

The comparison between the calculated and the experimental results of molecular weight as a function of time for blank microspheres are shown in Fig. 4.4. Model parameters used in the simulations are presented in Table 4.2. The case of sub-micron particles was not considered in the model, hence, only

particles having 20 $\mu$ m and 50 $\mu$ m sizes are used for the validation. It can be observed that the model is able to capture the size effect of microsphere degradation (Fig. 4.4) Mean absolute relative error of molecular weight reduction is 0.04 and 0.003 for blank samples with 20 $\mu$ m and 50 $\mu$ m, respectively.

Table 4.2 Parameters used in the model to fit with experimental data

	<b>Model parameters</b>	<b>Units</b>	<b>Values</b>
Group I	$M_{n0}$	g mol <sup>-1</sup>	1-3x10 <sup>4</sup>
	$M_{unit}$	g mol <sup>-1</sup>	65
	$C_{e0}$	mol m <sup>-3</sup>	20615
	$m$	no unit	4
	$\alpha$	no unit	0.4
	$\beta$	no unit	1
	$K_a$	no unit	1.35x10 <sup>-4</sup>
	$K_b$	no unit	
	$D_{ol,pore}$	m <sup>2</sup> week <sup>-1</sup>	1.0x10 <sup>-5</sup>
	$D_{drug,pore}$	m <sup>2</sup> week <sup>-1</sup>	1.0x10 <sup>-5</sup>
	$k_1$	week <sup>-1</sup>	5x10 <sup>-4</sup>
Group II	$k_2$	m <sup>3</sup> mol <sup>-1</sup> week <sup>-1</sup>	1x10 <sup>-1</sup>
	$k_3$	m <sup>3</sup> mol <sup>-1</sup> week <sup>-1</sup>	1x10 <sup>1</sup>
	$D_{ol,0}$	m <sup>2</sup> week <sup>-1</sup>	5.0x10 <sup>-11</sup>
	$D_{drug,0}$	m <sup>2</sup> week <sup>-1</sup>	2.0x10 <sup>-8</sup>
	$K_p$	no unit	0.3-0.75

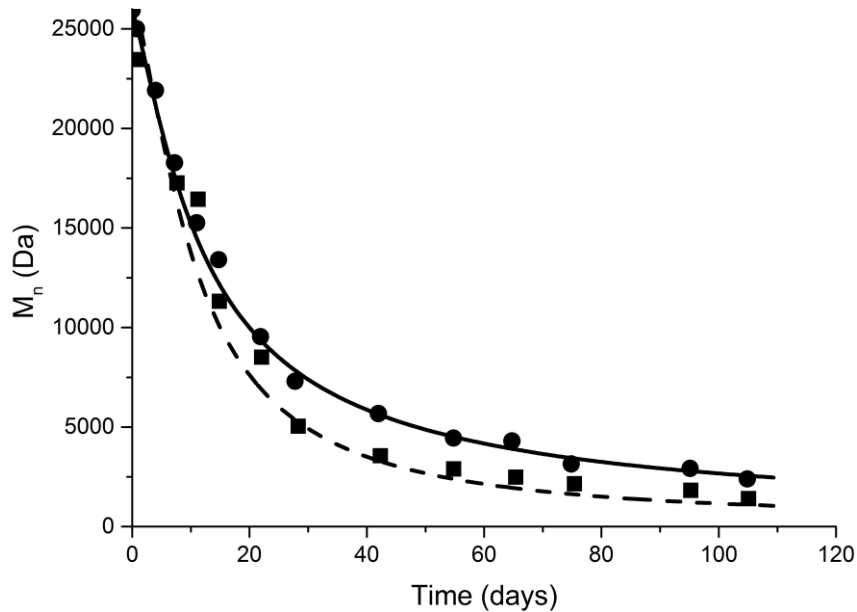


Fig. 4.4 Comparison between the model result and experimental data (Dunne *et al.*, 2000) for blank PLGA microspheres. Lines represent the model prediction for various sizes and discrete symbols represent corresponding experimental data for  $r = 20\mu\text{m}$  (solid line, circles) and  $50\mu\text{m}$  (dashed line, squares).

The effect of drug loading on molecular weight reduction is shown in Fig. 4.5. The drug related parameters are again shown in Table 4.2.  $K_p$ , was set as 0.75, 0.7 and 0.3 for 2.4%, 14.3% and 19.7% loaded microspheres respectively. The increasing drug loading led to a decrease in the value of  $K_p$ . This is reasonable since the amount of interacted drug decreases as drug loading increases.

Fig. 4.6 represents the model fitting for drug release for various drug loadings. Mean absolute relative error of molecular weight reduction is 0.05, 0.1 and 0.34 for 2.4%, 14.3%, and 19.7% loaded microspheres respectively. This value is respectively 0.48, 0.16 and 0.08 for release data of 2.4%, 14.3% and 19.7% loaded microspheres respectively.

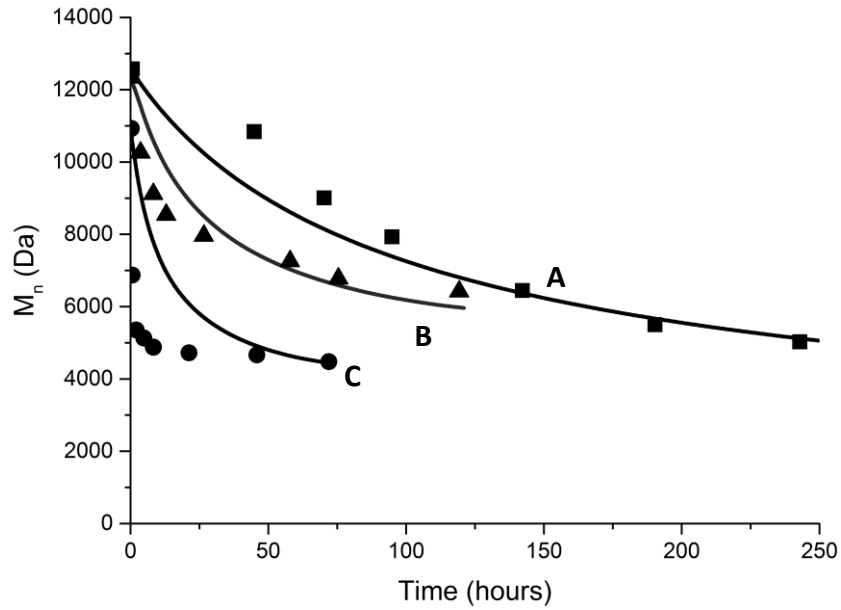


Fig. 4.5 Comparison of  $M_n$  reduction between model results and experimental data. Solid lines represent the model prediction for microspheres with various levamisole loadings and discrete symbols represent corresponding experimental data (Fitzgerald and Corrigan, 1996) (A) 2.4% w/w (solid line, square) (B) 14.3% w/w (solid line, triangle) and (C) 19.7% w/w (solid line, circle).

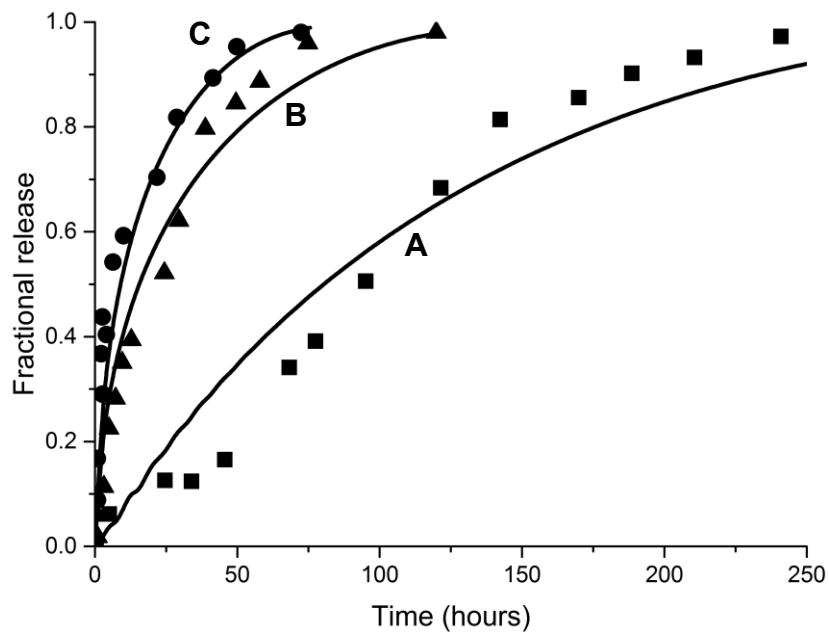


Fig. 4.6 Comparison of drug release between model results and experimental data. Solid lines represent the model prediction for microspheres with various levamisole loadings and discrete symbols represent corresponding

experimental data (Fitzgerald and Corrigan, 1996) (A) 2.4% w/w (solid line, square) (B) 14.3% w/w (solid line, triangle) and (C) 19.7% w/w (solid line, circle).

Under assumed interaction between drug and polymer matrix in the model, we could adjust the three parameters,  $k_3$ ,  $D_{drug,0}$  and  $K_p$  to fit the 61 data points in Fig. 4.5 and Fig. 4.6. The model fits the experimental data, however, fittings for Case B is relatively poor compared to Case A due to the self-imposed restriction. If an independent set of  $k_1$ ,  $k_2$  and  $D_{ol0}$  were used a much better fitting can be obtained. The fact that the model can capture the general trend as shown in Fig. 4.5 and Fig. 4.6 for drug loaded spheres using the same  $k_1$ ,  $k_2$  and  $D_{ol0}$  obtained from blank polymers indicates that the assumed mechanism of interaction between drug and polymer matrix is valid. The less satisfactory fitting in these figures shows the complexity of the interaction. This complexity is a result of the fact that drug release from biodegradable polymer is controlled by many factors, including hydrophilicity-hydrophobicity, crystallization of drug and polymer, the physicochemistry of drug, preparation method and *etc.* In the current model, we only focused on the physicochemistry of basic drug and its interaction with the polymer. And the model is capable of showing this interaction. It can be observed from Fig. 4.5 and Fig. 4.6 that the model can indeed capture the strong effect of drug loading on both polymer degradation and drug release.

The partition coefficient of drugs and carboxylic ends,  $K_p$ , determines the level of degradation, therefore, degradation rate is very sensitive to the choice of  $K_p$ . The effect of the partition coefficient on molecular weight is illustrated in Fig. 4.7 by fixing the other parameters (e.g., oligomer and drug diffusivities, drug loading,  $k_1$ ,  $k_2$ ,  $k_3$ ,  $m$ ,  $\alpha$  and  $\beta$ ). As can be seen from the figure, the smaller partition coefficient leads to the more enhanced degradation rate. This is reasonable, since as the value of  $K_p$  increases, the number of free carboxylic acids and drug molecules would be reduced, therefore, the acid and base catalyst part of the chain scission reaction would be less dominant. The partition coefficient is limited with the lower and higher boundaries corresponding to  $K_p = 0$  and  $K_p = 1.0$ .

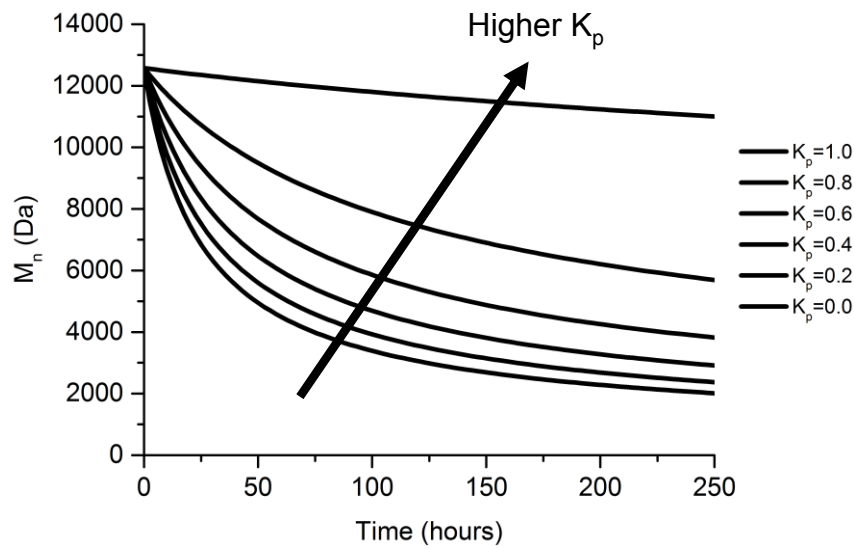


Fig. 4.7 The effect of partition parameter,  $K_p$ , on molecular weight

The mechanistic model presented above is tested using two sets of independent experimental data taken from the literature. It is worth to highlight that our emphasis is to explore the validity of the mechanism-based model. The idea is that to make predictions for both blank spheres and drug-loaded spheres using a common set of model parameters. If the model can indeed capture the interaction between drugs and polyester, then the model calculation should fit with the degradation rates of blank and drug-loaded spheres and the drug release profile of the drug-loaded spheres well. Our numerical results showed that the model could indeed capture the degradation behaviour and drug release profile of the blank and loaded microspheres.

## 4.5 Conclusion

A comprehensive mechanism-based model is presented describing the polyester degradation coupled with drug release from microspheres. The key issue in the model is to consider the full ionic interaction between basic drugs and polymer chain ends as well as the catalytic effect of free acidic and basic species on hydrolysis reaction. The model predictions are compared with the experimental data from the literature with various basic drug types and several loadings. It is shown that, the index of the polymer-drug interactions,  $K_p$ , is the primitive factor

controlling release of basic drugs. Together with our previous paper [24] on micro-spheres loaded with acidic drugs, our work models the impact of various drug types on poly-mer degradation for the first time from our knowledge. The mechanistic model presented here can be used in the design of microsphere systems as well as other drug loaded devices. The model can also facilitate the understanding of the underlying physicochemistry responsible for the release of basic drugs.

## **Part 3**

# **A model by combination of hydrolytic degradation-erosion and its applications**

## **Chapter 5. Combined hydrolytic degradation and erosion model for drug release**

For many biodegradable polymers, there is a strong interplay between the degradation and erosion processes – degradation leads to a certain decrease in molecular weight which is the key process for erosion initiation. Eventually, degradation leads to erosion and subsequently the loss of the material from the polymer.

In this chapter, the reaction and diffusion equations provided in Section 2.2 are combined with erosion models in the literature in order to identify and understand how each mechanism is involved in the mass loss and how different mechanisms dominate at different stages of the mass loss. Various kinetic mechanisms are incorporated in the model in an attempt to explain every possible mass loss behavior obtained from the experimental data. In the combined model, chain scission, oligomer production, diffusion and microstructure evolution are modeled together with surface erosion and interior erosion using a set of differential equations and Monte Carlo technique. Oligomer diffusion is modeled using Fick's laws with a diffusion coefficient dependent on the porosity. The porosity of the system is taken as dependent on the formation of cavities which is a result of polymer collapse. Comparisons are made between the mass loss profiles of individual mechanisms such as diffusion, surface erosion and interior erosion. This way of representation has never been proposed in the literature before. The model developed here has potential to deal with large mass losses, even up to 100%. This level of mass loss cannot be explained with a simple degradation-diffusion model. It is also important to state that modeling PLA/GA degradation-erosion is a pre-requirement for drug release modeling. The model constructed here would be the basis of the drug release model which would be proposed in Chapter 7. This part of the thesis has been published in *Acta Biomaterialia*.

## 5.1 Introduction

Most of the biomedical applications benefit from the fact that the polymer disappears after providing its function. Two major mechanisms are involved in the process: degradation of the polymer chains and erosion of the polymer matrix. Erosion leads to a visible change in microscopic and macroscopic level (Gopferich and Langer, 1993) as well as the large increase in mass loss and drug release. However, little is known about the basic principles of erosion process and its link with the degradation. The number of parameters and complexity of each process involved in the erosion hinder the development of new erosion models.

According to the general knowledge in the literature, degradation is a chemical process which can be explained by the chain cleavage. The degradation products, monomers, and oligomers, are released by diffusion. Assuming that chain cleavage is a random process affecting each bond with the equal probability, the oligomers are produced from the beginning of the degradation. If these products are released immediately from the beginning, there would be a large mass loss from the beginning of the degradation (Gopferich, 1997). However, the mass loss obtained by degradation is generally less than 5-10% of the total molecular weight of the device and happens after a certain time of the degradation. The level of mass loss that can be obtained with degradation is not sufficient to explain all the observed mass loss behaviours in the literature. Therefore, there must be other mechanisms causing a larger mass loss.

Recently Zhang *et al.* (Zhang et al., 2017) developed a combined degradation and erosion model. This is an advanced model which follows oligomer diffusion at the continuum scale and random chain scissions and polymer erosion at the microscopic scale. However, the model is over-complicated for applications in practical device design. The important autocatalytic effect of the hydrolysis reaction was not considered, which means the model is unable to capture size effect of the degradation. Gopferich (1997) suggested a two-phase mass loss profile for an eroding polymer. During the first phase, no significant mass loss can be obtained, while molecular weight is significantly reduced. This phase was

designated as degradation. As soon as the molecular weight reaches a critical level at which the polymer becomes water soluble, an erosion phase initiates and the eroded material could be released into the surrounding medium leading to a large mass loss (Husmann et al., 2002). In their work a mechanism based link between the degradation and erosion processes was not made. Moreover, up to date, there is no appropriate model to directly link erosion model with a solid degradation model and the models are far from covering all the aspects of erosion.

In summary, significant mass loss of the particles can be only observed when the polymer erosion is the active mechanism. Therefore, polymer molecular weight change is the measure for quantifying the degradation whereas mass loss is the measure for quantifying erosion (Zhu and Braatz, 2015). It is assumed that degradation is a necessary condition for the erosion and a degraded polymer can only erode after it has contact to a pore of the matrix surface (Gopferich, 1997).

The objective of this chapter is to combine a hydrolytic degradation model with a polymer erosion model so that the different behaviors of mass loss can be captured in a single model. The reaction-diffusion equations previously developed by Pan and his co-workers (2014, Wang et al., 2008) are adopted which consider the autocatalytic effect and are valid for aliphatic polyesters such as PLAs, PGAs and their copolymers. The degradation equations form the basis of the current chapter and would be summarized clearly before they are linked with the erosion model. These equations are coupled mechanistically with an erosion model to provide a full picture of mass loss and drug release. It is shown that all the observed trends such as biphasic and triphasic mass losses can be obtained by using the combined model.

## **5.2 Hypothesis of the model and representation of the polymer matrix**

In formulating the algorithm, the composite and elementary events are distinguished. The degradation and erosion mechanisms are assumed to be elementary events which cannot be divided into simpler events, while transport

of the degradation products is assumed to be the composite elements that can be linked with the elementary events. A two-dimensional model is used for the plates. To minimize the computational time, the symmetry about the vertical and horizontal center lines are presented and quarter models are constrained in the simulations. The polymer matrix is divided into  $n_x \times n_y$  grid points and each square pieces are called as pixels. The grid lines  $i=n_x$  and  $j=n_y$  represent the surface of the plate in contact with aqueous media;  $i=1$  and  $j=1$  are the sides of the plate which are not connected with the environment. Each pixel in the two-dimensional grid represents a polymer chain and all pixels have the same size. The following algorithm has been used to introduce the randomness of the erosion, initial molecular weight has been distributed randomly to follow normal distribution throughout the plate. Monte Carlo sampling method is used for the random distribution. Initially, all pixels are assumed to be non-eroded except the ones at the surface. Surface erosion starts at  $t=0$ , with a constant speed. To simulate the overall polymer degradation, chain scission equations has been defined at each pixel in the 2-dimensional grid system. Degradation produces monomers and oligomers which are ready to diffuse out of polymer matrix. Degradation also leads to a certain decrease in the molecular weight. As soon as an inner pixel reaches to the critical molecular weight and contacts with an eroded neighbour, it is assumed to be eroded instantaneously: this phenomenon is named as interior erosion in the current chapter. The porosity of the matrix is largely dependent on the cavities formed by erosion. The described algorithm has been transformed into mathematical expressions in the following sections.

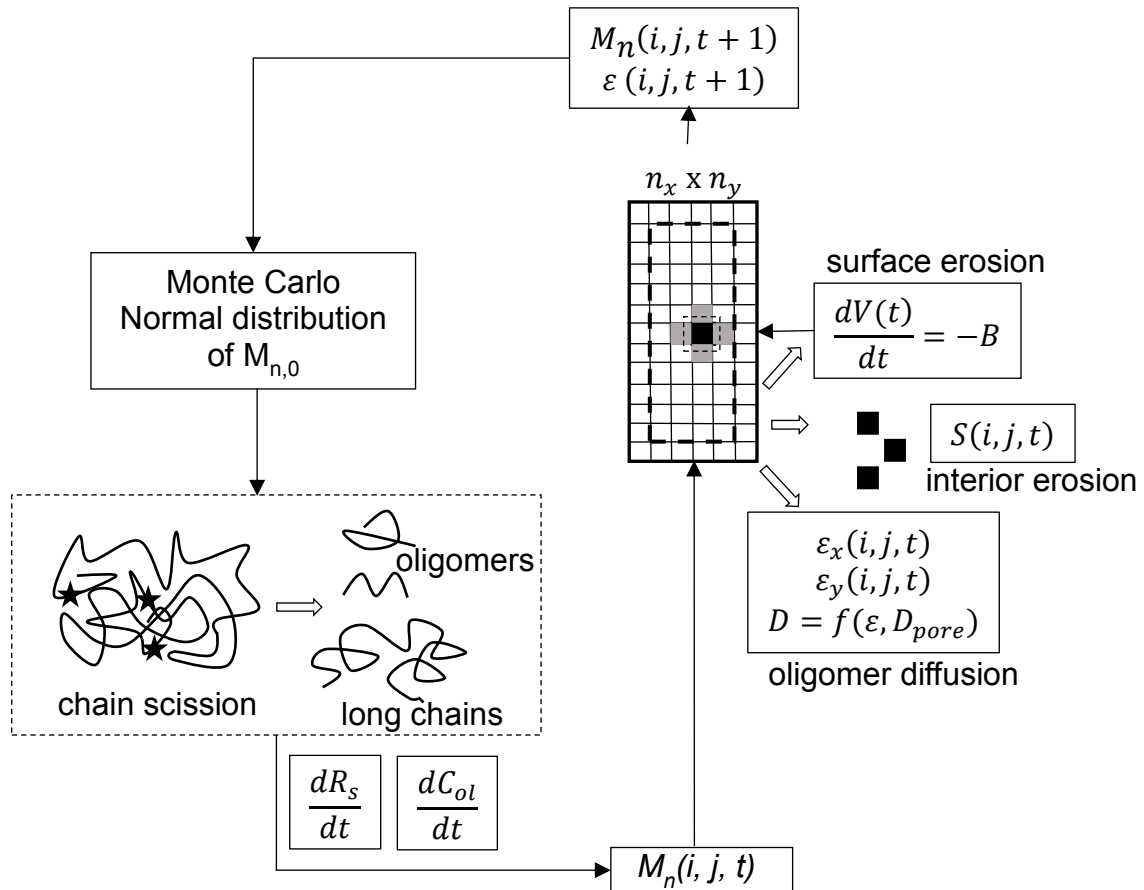


Fig. 5.1 The coupling of hydrolytic degradation and erosion

### 5.3 Initializing the computational grid prior to erosion

We consider the cases where matter transport is limited to 2-dimensions although the mathematical model is generally valid in 3-dimensions. The case studies presented later in this paper can all be modelled under the assumption of 2-dimensional matter transport. We limit our effort to these cases for the sake of simplicity. A polymer is represented by using a set of regular pixels as shown in Fig. 5.2. The centres of the pixels correspond to nodes in a finite difference grid. Again the model is not limited to this particular approach of discretization. In general, the finite element method can be used to solve the governing equations. However for the sake of simplicity, we focus our effort on using the simplest discretization method. This allows us to demonstrate the capacity of the model before its extension to general polymer implants. The polymer morphology and pores are treated explicitly by using pixels of different state. As shown in Fig. 5.2,

each pixel is identified by its indices  $(i,j)$  in the x- and y-directions. The state of each pixel is defined by its number averaged molecular weight,  $M_n(i,j,t)$ , erosion index,  $S(i,j,t)$  and the local drug concentration  $C_{drug}(i,j,t)$ . The erosion index is defined as

$$S_{i,j,t} = \begin{cases} 1 & \text{non-eroded pixel} \\ 0 & \text{eroded pixel} \end{cases} \quad (5.1)$$

Water diffusion is a fast process in comparison to polymer degradation and erosion (Wang et al., 2008, Han and Pan, 2009). It is therefore assumed that water molecules are always abundant in the polymer. The hydrolytic degradation is reflected by the reduction in  $M_n$  and polymer erosion is reflected by changes of  $S(i,j,t)$  from 1 to 0. The initial molecular weights of the pixels are set such that they follow a normal distribution using a direct Monte Carlo technique. A random number generator,  $R$ , is linked with a specified standard deviation to ensure that the molecular weight follows a normal distribution such that

$$M_{n,0} = M_{n,mean} + R \times M_{n,st\_dev} \quad (5.2)$$

in which  $M_{n,mean}$  and  $M_{n,st\_dev}$  represent the mean value and standard deviation of the molecular weight distribution respectively.

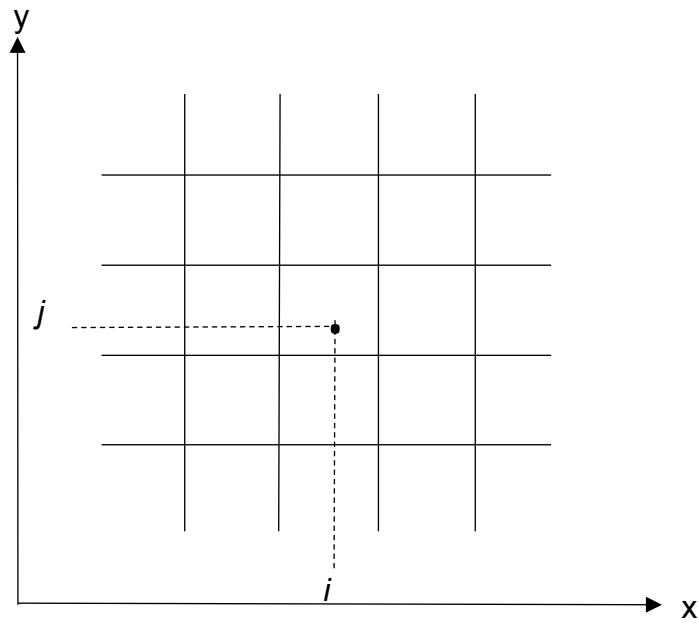


Fig. 5.2 Schematic illustration of discretised polymer

#### 5.4 A brief summary of the reaction-diffusion model

After the grid is set up the rules, the hydrolytic degradation is the first phase prior to the erosion which takes place in elementary level by cleavage of the backbone chains. The detailed mechanism of degradation is provided in Section 2.2, a brief summary of their model is provided here for the convenience of readers. The rate of polymer chain scission follows the governing equation (Wang et al., 2008, Pan, 2014)

$$\frac{dR_s}{dt} = C_{e,0} \left[ 1 - \alpha \left( \frac{R_s}{C_{e,0}} \right)^\beta \right] \left( k_1 + k_2 \left[ K_a \left( \frac{C_{ol}}{m} \right) \right]^{0.5} \right). \quad (5.3)$$

in which  $R_s$ ,  $C_{e,0}$  and  $C_{ol}$  represent the mole concentrations of chain scission, initial ester bonds and short chains,  $k_1$  and  $k_2$ , the kinetic rate constants for non-catalytic and autocatalytic hydrolysis reactions,  $\alpha$  and  $\beta$  are constants indicating the nature of chain scissions (random or end scissions),  $K_a$  represents the equilibrium constant for acid disassociation of the carboxylic ends, and  $m$ , the average degree of polymerization of the short chains which is generally taken as

4 (Pan, 2014). The production rate of short chains due to polymer chain cleavage is given by (Wang et al., 2008, Pan, 2014)

$$\frac{dR_{ol}}{dt} = \alpha\beta \left( \frac{R_s}{C_{e,0}} \right)^{\beta-1} \frac{dR_s}{dt}. \quad (5.4)$$

in which  $R_{ol}$  is the concentration of ester bonds of all the short chains. The average molecular weight  $M_n$  of the polymer is calculated using (Wang et al., 2008, Pan, 2014)

$$M_n = M_{n,0} \frac{1 - \alpha \left( \frac{R_s}{C_{e,0}} \right)^\beta}{1 + N_{dp,0} \left( \frac{R_s}{C_{e,0}} - \frac{\alpha}{m} \left( \frac{R_s}{C_{e,0}} \right)^\beta \right)}. \quad (5.5)$$

in which  $M_{n,0}$  is the initial molecular weight and  $N_{dp,0}$ , the degree of polymerisation of the polymer.

## 5.5 Surface erosion model

As stated in Section 1.3.2, polymer undergoes surface erosion causing the material to shrink from its outer surface towards its center; maintaining the bulk integrity. The speed of moving boundary is given by (Thombre and Himmelstein, 1984).

$$\frac{dV(t)}{dt} = -B. \quad (5.6)$$

in which  $\frac{dV(t)}{dt}$  represents the volume of material lost per unit surface area per unit time, and B is a material constant. For a pixel in contact with the surrounding medium,  $S(i, j, t)$  is set as zero when its volume is reduced to zero through Eq. 5.6.

## 5.6 Interior erosion model

Siepmann *et al.* (2002) used a Monte Carlo model to simulate the random behavior of polymer erosion in which they are motivated from Gopferich's study

(1997). In their model, they treated erosion as a random process by assigning individual lifetimes for each pixel. The lifetimes start to decrease upon contact with water. The pixels counted to be eroded as soon as their lifetimes are consumed. The interior erosion model is motivated by their study as well as the criteria set by Gopferich (1997) which is discussed in section 5.1.

## 5.7 Combined hydrolytic degradation and erosion model

Degradation equations show the actual chemical equations in the plate. For each cell  $(i, j)$  number average molecular weight,  $M_n$ , is obtained with the reaction equations. In each iteration  $M_n$  is being updated. As time proceeds, two main criteria proposed by Gopferich (1997) must be satisfied for pixels to be eroded from interior: molecular weight at the pixels must be below critical value, and pixels should be in contact with an eroded neighbour. As a yield of the random distribution of the initial molecular weight throughout the grid, each pixel will hit to the critical molecular weight at different time. Once pixels satisfied both of the criteria, they are assumed to fall apart instantaneously.

### 5.7.1 Rule of interior erosion

For computational reasons, we principally defined a temporary function,  $S_m$  to describe the current state of the pixels representing the temporary states of the pixels

$$S_m(i, j, t) = 0 \quad M_n < M_{n,critical} \quad (5.7)$$

in which  $M_{n,critical}$  represents the critical molecular weight. However, a pixel cannot be counted as eroded until it is in contact with an eroded neighbour. This can be mathematically represented as

$$S(i, j, t) = 0 \quad \text{if } S_m(i, j, t) = 0 \text{ and the pixel has an eroded neighbour} \quad (5.8)$$

Here,  $S(i, j, t)$  is a function representing actual states of the pixels at time  $t$ - only by action of interior degradation. This erosion model leads to a sudden release

of oligomers when the critical molecular weight is reached. While some polymers do show this sudden mass loss in the degradation experiment, other polymers show a gentler trend in mass loss (Li et al., 1990a, Li et al., 1990b). The slow mass erosion can be captured by introducing an incubation period,  $t_{inc}$ , in the model. A pixel of low molecular weight only changes its state from  $S = 1$  to  $S = 0$  after being in contact with an eroded neighbour for an incubation period of  $t_{inc}$ .

### 5.7.2 Rule of surface erosion

The speed of the moving boundary is calculated in the same way with Thombre and Himmelstein (1984) suggested. For a pixel in contact with the surrounding medium,  $S(i, j, t)$  is changed to zero when its volume is reduced to zero through Eq. 5.6 which can be shown as

$$V_{cell} = V_{cell} - \frac{dV}{dt} A dt \quad (5.9)$$

$$S(i, j, t) = 0 \quad \text{if} \quad V_{cell} = 0 \quad (5.10)$$

### 5.7.3 Rate equation for oligomer and drug diffusion

Oligomers are capable to diffuse through the polymeric matrix. Assuming Fick's law for diffusion, the oligomer concentration,  $C_{ol}$ , is governed by (Sevim and Pan, 2016)

$$\frac{\partial C_{ol}}{\partial t} = \frac{\partial R_{ol}}{\partial t} + \frac{\partial}{\partial x} \left( D_{ol,x} \frac{\partial C_{ol}}{\partial x} \right) + \frac{\partial}{\partial y} \left( D_{ol,y} \frac{\partial C_{ol}}{\partial y} \right) \quad (5.11)$$

in which  $D_{ol,x}$  and  $D_{ol,y}$  are the diffusion coefficients in x and y-directions. Here the current oligomer concentration,  $C_{ol}$  is coupled back to Eq. 5.3.

The diffusion coefficients depend on the local porosity of the polymer matrix. They are also hugely affected by the way in which the pores are connected locally, i.e. the diffusion coefficients have very different values in different directions. Two "porosities",  $\varepsilon_x$  and  $\varepsilon_y$  are introduced to reflect the direction dependence such that (Pan, 2014)

$$D_{ol,x} = D_{ol,poly} + (1.3\varepsilon_x^2 - 0.3\varepsilon_x^3)(D_{ol,pore} - D_{ol,poly}) \quad (5.12)$$

and

$$D_{ol,y} = D_{ol,poly} + (1.3\varepsilon_y^2 - 0.3\varepsilon_y^3)(D_{ol,pore} - D_{ol,poly}) \quad (5.13)$$

in which  $D_{ol,poly}$  and  $D_{ol,pore}$  represents the diffusion coefficients in fresh bulk polymer and in water filled pores respectively. A local “porosity” in a particular direction is defined as the fraction of eroded pixels over a pre-defined number of pixels,  $2n_{range}$ , vertical to that direction.  $\varepsilon_x$  and  $\varepsilon_y$  are therefore calculated as

$$\varepsilon_x(i, j, t) = \frac{1}{2 \times n_{range} + 1} \sum_{j=j-n_{range}}^{j=j+n_{range}} S(i, j, t) \quad (5.14)$$

$$\varepsilon_y(i, j, t) = \frac{1}{2 \times n_{range} + 1} \sum_{j=j-n_{range}}^{j=j+n_{range}} S(i, j, t) \quad (5.15)$$

The mass loss  $W_t$  is calculated by summation of mass losses due to short chain diffusion,  $W_d$ , and erosion,  $W_e$ , such as

$$W_t = W_d + W_e. \quad (5.16)$$

## 5.8 The numerical procedure

This section provides the details of the computer implementation of the numerical methods for determining a solution to the proposed model. Options can be specified by turning on and off the certain portions of the code to investigate the effects of the involved mechanisms separately. Switching between the reaction-diffusion, surface erosion and bulk erosion are possible through the use of the selections. The codes developed are provided in Appendix C.

The central finite difference scheme is used for spatial discretization of the second term on the right hand side in Eq. 5.11. The time integration is performed

by using the direct Euler scheme, i.e. values of  $R_s$  and  $C_K$  at  $t=t+\Delta t$  can be calculated as

$$R_s(t + \Delta t) = R_s + \frac{dR_s}{dt} \Delta t \quad (5.17)$$

$$C_{ol}(t + \Delta t) = C_{ol} + \frac{dC_{ol}}{dt} \Delta t \quad (5.18)$$

It is assumed that  $C_{ol}(i, j, 0) = 0$  and  $R_s(i, j, 0) = 0$  at  $t=0$ . Perfect sink conditions are assumed at the interface between the polymer and its surrounding medium, which requires that  $C_{ol} = 0$  at the interfaces. Numerical convergence is obtained by gradually increasing the number of pixels and decreasing the time step.

The tablet domain is initially indicated by solid boundaries in Fig. 5.3. The moving boundaries are indicated by dashed lines. Moving boundaries are only the case when the surface erosion is in the game. New locations of the moving boundaries are labelled as  $x_e$  and  $y_e$  in the figure. In the simulations, no new boundary has been defined at new locations because of the characteristic of the problem. This is because when we consider Eq. 5.12 and 5.13, the diffusion coefficients remain at  $D_{ol,pore}$ , for fully eroded surface, which is a very large number (taken by consideration of diffusion of oligomers in water). This makes concentration at the new boundary identical with the initial boundary. To sum up, the diffusion coefficient acts as a state variable, preventing the need for a time dependent boundary condition.

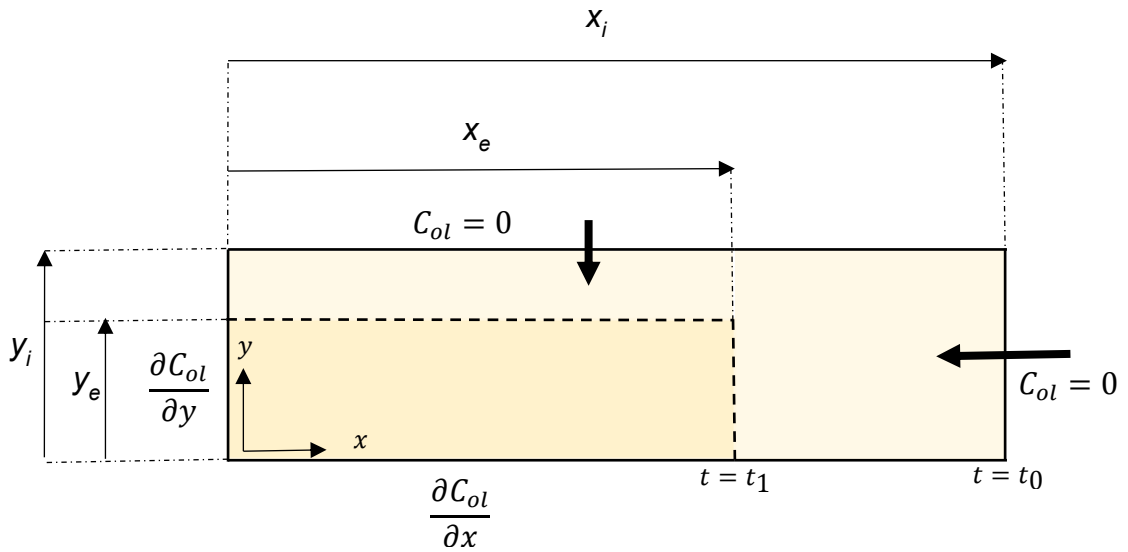


Fig. 5.3 Moving boundaries at different times and boundary conditions

It is assumed that there is no oligomer at the grids initially and no chain scission started at  $t=0$ , which can be represented mathematically as  $C_{ol}(i, j, 0) = 0$  and  $R_s(i, j, 0) = 0$ . Moreover, it is assumed that a combination of random and end chain cleavage occurred in degradation. By virtue of the boundary conditions only upper and right side of the plate is exposed to the release medium. Perfect sink conditions are assumed for these surfaces that requires  $C_{ol}(n_x, j, t) = 0$  and  $C_{ol}(i, n_y, t) = 0$ . For the boundaries isolated from the solution it is assumed that,  $C_{ol}(1, j, t) = C_{ol}(2, j, t)$  and  $C_{ol}(i, 1, t) = C_{ol}(i, 2, t)$ ;  $R_s(1, j, t) = R_s(2, j, t)$  and  $R_s(i, 1, t) = R_s(i, 2, t)$ .

With the defined initial and boundary conditions the equations are then solved numerically by use of finite difference method and spatiotemporal evaluations of the polymer matrix are determined. The simulated grid is spatially discretized into nodes in order to apply central finite difference method and the time integration is performed by use of direct Euler scheme. The plate is divided into  $i$ -space intervals in  $x$  direction and into  $j$ -space intervals in  $y$  direction. A very small time step is used in calculations ( $\Delta t=0.5s$ ). Numerical convergence is tested by gradually increasing the number of nodes and decreasing the time step. For each grid point, polymer chains scission and oligomer production is modelled using

degradation model mentioned above. Meanwhile, the surface erosion acts in a way to constantly leads to plate shrinking. For the interior pixels, as soon as, molecular weight reaches to a critical value,  $M_{n,critical}$ , and next to a hole, its lifetime decreases and grid is counted as eroded when it consumes all the volume. By considering the stated algorithm, concentration profiles, molecular weight changes, porosities and mass losses at  $t=0+\Delta t$ ,  $0+2\Delta t$  can be calculated consecutively. The simulations are performed in supercomputer, which took approximately 100 hours when utilizing 1 processor of the supercomputer. Fig. 5.4 shows the algorithm flow chart of the combined model developed in this chapter. The codes of the FORTRAN program are provided in Appendix C.

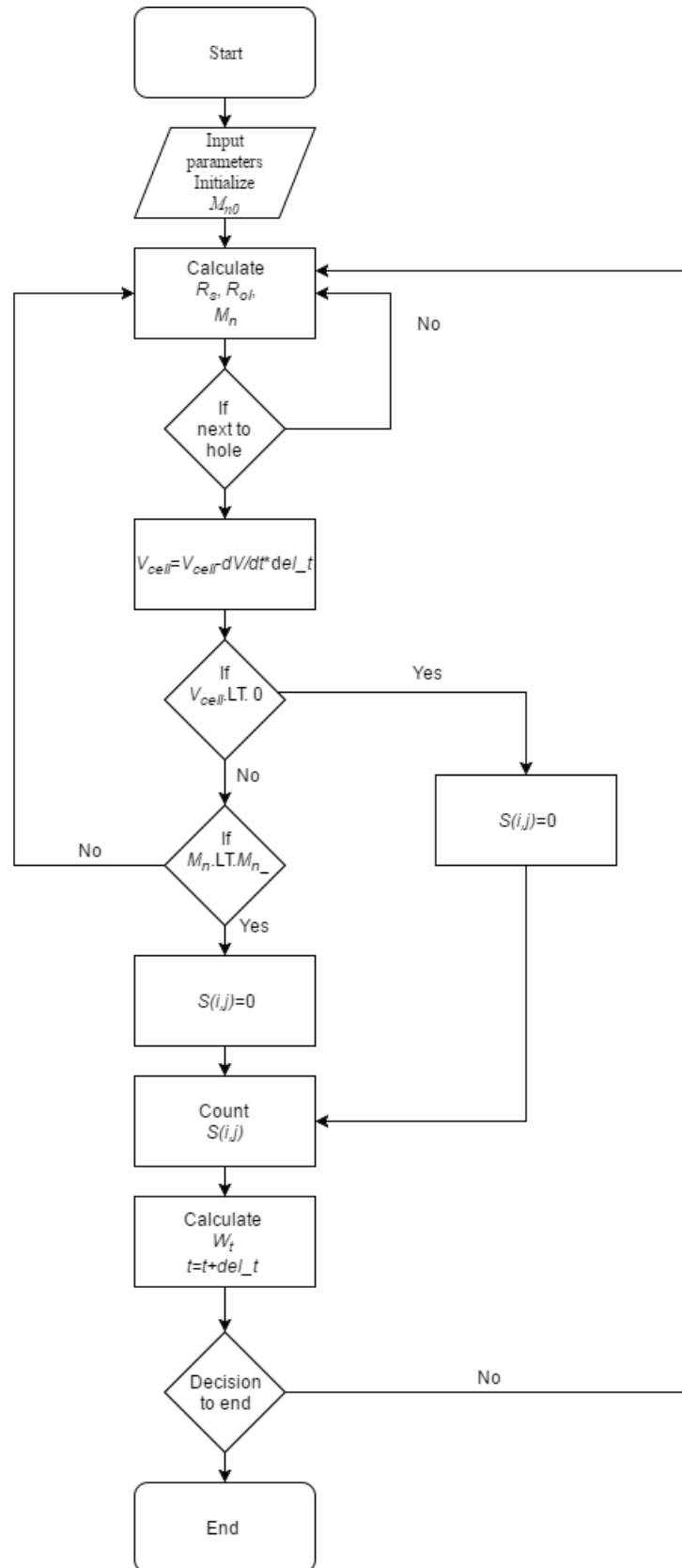


Fig. 5.4 Flow chart of the combined degradation-diffusion and erosion model

## 5.9 Different behaviors of mass loss that can be obtained using the combined model

The mathematical model developed here can be used to establish the conditions under the each mechanism: degradation-diffusion, surface erosion, interior erosion without incubation period, interior erosion with incubation period. Scenarios for each mechanism or different combinations of the mechanisms are shown in Fig. 5.5 to 5.10. An infinitively large plate is considered in the simulations. The following model parameters are used to generate figures which are broadly based on experimental data from Wang et al. (2006). The values of molecular weights are set as  $M_{n,mean}=7.5 \times 10^4$  g/mol,  $M_{n,st\_dev}=2.0 \times 10^4$  g/mol,  $M_{n,critical}=2.7 \times 10^4$  g/mol  $M_{unit}=65$  g/mol. The size of the representative unit of the plate is taken as  $80 \times 320 \mu\text{m}$ .  $D_{ol,poly}=5.0 \times 10^{-15}$  m<sup>2</sup>/week and  $D_{ol,pore}=1.0 \times 10^{-8}$  m<sup>2</sup>/week. The rate of surface erosion is set as  $B = 6.5 \times 10^{-14}$  m<sup>2</sup>/week and hydrolysis reaction constants are set as  $k_1=5.0 \times 10^{-6}$  week<sup>-1</sup>,  $k_2=2.0 \times 10^{-2}$  m<sup>3</sup> mol<sup>-1</sup> week<sup>-1</sup>. The number of pixels in x- and y-directions,  $n_x, n_y$ , are set as 250 x 1000. The values of parameter  $C_{e,0}$ ,  $m$ ,  $\alpha$  and  $\beta$  were obtained from Pan et al. (2014).

For the sake of comparison, all the simulations were terminated at 30 days. The model is first established to calculate the mass loss from the reaction-diffusion equations (Fig. 5.5). All other contributions to the mass loss are switched off in order to assess the effect of diffusion on mass loss.

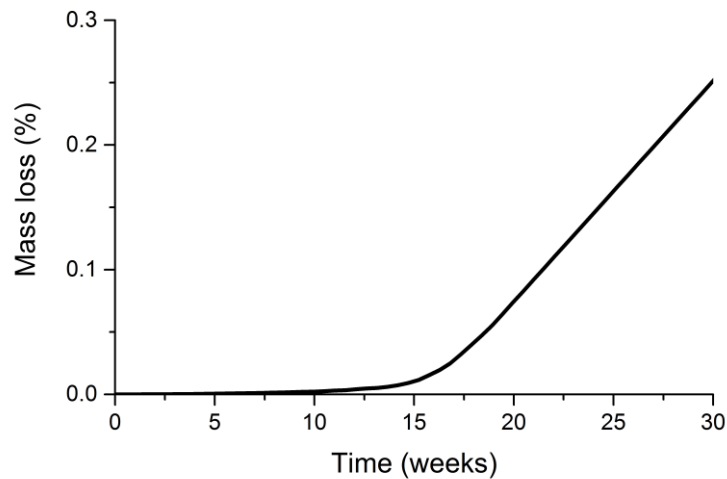


Fig. 5.5 Mass loss due to diffusion of short chains

It can be observed from Fig. 5.5 that the short chain diffusion accounts for 0.3 % of total polymer weight (0.3 wt. %). Sample shows a zero mass loss for a long period followed by a rapid increase at week 10. This is attributed to the fact that the soluble chains are unable to diffuse out of the matrix unless polymer is degraded to a certain degree. However, even at the later stages of degradation, short chains has only very little contribution to mass loss. The reason for such a small contribution is due to the fact that diffusion coefficient through polymer bulk is set as very small; which has been assigned deliberately by considering the diffusion coefficients used in the literature for short chain diffusion in polymer bulk.

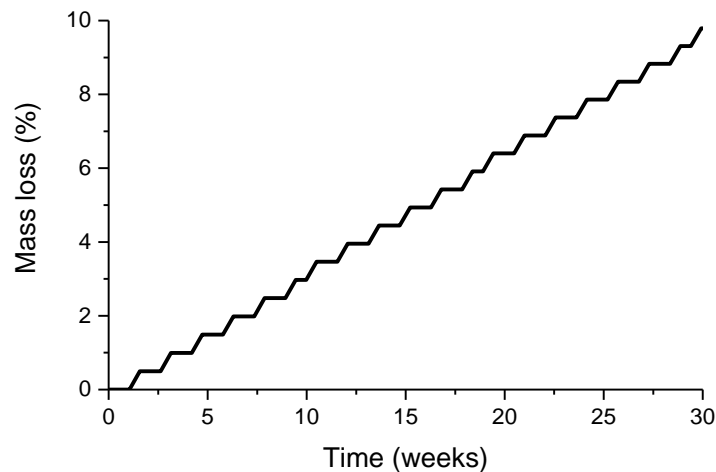


Fig. 5.6 Mass loss due to surface erosion

Fig. 5.6 shows mass loss due to surface erosion. Surface erosion starts at  $t=0$ , with a constant speed which leads to shrinking of the device. 15% mass loss is reached with the specified speed. The contribution of the surface erosion can be controlled by changing the speed of moving boundary. The sudden jumps in the figure are related to the characteristic of the surface erosion model and can be explained with the theory that a pixel cannot be eroded until it consumes its volume. The analyses are repeated with smaller mesh size and short time step to reflect the convergence of the model.

Fig. 5.7 shows the mass loss when the interior erosion is in action. The sample demonstrates a zero mass loss followed by a dramatic release of oligomers. The zero mass loss at the early stages of interior erosion can be explained by the fact that it takes time for chains to reach the critical molecular weight. The other reason might be that although interior pixels reach to the critical molecular weight, they need to be in contact with an eroded neighbour to be able to release. As soon as both of the criteria are satisfied, the interior pixels erode swiftly leading to an enormous mass loss.

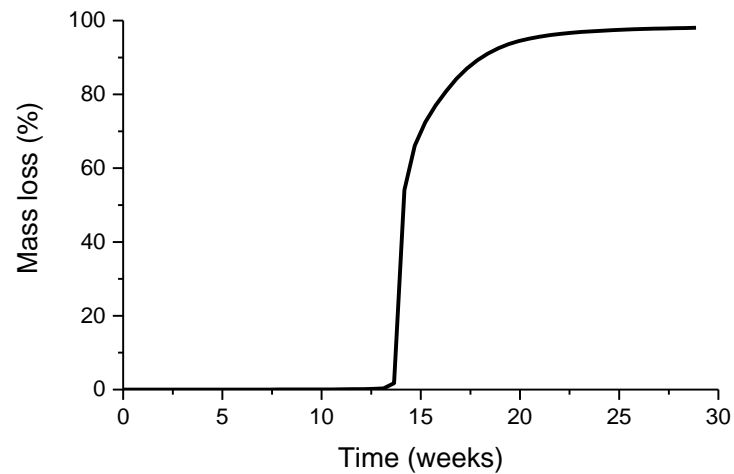


Fig. 5.7 Mass loss due to interior erosion

In some of the experimental studies in the literature (Li *et al.*, 1990a, Li *et al.*, 1990b), the mass loss trend follows a smooth curve after a zero mass loss. To be able to explain such mechanisms, an option of an incubation period,  $t_{inc}$ , for the polymer erosion is also introduced into the model to reflect observed mass loss behaviour. For this type of profiles, pixels must meet the third criteria in addition to first two: the incubation period should be exceeded to release the oligomers. By assuming the incubation period as 0.5 weeks, the mass loss profile is represented in Fig. 5.8. The slope of the curve can be controlled by the change in the incubation period.

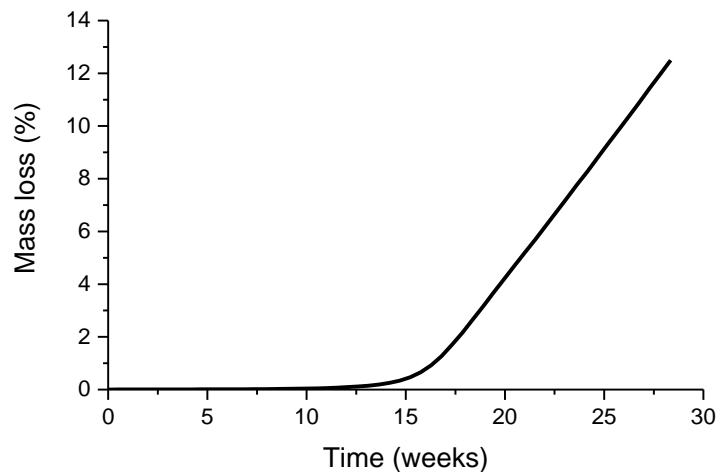


Fig. 5.8 Mass loss due to interior erosion with incubation period of 0.5 weeks

The introduction of an incubation period for interior erosion produces the mass loss trend shown Fig. 5.8 that is most widely observed in the literature. The trend is achieved by assuming that a polymer of very low molecular weight cannot dissolve immediately when being in contact with water.

A summary of the mass loss profiles for individual mechanisms is plotted in Fig. 5.9. This kind of representation can be practical to assess the mechanisms involved in a degrading-eroding polymer. However, the mass loss profiles in the literature indicate that the various combinations of these mechanisms can be required in order to explain the observed mass loss trends. Fig. 5.10 shows the scenario for the combination of all the above mechanisms. These are degradation, diffusion, surface erosion and interior erosion with incubation period of 0.5 weeks. Up to week 13, surface erosion is dominated to the other mechanisms by representing a characteristic linear mass loss. Beyond that, surface erosion and interior erosion with incubation period are responsible with the observed profile. Since more than one mechanism is involved, it is expected to observe such a biphasic mass loss trend. By considering all the profiles mentioned, it can be concluded that the bolus oligomer release towards the end

of degradation is identical to the interior erosion. A more comprehensive discussion is presented in the next chapter of this thesis.

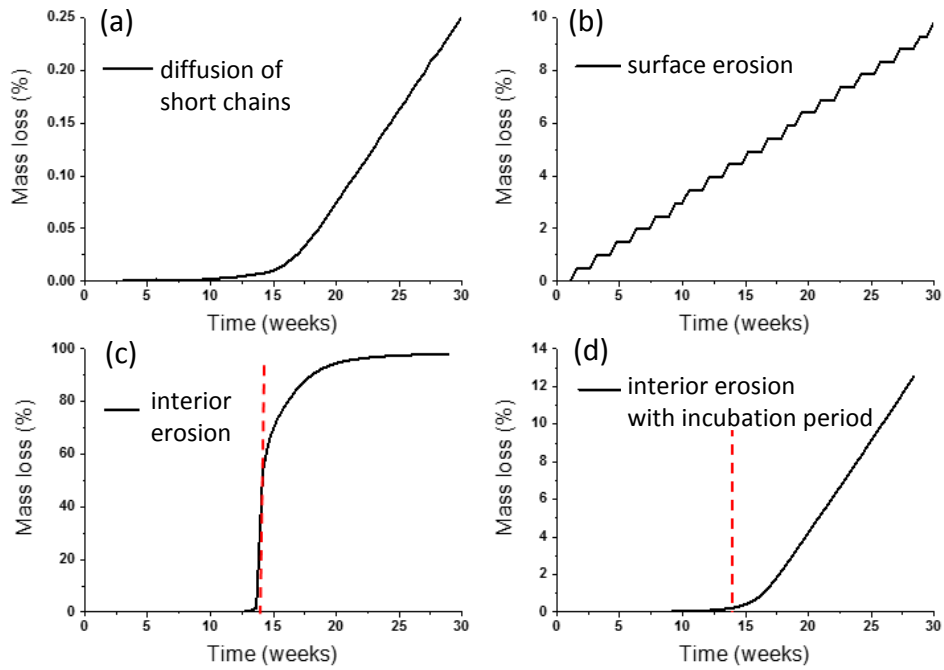


Fig. 5.9 A summary of the mass loss profiles due to individual mechanisms

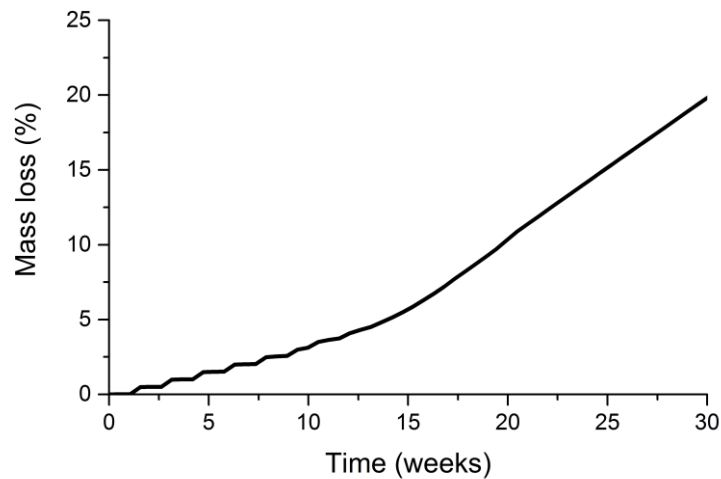


Fig. 5.10 Combined effect of all the mechanisms on mass loss: degradation-diffusion (5.9(a)), surface erosion (5.9(b)), interior erosion with incubation period of 0.5 weeks (5.9(d))

The combined model is able to capture the mass loss profiles of diffusion, surface erosion, interior erosion or interior erosion with incubation period. The key point here is to identify and understand particular mechanisms involved in the mass loss. The contribution of that mechanisms can be more or less dominant or completely uninvolved for the special cases. Often, more than one mechanism is involved at a given time or different mechanisms can dominate at different stages of mass loss as can be seen from Fig. 5.10. This has been succeed in the simulations by switching on and off the relevant mechanisms and controlling the speed of the involved mechanisms in the current model.

## 5.10 Conclusion

A combined mathematical model is developed in this chapter to simulate the degradation-erosion process of PLA/GA polymers. In the model, surface erosion and degradation initiates concurrently at  $t=0$ . Degradation equations feed molecular weight values to the erosion part. As soon as a pixel reaches to the critical molecular weight and has an eroded neighbor, interior erosion acts. Heterogeneity of polymer matrix is also considered by calculation of the porosities separately for each axial direction. The model calculates porosities in

a range rather than averaging them along the axis. Using the model, chain cleavage, diffusion, erosion and hole formation can be simulated in a single model.

The key finding of this study is that, the early mass losses with constant rate is an indicator of surface erosion, while the bolus mass losses after a certain time are indicative of interior erosion. For the cases including bolus mass loss with a smoother profile, one can claim that the interior erosion is functioning with an incubation period. Incubation behaviour is a general and important factor that has to be considered when understanding the degradation of aliphatic polyesters. Diffusion individually does not have a big contribution to the mass loss. The method used here is a very useful way to explain the different kind of mass loss profiles by considering all the sources that can contribute to the mass loss. Turning on and off the certain portions of the code provides a clear picture of how each particular mechanism is involved in the mass loss.

## Chapter 6. Case studies of polymer degradation using combined hydrolytic degradation and erosion model

In this chapter, the full model presented in Chapter 5 was applied to several case studies in the literature. For convenience, a summary of the combined model is provided at the beginning of the chapter. The aim is to demonstrate the model performance for the physically meaningful cases and provide an insight into the possible mechanisms underlying each case. This has been achieved by switching on and off the involved mechanisms and controlling the contribution of each mechanism.

### 6.1 Summary of the experimental data by Grizzi *et al.* (1995) and Lyu *et al.* (2007)

Grizzi *et al.* (1995) carried out a set of experiments using PLA50 in order to compare the degradation behaviour of plates with different sizes. For this, large and thin plates were allowed to age under iso-osmolar phosphate buffer solution, pH 7.4 at 37°C. The thicknesses of the samples are given as 15x10x2 mm and 15x10x0.3 mm and  $M_n=20000 \text{ gmol}^{-1}$  and  $34000 \text{ gmol}^{-1}$  for plates and films respectively. The level of degradation is monitored by molecular weight and mass loss change. Their experimental results are reproduced using the discrete symbols in Fig. 6.3 and Fig. 6.4, in which number average molecular weight and mass loss are shown as functions of time. The mass loss showed a sudden increase after an initial zero mass loss. For thin device this trend is much smooth compared to the thick plate. The greater thickness of the device showed a faster degradation. A quantitative discussion was made which revealed considerable insight into that degradation of the devices depends very much on size.

Lyu *et al.* (2007) studied the hydrolysis kinetics of amorphous poly(L-lactide-co-L, D-lactide) (70/30) co-polymer. In their study, they compared the 2<sup>nd</sup> order and 3<sup>rd</sup> order kinetic models with their experimental data. Moreover, the temperature effect on the hydrolysis of PLA is tested over a range 37°C to 90°C in a phosphate buffered solution (pH 7.4). Number average molecular weight of

the moulded samples is given as 290000 gmol<sup>-1</sup>. The test samples were discs 12.5 mm in diameter and 1 mm in thickness. The degradation results are shown as the change in  $M_n$  and mass loss as functions of time. The authors reported that the experimental results do not follow 2<sup>nd</sup> or 3<sup>rd</sup> order reaction kinetics. It has been suggested that the short chains does not have enough mobility in the early stages of degradation to act as the catalysis for the hydrolysis reaction. This suggestion was completed with the need for alternative models into the diffusion limited degradation. Here we use the model presented in Chapter 5 to analyse the underlying mechanisms of Grizzi *et al.* and Lyu *et al.*'s experimental data.

## 6.2 Summary of the combined model

The equations for combined degradation-erosion model are provided here for the convenience of the reader

### Chain scission

$$\frac{dR_s}{dt} = C_{e,0} \left[ 1 - \alpha \left( \frac{R_s}{C_{e,0}} \right) \right] \left( k_1 + k_2 \left[ K_a \left( \frac{C_{ol}}{m} \right) \right]^{0.5} \right) \quad (6.1)$$

$$\frac{dR_{ol}}{dt} = \alpha \beta \left( \frac{R_s}{C_{e,0}} \right)^{\beta-1} \frac{dR_s}{dt} \quad (6.2)$$

$$M_n = M_{n,0} \frac{1 - \alpha \left( \frac{R_s}{C_{e,0}} \right)^\beta}{1 + N_{dp,0} \left( \frac{R_s}{C_{e,0}} - \frac{a}{m} \left( \frac{R_s}{C_{e,0}} \right)^\beta \right)} \quad (6.3)$$

### Surface erosion

$$\frac{dV(t)}{dt} = -B \quad (6.4)$$

$$V_{cell} = V_{cell} - \frac{dV}{dt} * dt \quad (6.5)$$

$$S(i, j, t) = 0 \quad \text{if} \quad V_{cell} = 0 \quad (6.6)$$

### Interior erosion

$$S_m(i, j, t) = 0 \quad \text{if } M_n < M_{n,critical} \quad (6.7)$$

$$S(i, j, t) = 0 \quad \text{if } S_m(i, j, t) = 0 \quad \text{and the pixel has an eroded neighbour} \quad (6.8)$$

### Diffusion

$$\frac{\partial C_{ol}}{\partial t} = \frac{\partial R_{ol}}{\partial t} + \frac{\partial}{\partial x} \left( D_{ol,x} \frac{\partial C_{ol}}{\partial x} \right) + \frac{\partial}{\partial y} \left( D_{ol,y} \frac{\partial C_{ol}}{\partial y} \right) \quad (6.9)$$

$$D_{ol,x} = D_{ol,poly} + (1.3\varepsilon_x^2 - 0.3\varepsilon_x^3)(D_{ol,pore} - D_{ol,poly}) \quad (6.10)$$

$$D_{ol,y} = D_{ol,poly} + (1.3\varepsilon_y^2 - 0.3\varepsilon_y^3)(D_{ol,pore} - D_{ol,poly}) \quad (6.11)$$

Equations 6.1 to 6.11 provide a summary of the model which combines chain scission, surface erosion, interior erosion, and diffusion.

- ✓ Eq. 6.1 gives the autocatalytic chain scission rate for the amorphous polymer.
- ✓ Eq. 6.2 relates oligomer production rate with the chain scission.
- ✓ Eq. 6.3 relates the number of chain scission with the molecular weight.
- ✓ Eq.s 6.4-6.6 determine whether a pixel is surface eroded or not by considering the remaining volume of the cell. Pixels can be only surface eroded if they are in contact with the aqueous medium.
- ✓ Eq.s 6.7-6.8 determine whether a pixel is bulk eroded or not by checking two main criteria of interior erosion: rather molecular weight is below the critical value and pixels are in contact with an eroded neighbour.
- ✓ Eq.s 6.9-6.11 are used to calculate the effective diffusion coefficient of the oligomers taking into account the increasing porosity of the system. The porosities  $\varepsilon_x$  and  $\varepsilon_y$  are based on the number of eroded pixels in each direction.

### **6.3 Summary of the parameters used in the combined model**

When analyzing the experimental data, a set of parameters can be found which provides the best fitting with the model prediction. This set of parameters allows identifying the underlying mechanisms of degradation and erosion. In this section, the parameters have been varied to analyze two set of experimental

data. The selection of the case studies is done based on the fact that they require different combinations of the mechanisms to attain the best fitting. This has been established by switching on/off the mechanisms or controlling the contribution of each mechanism. The model parameters used in the fittings are provided in Table 6.1.

Table 6.1 Parameters used in the fittings

Model parameters	Units	Case study A (thick plate)	Case study A (thin plate)	Case study B
$M_{n,mean}$	g mol <sup>-1</sup>	2x10 <sup>4</sup>	3.4x10 <sup>4</sup>	2.1x10 <sup>5</sup>
$M_{n,st\_dev}$	g mol <sup>-1</sup>	5x10 <sup>3</sup>	1.5x10 <sup>3</sup>	1.5x10 <sup>5</sup>
$M_{unit}$	g mol <sup>-1</sup>	72	72	72
$k_1$	week <sup>-1</sup>	2.0x10 <sup>-4</sup>	7.0x10 <sup>-5</sup>	5.0x10 <sup>-7</sup>
$k_2$	m <sup>3</sup> mol <sup>-1</sup> week <sup>-1</sup>	1.0x10 <sup>-2</sup>	1.0x10 <sup>-2</sup>	3.0x10 <sup>-4</sup>
$m$	no unit	4	4	4
$\alpha$	no unit	0.4	0.4	0.4
$\beta$	no unit	1	1	1
$C_{e,0}$	mol m <sup>-3</sup>	17300	17300	17300
$K_a$	no unit	1.35x10 <sup>-4</sup>	1.35x10 <sup>-4</sup>	1.35x10 <sup>-4</sup>
$B$	m <sup>2</sup> week <sup>-1</sup>		0	0
$M_{n,critical}$	g mol <sup>-1</sup>	4.1x10 <sup>3</sup>	7.0x10 <sup>3</sup>	1.8x10 <sup>4</sup>
$D_{ol,poly}$	m <sup>2</sup> week <sup>-1</sup>	5.0x10 <sup>-15</sup>	5.0x10 <sup>-15</sup>	3.0x10 <sup>-15</sup>
$D_{ol,pore}$	m <sup>2</sup> week <sup>-1</sup>	1.0x10 <sup>-5</sup>	1.0x10 <sup>-5</sup>	1.0x10 <sup>-5</sup>

Here, the parameter  $m$ ,  $\alpha$  and  $\beta$  are obtained from Pan *et al.* (2014).  $C_{e,0}$ ,  $M_{unit}$  and  $K_a$  are the standard data for the polymers in the issue.  $M_{n,mean}$  is extracted and  $M_{n,critical}$  is estimated from the corresponding experimental data. The other parameters such as  $k_1$ ,  $k_2$ ,  $B$ ,  $M_{n,st\_dev}$  and  $D_{ol,poly}$  are obtained by varying the values systematically to give the best fit between the model prediction and experimental data.  $D_{ol,pore}$  is set by considering the diffusivity of species in water (Stewart, 2003). Two-dimensional plates are considered in the model. Initial oligomer concentrations are  $C_{ol} = C_{ol,0} = 0.035x C_{e,0}$  for thick plate; 0 for thin plate for Case study A; and  $0.015x C_{e,0}$  for Case study B. Symmetry is assumed across the plates, therefore, quarter models are used in the simulations, therefore sizes are set as  $a=1\text{mm}$  and  $b=5\text{mm}$  for thick plates and  $a=150\mu\text{m}$  and  $b=5\text{mm}$  for thin

plates in Case A. For case B, the values are  $a=500\mu\text{m}$  and  $b=6.25\text{mm}$ . Initial molecular weight is randomly distributed throughout the plate considering the mean values in the original study.  $M_{n,critical}$  is estimated from the case studies for amorphous polymer. In order to obtain a better fitting, a constant incubation period of 0.5 week is added to interior erosion.

## 6.4 Fittings of the combined model to experimental data

Using the mathematical model provided in Section 6.2 and the parameters provided in Section 6.3, it is now possible to suggest a mechanism for each case study.

### 6.4.1 Case study A

Fig. 6.1 shows the model results of molecular weight distribution for thick plates prior to degradation and at 1 week, 10 weeks and 13 weeks. The molecular weight is distributed to follow normal distribution prior to degradation. The distribution exhibits monomodal characteristic during the degradation and erosion processes which indicate polymer to stay in amorphous phase during the process. At  $t=0$ , the average molecular weight at the peak corresponds to the 20000. As time proceeds, the position of peaks is shifted to the left. The molecular weight distribution of thin films is shown in Fig. 6.2 prior to degradation and at 10 weeks, 18, weeks and 27 weeks. Similarly, the peaks represent a monomodal characteristic during the degradation and erosion processes.

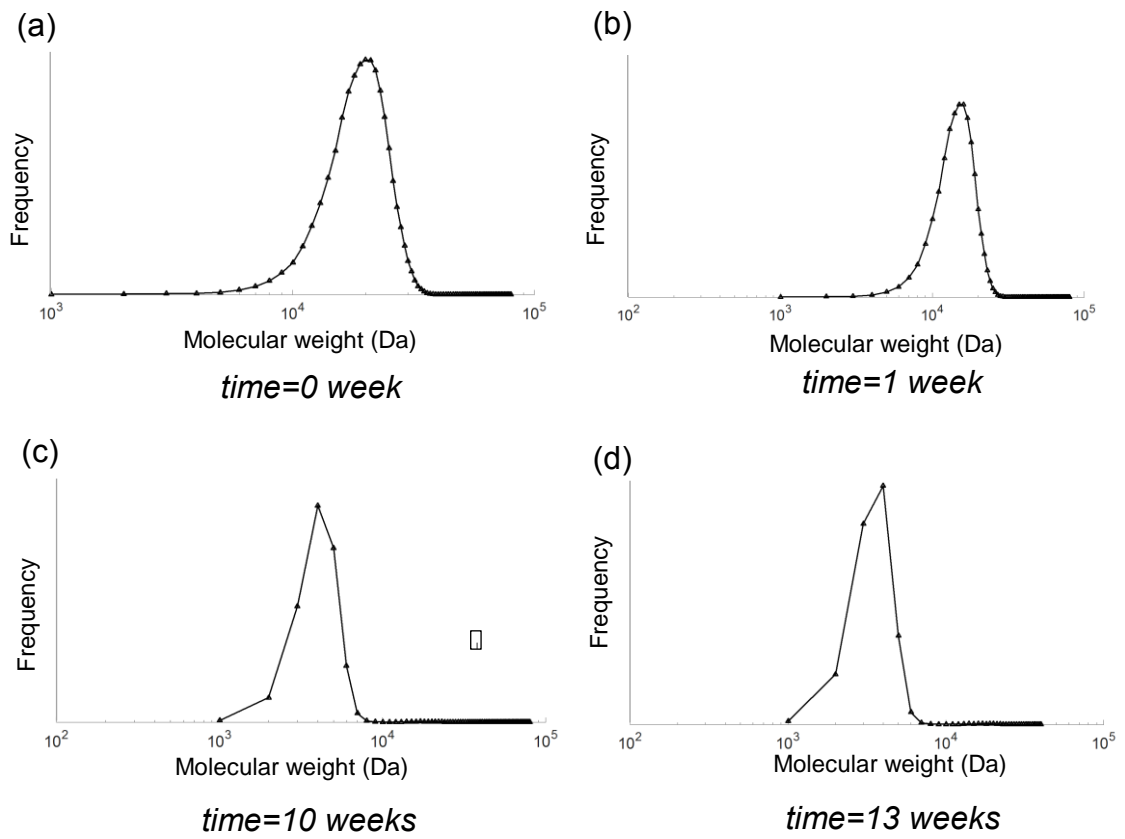


Fig. 6.1 Molecular weight distributions of plates at various times during the degradation (a)  $t=0$  week; (b)  $t=1$  week; (c)  $t=10$  weeks and (d)  $t=13$  weeks.

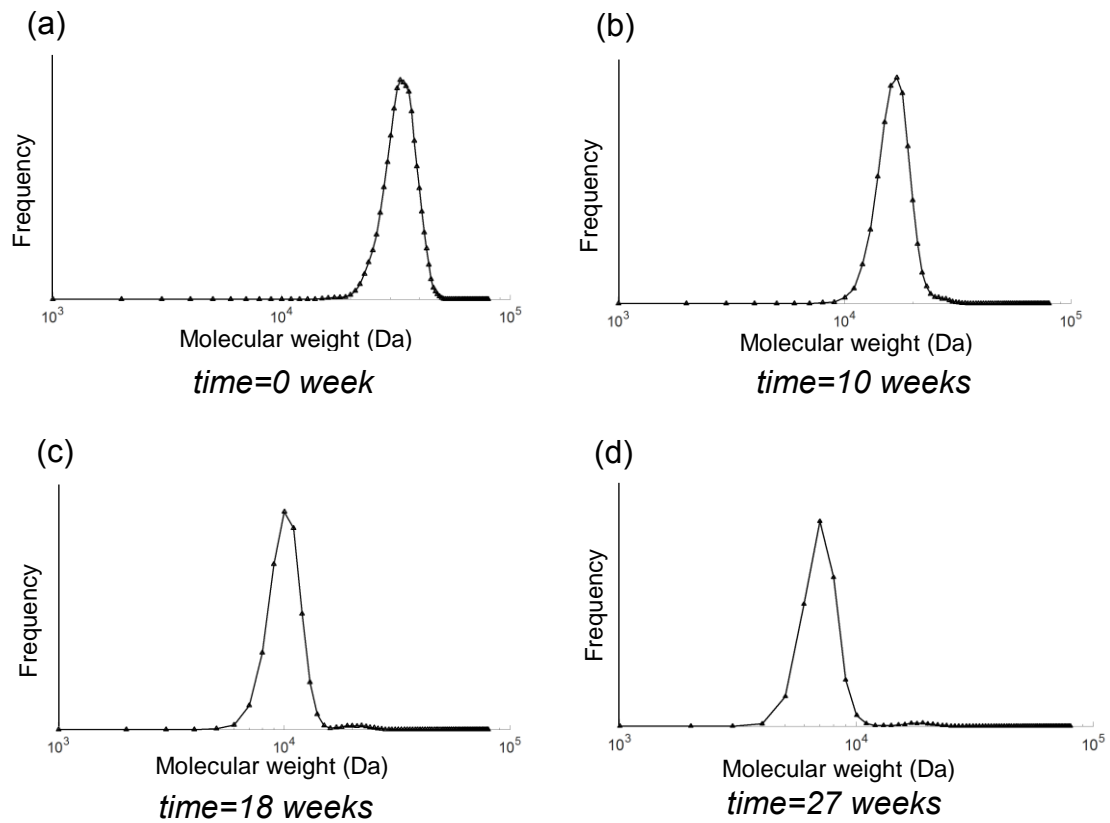


Fig. 6.2 Molecular weight distributions of plates at various times during the degradation (a)  $t=0$  week; (b)  $t=1$  week; (c)  $t=10$  weeks and (d)  $t=13$  weeks.

The best fit between the mathematical model and the experimental data is presented in Fig. 6.3 and Fig. 6.4 both for films and plates. The parameters  $n_x \times n_y$  is set as  $200 \times 1000$  for thick plates and  $30 \times 1000$  for thin plates which is compatible with the actual shape of the plates to ensure each pixel to be same the size. For thick plates, both degradation, diffusion and interior erosion are included in the numerical model. It can be observed that the model fits the experimental data for the mass loss and average molecular weight. The best fit is achieved by  $B=0$ , which indicates no surface erosion. This is reasonable since the initial mass loss is zero when considering the experimental data. The interior erosion without an incubation period is necessary for plates to produce the level of mass loss observed in the experimental study. Results show that the thick plate hits to the critical molecular weight is in 12 weeks. The greater amount of

mass loss in later stages is identical for interior erosion and produce a bolus mass loss in short period of time.

For thin plates, experimental results do represent no linear mass loss in early times of degradation. Therefore, surface erosion is again switched off in the numerical analysis for this case. However, it is obvious from the data that, there is a sudden mass loss at  $t=0$ ; which can be explained by the instant release of fabrication excess in the matrix when exposed to the medium. This instant mass loss is involved in the model; by setting 7% of initial mass loss at  $t=0$ . Similar to the thick plates, a fitting to mass loss is only possible for thin plates if interior erosion is included. However, the mass loss is much smooth for thin plates. The smooth trend is explained by interior erosion with incubation period. The best fitting is achieved by an incubation period of 0.2 weeks. As it can be observed from the figure, the time at which device hits the critical molecular weight is 27 weeks. As a summary, it can be concluded that interior erosion is the main mechanisms controlling mass loss from thick plates, while the interior erosion with an incubation period is responsible for observed mass loss for thin plates of Grizzi *et al.*'s study. A fitting to molecular weight is also presented in Fig. 6.3. The model results are also proved to be accurate in capturing the size dependent characteristic of degradation.

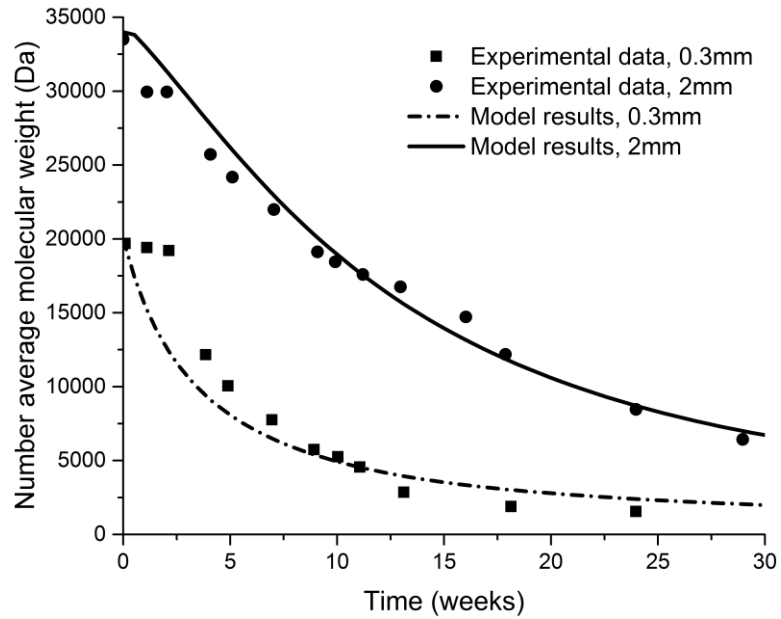


Fig. 6.3 Comparison of molecular weight change between model prediction and experimental data for samples with thickness of 0.3 mm and 2 mm. The solid and dashed lines represent the model predictions with the discrete symbols representing the experimental data (Grizzi *et al.*, 1995).

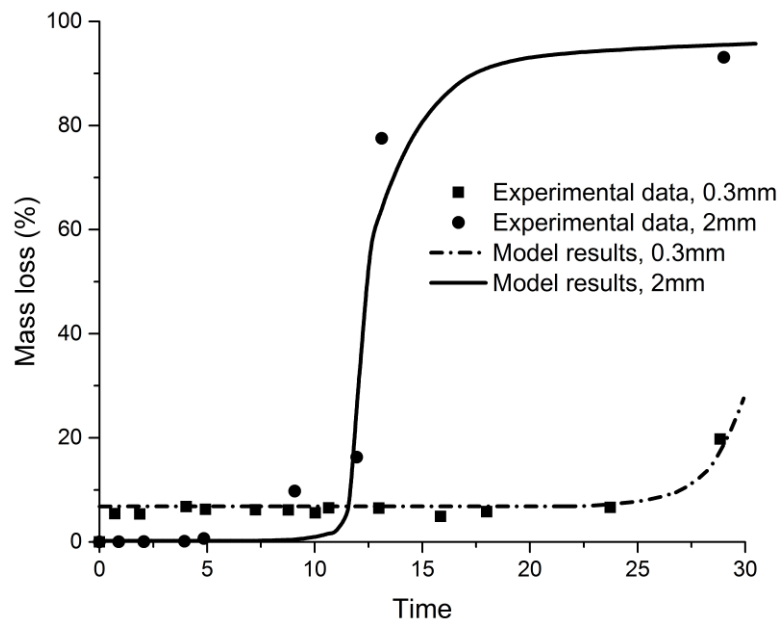


Fig. 6.4 Comparison of molecular mass loss between model prediction and experimental data for samples with thickness of 0.3 mm and 2 mm. The solid and dashed lines represent the model predictions with the discrete symbols representing the experimental data (Grizzi *et al.*, 1995)

Li *et al.* (1990c) conducted degradation experiments of PLA/GA specimens and observed specimens to be heterogeneous after degradation. Fig. 6.5 shows the cross section of their specimens after 10 days of degradation in distilled water. They observed a clear whitish layer at the surface and the hollow structure inside indicating a surface-centre differentiation of the specimens. The hollow structure inside the specimens can be well explained by the model proposed in this chapter. The time series of the representative thick plate that we obtained when the procedure was applied is represented in Fig. 6.6. Here, white pixels represent non-eroded polymer areas and black pixels, the eroded polymer areas. Obviously, there is no interior erosion until week 11, since the pixels are above critical molecular weight before that time. When grids reach to the critical value, erosion starts from the surface and quickly connects to the more degraded inner core. Fig. 6.6 shows that even after long erosion times there is still a clear skin layer in the upper and right-side lines forming a clear shell for the grids in contact with the aqueous environment. This finding agrees well with the experimental data obtained by Li *et al.* (1990c). By expanding the grid into 3-dimension, it can be visualized that the remainders form an interconnected network which is quite porous. Burkersroda (2002) also discussed that issue with the break of the surface layer at some point when a critical osmotic pressure builds up inside the matrix due to the accumulation of degradation products. That theory is explained with percolation phenomena which are based on the fact that degradation products cannot leave the matrix unless a critical degree of degradation is reached. The polymer then forms a network of pores to allow the release of degradation products which are accumulated inside the matrix. Percolation phenomena explain the hollow core surrounded by a whitish layer which is shown in Fig. 6.6.

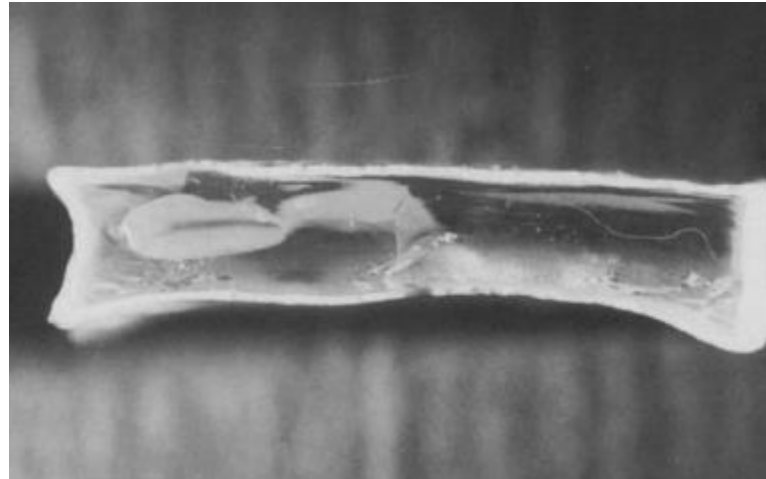


Fig. 6.5 Hollow structure of PLA37.5GA25 specimen after 10 days of degradation in distilled water (Li *et al.*, 1990c) with permission via the Copyright Clearance Centre.

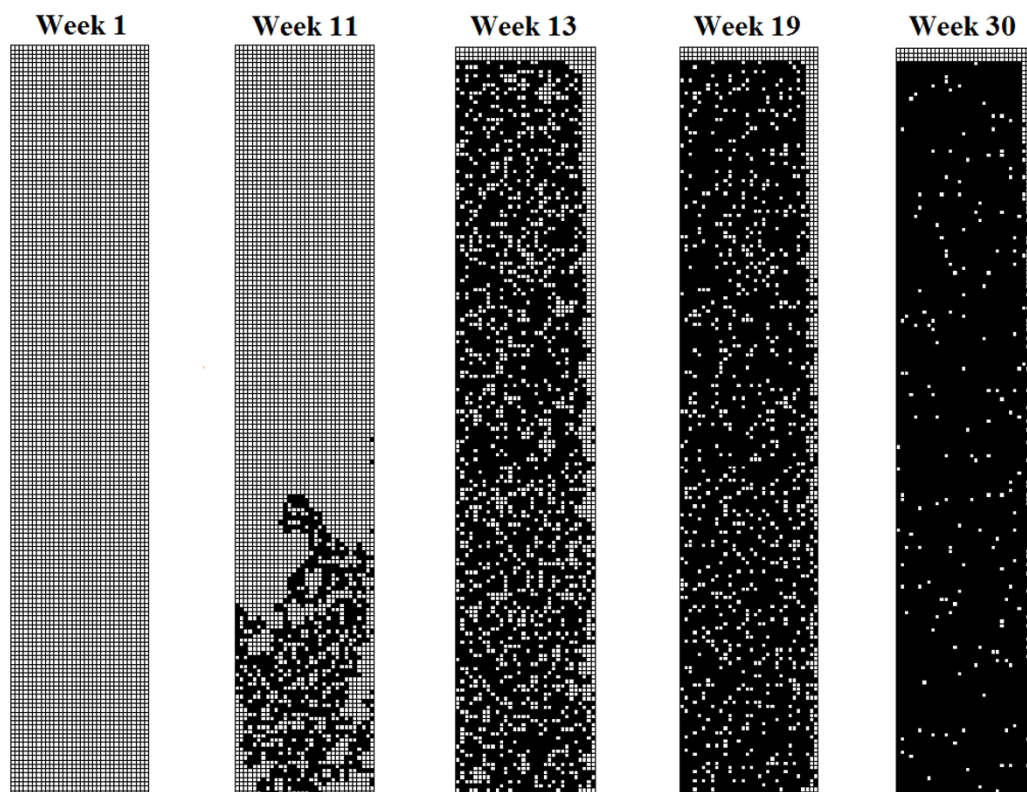


Fig. 6.6 Temporal evaluation of simulated the polymer matrix

### 6.4.2 Case study B

The solid lines Fig. 6.7 and Fig. 6.8 show the best fitting of the model, with the parameters provided in Table 6.1. The parameters  $n_x \times n_y$  is set as 100 x 1250 which is compatible with the actual shape of the plate to ensure each pixel to be same the size. Model again fits the experimental data. The best fitting observed by setting  $B=0$ , which indicates surface erosion is switched off in the simulations. The plates reach the critical molecular weight at 65 weeks, beyond which mass loss initiates. The fast mass loss indicates that interior erosion is the active mechanism. Therefore, no incubation period is attributed to the simulations. The main mechanisms responsible for the observed mass loss is interior erosion for this case. The value of  $D_{ol,poly}$  is chosen to give the best model fitting.  $D_{ol,poly}$  has no significant effect on mass loss as expected; however, determines the level of degradation. Again the qualitative analysis scheme has been shown to be successful to identify the mechanisms dominated during the degradation experiments.

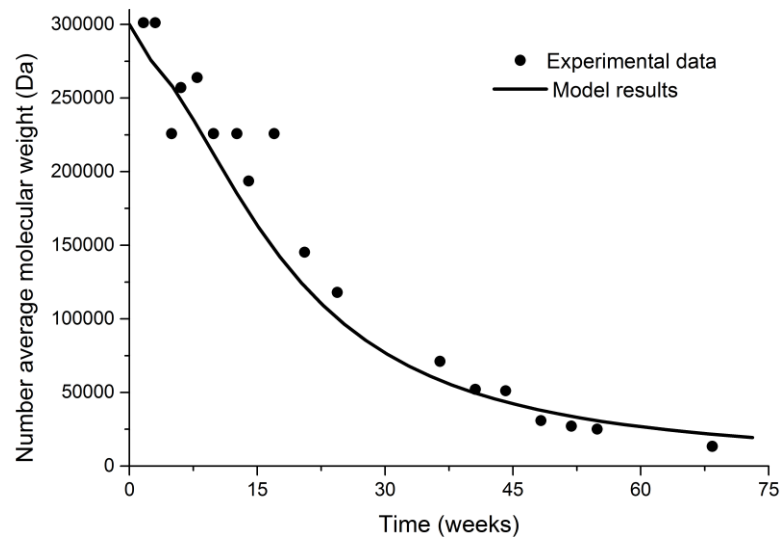


Fig. 6.7 Comparison of molecular weight change between model prediction and experimental data. The solid line represents the model prediction with the discrete symbols representing the experimental data (Lyu *et al.*, 2007)

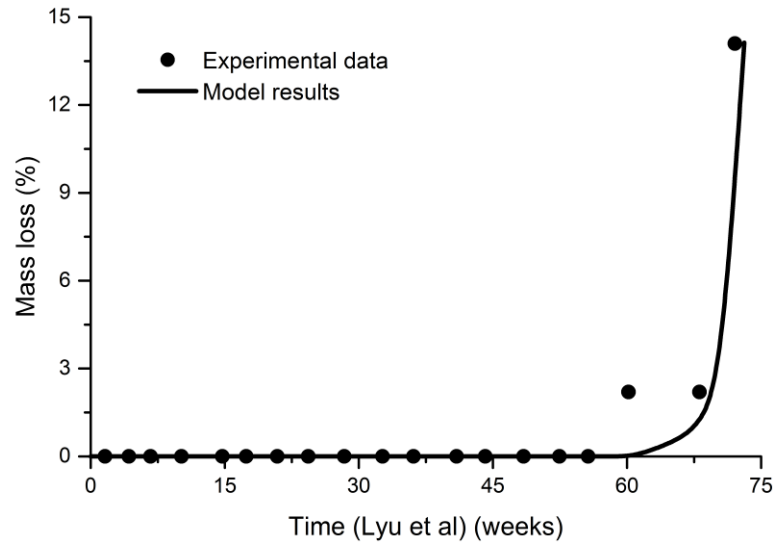


Fig. 6.8 Comparison of mass loss between model prediction and experimental data. The solid line represents the model prediction with the discrete symbols representing the experimental data (Lyu *et al.*, 2007)

## 6.5 Conclusion

In this chapter, the mathematical model developed in Chapter 5 was validated by two independent case studies from the literature. The case studies were chosen considering that they require different combinations of degradation, diffusion, surface erosion and interior erosion. The parameters were determined by varying them in a range in order to obtain the best fitting. Therefore, one can claim that the model presented in the chapter is a mechanistic model as well as being a parameter estimation problem. The model proved to be accurate in predicting the molecular weight distribution, change in molecular weight and mass loss efficiently. The high level of fitting accuracy indicates the model's ability to fit various experimental data sets detailed in the literature. Moreover, the temporal evolution of fragmentation stages of the polymer matrix is presented, which has proved to be consistent with the theories demonstrated by literature. The method used here effective to capture the large mass losses and the model results offer physical insight into the experimental studies. Moreover, the computational model presented here can be a useful tool in the estimation of the relation

between degradation and erosion processes and has shown to be a very useful way to theoretically capture enormous mass losses.

## **Chapter 7. Case studies of drug release from stents using the combined hydrolytic degradation and erosion model**

The release kinetics of drugs dissolved within a polymeric matrix layer generally follows a multiphasic release mechanism. This mechanism includes a diffusion controlled phase, a degradation controlled phase and/or an erosion-controlled phase. In this chapter, the full model presented in Chapter 5 is extended in a way to cover the presence of drug. The modified model is validated with a case study identifying the degradation and drug release from PLGA stent coating. Different drug loadings are modelled to identify whether the model can indeed capture the experimental results. The mathematical model is used to understand the underlying mechanisms of drug-eluting stents.

### **7.1 Introduction**

A coronary stent is a metal tube that is inserted into the arteries at the locations of narrowing and acts as a supporting material to the blood vessels. The stents can be either a balloon expandable or a self-expandable stent. The former functions under the pressure of the balloon; while self-expandable stents work when the sheath is retracted. For both of the cases, the stent provides support to the artery and keeps the artery open (Migliavacca *et al.*, 2004). The coronary stents are generally grouped as bare metallic stents (durable stents), coated metallic stents, biodegradable stents and drug eluting stent. Drug eluting stents with durable polymer coatings reduce the rates of target lesion compared to the durable stents. However, the problem of late stent thrombosis remains a high risk in most of the populations (Bangalore *et al.*, 2013).

The fully degradable drug eluting stents, in which the stent is made from biodegradable polymers have great potential for delivering drugs into human coronary arteries. The device enables prolonged delivery of the drugs. Currently, sirolimus and paclitaxel are the only drugs used in drug eluting stents approved by the Food and Drug Administration (Acharya and Park, 2006). Both are big

molecules ( $M_w$ : 914.19 g/mol, sirolimus and 853.96 g/mol, paclitaxel (Ultra, 2001)) and have very low solubility in aqueous solution (logP: 4.3, sirolimus and 3.2, paclitaxel (Wishart *et al.*, 2006)). Therefore, the release of these drugs from the polymers are extensively governed by degradation and erosion mechanisms. The polymers commonly used for that purpose include the PLA/GA group of biodegradable polymers (Wang *et al.*, 2006, Zhu *et al.*, 2014). Particularly PLGA copolymers are well recognized for their suitability in drug eluting stents due to administering a complete drug release by virtue of degradation and erosion of polymer matrix (Zhu and Braatz, 2015). There are several study in the literature suggesting drug release mechanisms from biodurable stent coatings such as the models considering the drug-vascular tissue interactions (Hossainy and Prabhu, 2008), analytical solutions for drug diffusion in one dimensional wall (Pontrelli and de Monte, 2010) and mechanics and fluid dynamic simulations considering stent expansion and interaction with coronary artery (Zunino *et al.*, 2009). However, there is limited work in mathematical models quantifying drug release from biodegradable and bioerodible stents. Most of the models suggested so far describe the drug release based on degradation only models. A broader perspective has been recently adopted by Zhu and Braatz (2015). In their study, Zhu and Braatz coupled degradation, erosion and drug release from PLGA stent coating. They focused on the two stage release of PLGA drug release systems involving an initial slow release followed by an enhanced release which is obtained by erosion. Drug diffusion is achieved through polymer solid and liquid filled pores. Drug release is modelled taking into account various factors such as molecular weight change, diffusivity in polymer and liquid filled pores and drug partitioning between solid and liquid phases. However, one major limitation of their study is to propose an analytical expression for mass loss. The model would have been more useful if they considered a mechanistic approach for erosion.

As repeatedly stated in Chapter 5 and Chapter 6, degradation and erosion mechanism are fairly interconnected with each other. When designing a stent system made of biodegradable polymers, it is important to understand these particular mechanisms involved in the release process. Often, more than one mechanisms are involved at a given time or different mechanisms may dominate

at different stages of the drug delivery (Siegel and Rathbone, 2012). It is, therefore, a very attractive proposition to suggest different mechanisms for a specific device. In that perspective, the model proposed in Chapter 5 provides a solid foundation for modelling drug release from biodegradable stents. In the current chapter, the model provided in Chapter 5 is further improved to include the drug term. So that drug release from stents is treated as a combination of degradation, diffusion, surface erosion and interior erosion. The modified model is then validated with a case study from the literature for in vitro sirolimus release. By switching on and off the involved mechanisms, the model results giving the best fit is represented.

## 7.2 Summary of the experimental data by Wang *et al.* (2006)

Wang *et al.* (2006) studied the release of sirolimus from bi-layer and tri-layer biodegradable films made of supporting layer(s) and a drug eluting layer. Supporting layer is made of PLLA and the drug-eluting layer is made of PLGA for bi-layer films. For the case of tri-layer films, the drug eluting layer is kept between two supporting layers: one layer made of PLLA and one mode of PLGA 50/50. Diagrams of the bi-layer and tri-layer polymer matrix are shown in Fig. 7.1. These layers are separately dissolved in DCM during the casting, thus, they can be considered independently.  $M_{n,0}=75000 \text{ gmol}^{-1}$ ; and  $M_{unit}=65 \text{ gmol}^{-1}$  (considering 53% PLA and 47% PGA wt/wt). 1% and 2% wt% drug loadings are studied to analyse the effect of drug loadings on the final release profile. The layer thicknesses are controlled within  $60-80\pm 5\mu\text{m}$ . Degradation and drug release assessments are performed in the release medium (5% Dichloromethane (DMSO)+95% pH 7.4 PBS) at 37 °C. The changes in molecular weight and mass loss of drug-eluting layer is shown as functions of time. Moreover, drug release and the micrographs of the surface morphology are monitored during the degradation. The experimental results are reproduced using the discrete symbols in Fig. 7.3, Fig. 7.4 and Fig. 7.5. It is shown that molecular weight decrease, mass loss and drug release occur in two stages: an initial steady state and subsequently a more drastic stage. They argued this trend by the relative dominance of the mechanism during the degradation as a diffusion dominated

phase and a degradation-erosion dominated phase. Moreover, it is concluded that changing drug loading does not affect the release kinetics. This could be attributed to the fact that the drug loadings studied are quite close to each other. A further study with more loadings is therefore suggested.

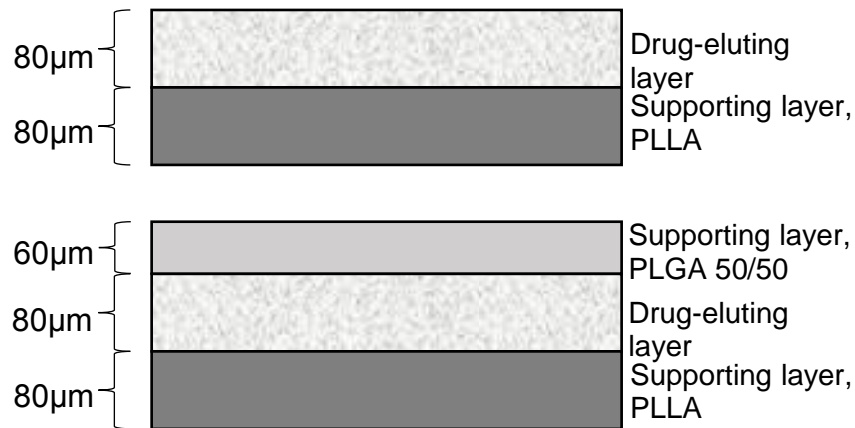


Fig. 7.1 Diagrams of the bi-layer and tri-layer polymer films of Wang *et al.* (Wang *et al.*, 2006) with the corresponding layer thicknesses (reproduced from relevant study)

### 7.3 Modification of the combined degradation-erosion model to include drug term

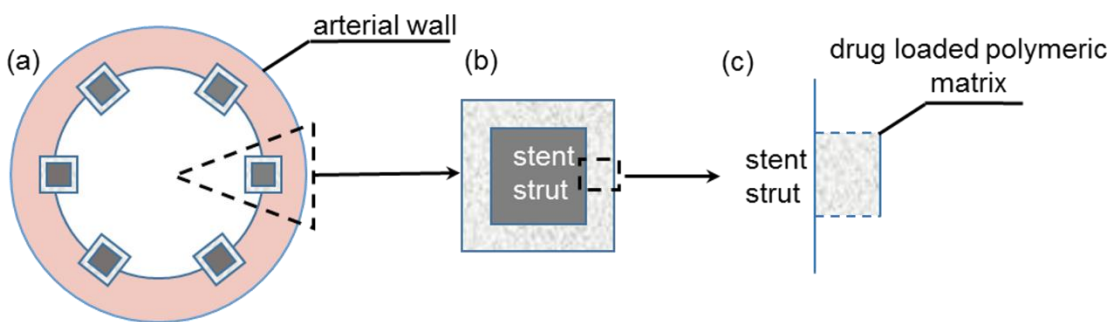


Fig. 7.2 shows the schematic of the stent and the drug loaded polymer coating which is the topic of the mathematical model presented in this chapter. Once a strut is in contact with a solvent, the solvent molecules (such as water) penetrate

into the polymer matrix leading to concurrent events: solubilization of drug molecules depending on their kinetics and cleavage of polymer chains.

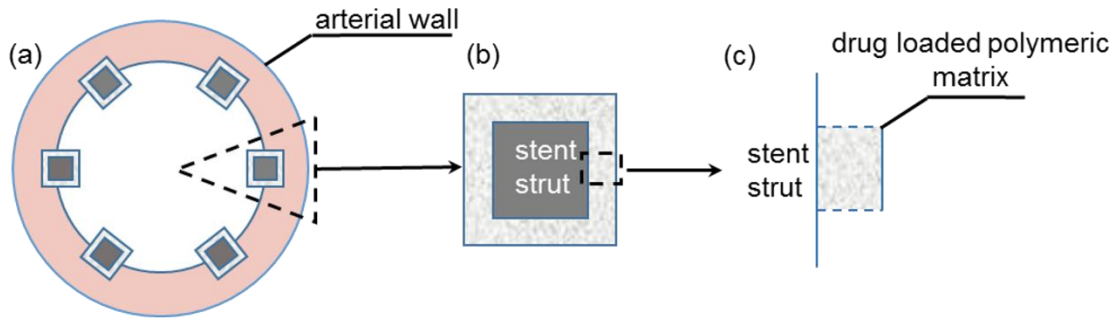


Fig. 7.2 a) Cross section of an implanted stent in a coronary artery; b) schematic of a single stent strut with drug-loaded polymer matrix; c) schematic of the drug loaded polymeric matrix which is modelled in the current chapter.

Two key components are considered in modelling drug release from PLGA stent: 1) capture the dynamic changes in the polymer matrix such as degradation, erosion and corresponding porosity changes; 2) description of the drug diffusivity based on the dynamic changes in the polymer matrix. The model presented in Chapter 5 is applied for the calculation of PLA/GA degradation, erosion and the corresponding porosity. The model is then modified considering the drug transport in the coating which is proceeded by diffusion mechanism. Assuming that the drug is uniformly dispersed in the polymer matrix initially, the drug release is described by Fick's law of diffusion such as

$$\frac{\partial C_{drug}}{\partial t} = \frac{\partial R_{drug}}{\partial t} + \frac{\partial}{\partial x} \left( D_{drug} \frac{\partial C_{drug}}{\partial x} \right) + \frac{\partial}{\partial y} \left( D_{drug} \frac{\partial C_{drug}}{\partial y} \right). \quad (7.1)$$

Here  $D_{drug}$  is the effective diffusivity that is dependent on the porosity of matrix. Diffusion coefficient of drug changes significantly by generation of pores during the degradation. Again, considering the heterogeneous structure within the matrix which is largely based on erosion, the diffusion coefficient are calculated separately for each direction. Eq. 5.22 is modified for the drug case such that

$$D_{drug,x} = D_{drug,poly} + (1.3\varepsilon_x^2 - 0.3\varepsilon_x^3)(D_{drug,pore} - D_{drug,poly}) \quad (7.2)$$

and

$$D_{drug,y} = D_{drug,poly} + (1.3\varepsilon_y^2 - 0.3\varepsilon_y^3)(D_{drug,pore} - D_{drug,poly}). \quad (7.3)$$

Drug release is accomplished by combinations of several sources as drug diffusion, surface erosion, and bulk erosion. The final drug release,  $M_t$  can be calculated by the sum of all the sources contributed:

$$M_t = M_d + M_s + M_b \quad (7.4)$$

$M_d$ ,  $M_s$  and  $M_b$  are the drug release governed by drug diffusion, surface erosion and bulk erosion respectively. The contribution of this mechanisms are controlled by rather switching on/off the relevant bids in the simulations or changing the domination of each mechanism.

#### 7.4 Summary of the parameters used in case study

The set of parameters used in this section allows identifying the underlying mechanisms of degradation, erosion and the drug release for the case study of Wang *et al.* (2006). This has been established by switching on/off the mechanisms or controlling the contribution of each mechanism. The selection of the parameters is made based on targeting a good fitting. The model parameters used in the fittings are provided in Table 6.1.

Table 7.1 Values of the model parameters used in the fittings

<i>Model parameters</i>	<i>Units</i>	<i>Case study</i>
$M_{n,mean}$	g mol <sup>-1</sup>	7.5x10 <sup>4</sup>
$M_{n,st\_dev}$	g mol <sup>-1</sup>	2.0x10 <sup>4</sup>
$M_{unit}$	g mol <sup>-1</sup>	65
$k_1$	week <sup>-1</sup>	5.0x10 <sup>-6</sup>
$k_2$	m <sup>3</sup> mol <sup>-1</sup> week <sup>-1</sup>	2.5x10 <sup>-2</sup>
$m$	no unit	4
$\alpha$	no unit	0.4
$\beta$	no unit	1
$C_{e,0}$	mol m <sup>-3</sup>	20615
$K_a$	no unit	1.35x10 <sup>-4</sup>
$M_{n,critical}$	g mol <sup>-1</sup>	2.0x10 <sup>4</sup>

$D_{ol,poly}$	$m^2 \text{ week}^{-1}$	$5.0 \times 10^{-15}$
$D_{ol,pore}$	$m^2 \text{ week}^{-1}$	$1.0 \times 10^{-5}$
$D_{drug,poly}$	$m^2 \text{ week}^{-1}$	$5.0 \times 10^{-17}$
$D_{drug,pore}$	$m^2 \text{ week}^{-1}$	$1.0 \times 10^{-5}$

Again, the parameter  $C_{e,0}$ ,  $m$ ,  $\alpha$  and  $\beta$  is obtained from Pan *et al.* (2014).  $M_{n,mean}$  is the initial molecular weight of the polymer prior to degradation, which is taken from (Wang *et al.*, 2006).  $M_{n,critical}$  is estimated from the experimental data representing  $M_n$  reduction.  $D_{ol,pore}$  and  $D_{drug,pore}$  are the diffusion coefficients in liquid filled pores for oligomers and drug respectively, which are simply assumed to be big numbers considering the diffusivity of species in water (Stewart, 2003).  $D_{ol,poly}$  is set as a very small number considering the diffusivity of oligomers in fresh bulk polymer. The set of  $M_{n,st\_dev}$ ,  $k_1$ ,  $k_2$  and  $D_{drug,poly}$  is then obtained by fitting the model calculations with the experimental data.

The polymer matrix is simulated as a 2-dimensional plate. The parameters  $n_x \times n_y$  is set as 40 x 2500 which is compatible with the actual shape of the plate to ensure each pixel to be square size. Quarter model is used in the simulations because of the symmetry of the plates. Therefore, the sizes of the plate is set as  $a=40\mu\text{m}$  and  $b=2.5\text{mm}$ . For the sake of a better fitting, an incubation period of 1.25 weeks is used with the interior erosion.

## 7.5 Fittings of the modified model with experimental data

Fig. 7.3, 7.4 and 7.5 shows the best fit between the model results and the experimental data obtained by Wang *et al.* (2006). The model parameters used in the fitting are provided in Table 7.1. The initial oligomer concentration is set as  $C_{ol,0}=0$ . The experimental data gives the hint of a sudden mass loss at  $t=0$ ; which can be explained by the instant release of fabrication excess in the matrix when exposed to the medium. This instant loss is involved in the model; by setting 3.8% of initial mass loss at  $t=0$ . Surface erosion mechanism is switched off in the simulations. The increased mass loss to the end of the degradation is representative of the interior erosion. The gradual increase in the mass loss

indicates the incubation for release of oligomers, therefore, we set an incubation period of 1.25 weeks in the simulations.

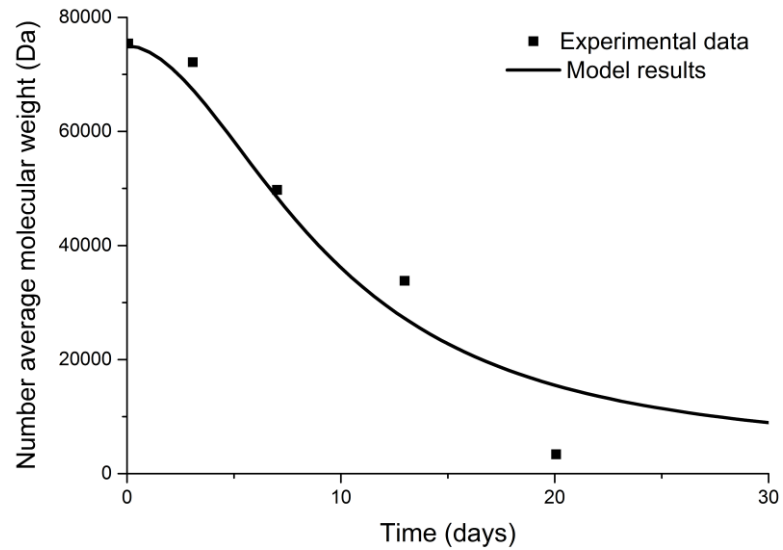


Fig. 7.3 Comparison of molecular weight decrease of PLGA between model prediction and experimental data. The solid line represents the model predictions with the discrete symbols representing the experimental data (Wang *et al.*, 2006).

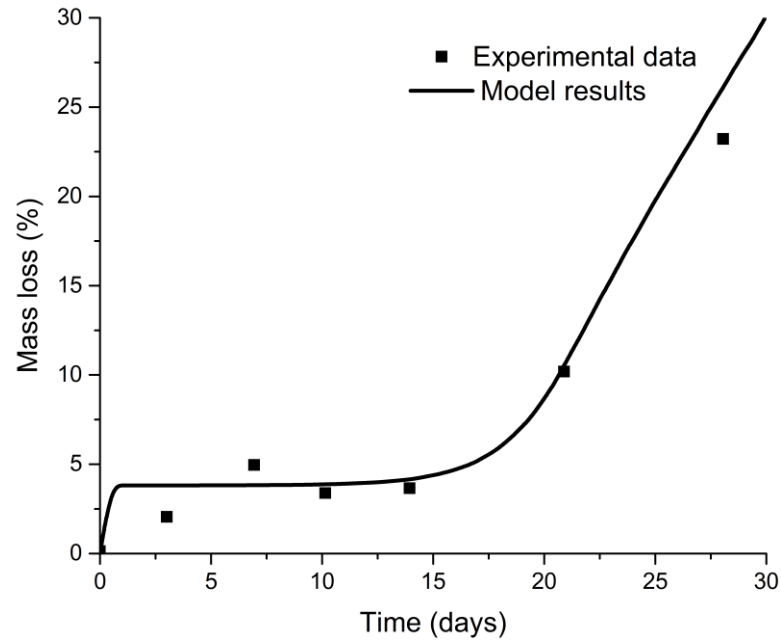


Fig. 7.4 Comparison of mass loss of PLGA between model prediction and experimental data. The solid line represents the model predictions with the discrete symbols representing the experimental data (Wang *et al.*, 2006).

Water penetration into the matrix induces the drug dissolution. Free drug molecules are available to diffuse out of the polymer matrix. In their experimental study, Wang *et al.* (2006) worked with the drug loadings below the solubility limit of the drug inside the polymer. Therefore, there was no solid aggregate of the drug during the degradation. Fig. 7.5 illustrates the model fitting of drug release with the experimental data. Experimental data is again represented as symbols while the model prediction is represented as a solid line. Sirolimus release of two loadings, 1 and 2% loading, was simulated. Since the drug loadings are very similar in magnitude, release profiles overlap for two loadings, both in the experimental study and in the model. In order to prevent the confusion, only the results for 1% loading is shown in Fig. 7.5. Only two additional parameters are used for covering the presence of drug in addition to the parameters set for blank polymer: the drug diffusivity,  $D_{drug,poly}$  and  $D_{drug,pore}$ .

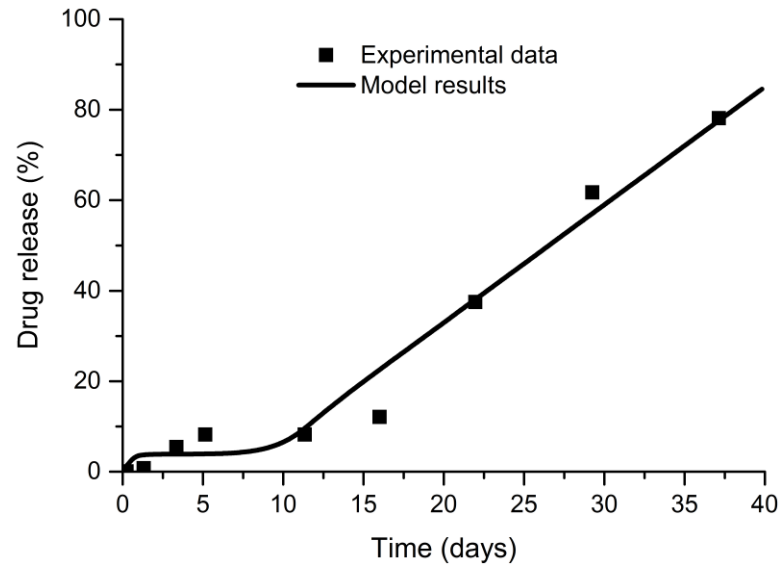


Fig. 7.5 Comparison of sirolimus release from PLGA between model prediction and experimental data. The solid line represents the model predictions with the discrete symbols representing the experimental data (Wang *et al.*, 2006).

As can be seen from Fig. 7.4, drug diffusion and the interior erosion are the active mechanisms responsible for the observed drug release profile. Overall, drug release has been completed in two stages: a diffusion controlled stage and an erosion-controlled stage. The diffusion coefficient of the drug is set as a very small number considering the size and the molecular weight of the sirolimus. Therefore, drug release is very slow in the first stage in which release is fully controlled by diffusion. The second stage begins as soon as pixels reach to the critical molecular weight. Drug release profile follows a similar trend with the mass loss profile representing the consistency of the mechanisms responsible for the release of oligomers and drug. Overall, good agreement is exhibited in all the figures indicating the accuracy of the model developed. It is not possible to explain the two stage release of drugs with a simple degradation diffusion model. Therefore, it is crucial to consider a combined degradation diffusion and erosion model to be able to explain such drug release behaviour.

Fig. 7.6 shows the Field Emission Scanning Electron Microscopy (FESEM) micrographs of the polymer matrix during hydrolytic degradation and erosion. The figure is taken from the study of Wang *et al.* (2006). The micrographs present the status of the surface prior to degradation and at time 7 days, 14 days and 21

days. As can be seen from the figure, cavities are formed during degradation and erosion which links interior to the surface. The cavity formation is unclear up to time 21 days. However, at 21 days, cavity formation is obvious in the matrix surface which leads relatively significant mass loss (10%) and drug release (30%) at that time.

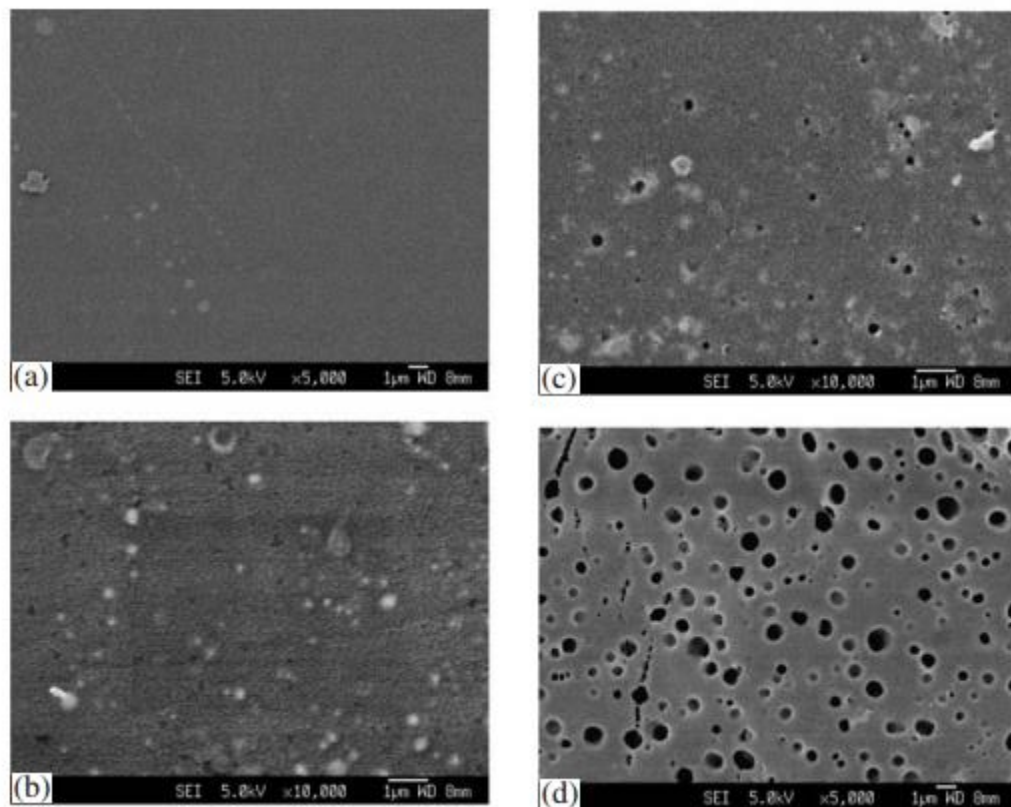


Fig. 7.6 Micrographs of the surface morphology of degrading PLGA 53/47 taken from (Wang *et al.*, 2006) (a) 0 days, (b) 7 days, (c) 14 days and (d) 21 days.

Fig. 7.7 shows the simulation results which represent the status of the drug loaded polymer matrix at 21 days. Grey part in the figure represents the stent strut which is excluded in the simulations and only represented here for a clear picture. White pixels indicate the non-eroded polymer matrix whereas black pixels represent the eroded polymer matrix. The status of the surface shown in Fig. 7.7 fairly match with the FESEM micrographs represented in Fig. 7.6. This is

because, model results validate the formation of microcavities which builds up a network in the polymer and links the surface with the more degraded interior. The microcavities are formed based on the erosion of the pixels which gives rise to rapid oligomer and drug release. The level of matching between the model results and experimental data confirms the validity of the model established. To conclude, the oligomer and sirolimus release from PLGA polymer is divided into two stages: a diffusion controlled stage which gives a constant slow release of oligomer at initial times and an erosion-controlled stage which results in a rapid release of oligomers an drug at later stages.

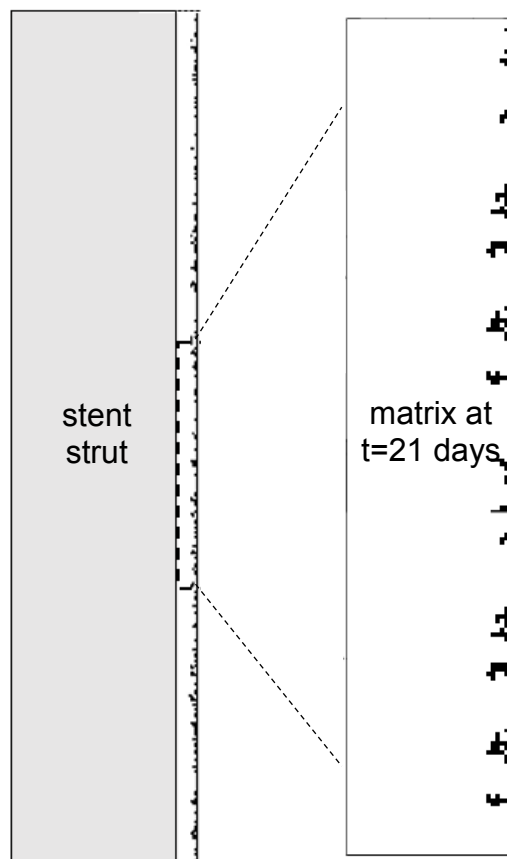


Fig. 7.7 Simulation results for drug loaded polymer matrix at  $t=21$  days.

## 7.6 Conclusion

This chapter provides a complete model set for describing polymer degradation and erosion and coupled drug release from a stent coating. Understanding the degradation and erosion kinetics of biodegradable polymers such as PLGA is a prerequisite for the design of a drug-eluting polymer stent. Considering this, the mathematical model in Chapter 5 is modified and coupled with drug release with an attempt to explain the number average molecular weight, mass loss and drug release behaviour from the coating. The model results were then validated with the experimental data from the literature.

Simultaneous drug diffusion from polymer matrix and liquid-filled pores was modelled. Effective drug diffusivity was taken as dependent on the porosity of the matrix which is a function of cavity formation. Erosion is the main mechanism responsible for the formation of the cavities. The model was then verified for sirolimus release from the stent coating and showed a good level of fitting. The comparison between the model in this chapter and the degradation model revealed that the multiple stages of drug release cannot be captured with a single degradation model.

## Chapter 8. Major conclusions and future work

### 8.1 Major conclusions

In this thesis, several mathematical models were developed and used to predict the drug release behaviour of PLA/GA polymers. The works in separate chapters were motivated by experimental studies documented in the literature, which demonstrated drug-polymer interaction within the polymer matrix, as well as two stage degradation-erosion behaviour of polymers. The degradation models were considered as autocatalytic because of the characteristics of PLA/GA polymers. The reaction-diffusion models considered the pore evaluation and enhanced diffusivity of oligomers and drugs during degradation and erosion. The models were not developed to be valid for all cases for controlled drug delivery systems, instead, they had been used to further understand the underlying background of the experimental data.

The mathematical models presented in this thesis were based on previous models from the group at the University of Leicester, they were either improved, to include the further catalysts effects arising from drugs and the interactions with the drug and polymer or coupled with erosion models, in order to capture the enormous mass losses of polymers as well as multi-stage drug release behaviour. The models were used to further understanding of the factors in hydrolytic degradation and drug release.

The effect of drug incorporation on polymer degradation rate was presented by considering the interaction between drugs and polymers as well as the catalyst effect of free acidic and basic species. It was found that acidic drugs significantly accelerates the polymer degradation by releasing protons during dissociation. For the basic drugs, it was found that drugs can either accelerates or decelerates the polymer degradation depending on the ionic interaction between basic drugs and polymer chain ends. The index of the polymer - basic drug interactions,  $K_p$ , was found to be the primitive factor controlling the release of basic drugs. Namely, the increase in the value of  $K_p$  resulted in a decrease in degradation

rate, because of the decrease in the number of free carboxylic acids and drug molecules.

A coupled mathematical model was also developed in this thesis to simulate the hydrolytic degradation and erosion process of PLA/GA polymers. The key finding of the study was that, the mechanism of diffusion has very small contribution to the mass loss and drug release. Moreover, the early mass loss with constant rate was an indicator of surface erosion, while the bolus mass losses after a certain time were indicative of interior erosion. For the cases including bolus mass loss with a smoother profile, it was found that the interior erosion is functioning with an incubation period. The model well captured the mass loss, drug release and microstructure evaluation for several case studies including the blank polymers and a drug eluting stent.

From our knowledge, it is the first time in the literature to combine the mechanisms of hydrolytic degradation, diffusion, surface and interior erosion into a single mathematical model. Our study fills a gap in the literature by including the autocatalysis into a probabilistic erosion model. The model highlight an issue which has never been paid enough attention – it is important to link hydrolytic degradation and erosion processes in order to understand different kinds of mass loss and drug release trends. The method used here is effective to deal with large mass loss as well as multiphasic drug release behaviour. Importantly, the model results offer physical insight into the experimental studies. The practical application of the model can be useful to guide the design of the polyester materials with required properties.

Many mechanisms are involved in the progressive drug release from controlled delivery systems. Moreover, experimental data gives the hint that release from each controlled drug delivery system is dominated by different phenomena. Therefore, it is not possible to propose models that would be valid for all the drug delivery systems. The main aim of this thesis was offering possible mechanisms to the experimental data rather than developing models that would be valid for all the cases. The models developed in this thesis offered a physical insight into the various experimental studies available in the literature. The good agreement

between the model results and the experimental data showed that this target was accomplished to a large extent.

## **8.2 Future work**

Despite the number of experimental studies in controlled release systems in recent years, the area of modelling controlled delivery systems is still under development. As discussed in the previous chapters of this thesis, the models in the literature are very simple and far from predicting the real data.

The mathematical modelling of drug delivery has a significant potential for development of new products and helps to enlighten complex behaviour of pharmaceutical dosage forms. With the developments in the information technology the accuracy of the models developed are improved in a great extent. Likewise the case for other disciplines, modelling drug delivery is expected to become a part of the drug development. However, one obstacle with modelling drug delivery systems is that it is challenging to establish a model which would be applicable for all different kind of polymers and drugs. Mathematical models are more likely to be applicable to specific devices with specific drug and polymer. Another obstacle is that many assumptions are needed in order to develop the models which decreases the convergence of the models to the reality. A fruitful aspect will be to go towards development of models with decision trees which identifies the appropriate model for specific kind of drug delivery systems. This would help understanding the underlying drug release mechanism of a specific system.

The other fruitful approach will be to combine these mathematical models for quantifying the drug release in living organism, such as drug transport to the different organs and cells. Yet, the drug release models predicts the resulting drug release kinetics. However, the resulting drug concentration at human body including the pharmacodynamics effects in patient is missing. The models considering the drug distribution, drug metabolism and prediction of clearance can provide valuable information to design new products.

---

## References

- ACHARYA, G. & PARK, K. 2006. Mechanisms of controlled drug release from drug-eluting stents. *Advanced Drug Delivery Reviews*, 58, 387-401.
- AGRAWAL, C. & RAY, R. B. 2001. Biodegradable polymeric scaffolds for musculoskeletal tissue engineering. *Journal of biomedical materials research*, 55, 141-150.
- AHOLA, M., RICH, J., KORTESUO, P., KIESVAARA, J., SEPPÄLÄ, J. & YLI-URPO, A. 1999. In vitro evaluation of biodegradable  $\epsilon$ -caprolactone-co-d,l-lactide/silica xerogel composites containing toremifene citrate. *International Journal of Pharmaceutics*, 181, 181-191.
- ARIFIN, D. Y., LEE, L. Y. & WANG, C.-H. 2006a. Mathematical modeling and simulation of drug release from microspheres: Implications to drug delivery systems. *Advanced drug delivery reviews*, 58, 1274-1325.
- ARIFIN, D. Y., LEE, L. Y. & WANG, C. H. 2006b. Mathematical modeling and simulation of drug release from microspheres: Implications to drug delivery systems. *Adv Drug Deliv Rev*, 58, 1274-325.
- BALA, I., HARIHARAN, S. & KUMAR, M. R. 2004. PLGA nanoparticles in drug delivery: the state of the art. *Critical Reviews™ in Therapeutic Drug Carrier Systems*, 21.
- BANGALORE, S., TOKLU, B., AMOROSO, N., FUSARO, M., KUMAR, S., HANNAN, E. L., FAXON, D. P. & FEIT, F. 2013. Bare metal stents, durable polymer drug eluting stents, and biodegradable polymer drug eluting stents for coronary artery disease: mixed treatment comparison meta-analysis. *BMJ : British Medical Journal*, 347.
- BASTIOLI, C. 2005. *Handbook of biodegradable polymers*, iSmithers Rapra Publishing.
- BATYCKY, R. P., HANES, J., LANGER, R. & EDWARDS, D. A. 1997. A theoretical model of erosion and macromolecular drug release from biodegrading microspheres. *Journal of Pharmaceutical Sciences*, 86, 1464-1477.

- 
- BERKLAND, C., KIM, K. K. & PACK, D. W. 2003. PLG microsphere size controls drug release rate through several competing factors. *Pharmaceutical research*, 20, 1055-1062.
- BERKLAND, C., KING, M., COX, A., KIM, K. & PACK, D. W. 2002. Precise control of PLG microsphere size provides enhanced control of drug release rate. *Journal of Controlled Release*, 82, 137-147.
- BODMEIER, R. & CHEN, H. G. 1989. Evaluation of biodegradable poly(lactide) pellets prepared by direct compression. *J Pharm Sci*, 78, 819-22.
- BODMER, D., KISSEL, T. & TRAECHSLIN, E. 1992. Factors influencing the release of peptides and proteins from biodegradable parenteral depot systems. *Journal of Controlled Release*, 21, 129-137.
- BOSWORTH, L. A. & DOWNES, S. 2010. Physicochemical characterisation of degrading polycaprolactone scaffolds. *Polymer Degradation and Stability*, 95, 2269-2276.
- BUCHANAN, F. J. 2008. *Degradation rate of bioresorbable materials: Prediction and evaluation*, Elsevier.
- BURKERSRODA, F. V. & GOEPFERICH, A. An approach to classify degradable polymers. MRS Proceedings, 1998. Cambridge Univ Press, 17.
- CAI, H., DAVE, V., GROSS, R. A. & MCCARTHY, S. P. 1996. Effects of physical aging, crystallinity, and orientation on the enzymatic degradation of poly(lactic acid). *Journal of Polymer Science Part B: Polymer Physics*, 34, 2701-2708.
- CAIRNS, D. 2012. *Essentials of pharmaceutical chemistry*, Pharmaceutical Press.
- CASALINI, T., ROSSI, F., LAZZARI, S., PERALE, G. & MASI, M. 2014. Mathematical modeling of PLGA microparticles: from polymer degradation to drug release. *Mol Pharm*, 11, 4036-48.
- CASCONE, M. G., SIM, B. & SANDRA, D. 1995. Blends of synthetic and natural polymers as drug delivery systems for growth hormone. *Biomaterials*, 16, 569-574.
- CHA, Y. & PITT, C. G. 1988. A one-week subdermal delivery system for l-methadone based on biodegradable microcapsules. *Journal of Controlled Release*, 7, 69-78.

- CHA, Y. & PITT, C. G. 1989. The acceleration of degradation-controlled drug delivery from polyester microspheres. *Journal of Controlled Release*, 8, 259-265.
- CHARLIER, A., LECLERC, B. & COUARRAZE, G. 2000. Release of mifepristone from biodegradable matrices: experimental and theoretical evaluations. *International journal of pharmaceutics*, 200, 115-120.
- CLUGSTON, M. & FLEMMING, R. 2000. *Advanced chemistry*, Oxford University Press.
- D'SOUZA, S., FARAJ, J. A., DORATI, R. & DELUCA, P. P. 2015. Enhanced Degradation of Lactide-co-Glycolide Polymer with Basic Nucleophilic Drugs. *Advances in Pharmaceutics*, 2015.
- DANIELS, A., CHANG, M. K., ANDRIANO, K. P. & HELLER, J. 1990. Mechanical properties of biodegradable polymers and composites proposed for internal fixation of bone. *Journal of Applied Biomaterials*, 1, 57-78.
- DEWICK, P. M. 2006. *Essentials of organic chemistry: for students of pharmacy, medicinal chemistry and biological chemistry*, John Wiley & Sons.
- DOMB, A. J. & KUMAR, N. 2011. *Biodegradable polymers in clinical use and clinical development*, John Wiley & Sons.
- DUNNE, M., CORRIGAN, O. I. & RAMTOOLA, Z. 2000. Influence of particle size and dissolution conditions on the degradation properties of polylactide-co-glycolide particles. *Biomaterials*, 21, 1659-1668.
- ENGINEER, C., PARIKH, J. & RAVAL, A. 2011. Review on hydrolytic degradation behavior of biodegradable polymers from controlled drug delivery system. *Trends Biomater Artif Organs*, 25, 79-85.
- FITZGERALD, J. F. & CORRIGAN, O. I. 1996. Investigation of the mechanisms governing the release of levamisole from poly-lactide-co-glycolide delivery systems. *Journal of Controlled Release*, 42, 125-132.
- FORD, A. N., PACK, D. W. & BRAATZ, R. Multi-scale modeling of PLGA microparticle drug delivery systems. 21st European Symposium on Computer Aided Process Engineering: Part B, 2011a. Interscience New York, 1475-1479.

- 
- FORD, A. N., PACK, D. W. & BRAATZ, R. D. 2011b. Multi-Scale Modeling of PLGA Microparticle Drug Delivery Systems. *Computer Aided Chemical Engineering*.
- FORD VERSYPT, A. N., PACK, D. W. & BRAATZ, R. D. 2013. Mathematical modeling of drug delivery from autocatalytically degradable PLGA microspheres — A review. *Journal of Controlled Release*, 165, 29-37.
- FRENNING, G. & STRØMME, M. 2003. Drug release modeled by dissolution, diffusion, and immobilization. *International Journal of Pharmaceutics*, 250, 137-145.
- GLEADALL, A., PAN, J., KRUFIT, M.-A. & KELLOMÄKI, M. 2014. Degradation mechanisms of bioresorbable polyesters. Part 1. Effects of random scission, end scission and autocatalysis. *Acta biomaterialia*, 10, 2223-2232.
- GLEADALL, A. C. 2015. *Modelling degradation of biodegradable polymers and their mechanical properties*. Department of Engineering.
- GOPFERICH, A. 1996. Mechanisms of polymer degradation and erosion. *Biomaterials*, 17, 103-114.
- GOPFERICH, A. 1997. Polymer bulk erosion. *Macromolecules*, 30, 2598-2604.
- GÖPFERICH, A. 1996. Mechanisms of polymer degradation and erosion. *Biomaterials*, 17, 103-114.
- GOPFERICH, A. & LANGER, R. 1993. Modeling of polymer erosion. *Macromolecules*, 26, 4105-4112.
- GRIZZI, I., GARREAU, H., LI, S. & VERT, M. 1995. Hydrolytic degradation of devices based on poly(DL-lactic acid) size-dependence. *Biomaterials*, 16, 305-11.
- HAN, X. 2011. *Degradation models for polyesters and their composites*. University of Leicester.
- HAN, X. & PAN, J. 2009. A model for simultaneous crystallisation and biodegradation of biodegradable polymers. *Biomaterials*, 30, 423-430.
- HAN, X., PAN, J., BUCHANAN, F., WEIR, N. & FARRAR, D. 2010. Analysis of degradation data of poly(l-lactide-co-l,d-lactide) and poly(l-lactide) obtained at elevated and

- physiological temperatures using mathematical models. *Acta Biomaterialia*, 6, 3882-3889.
- HELLER, J. 1987. Controlled drug release from monolithic systems. *Ophthalmic Drug Delivery*. Springer.
- HELLER, J. & BAKER, R. 1980. Theory and practice of controlled drug delivery from bioerodible polymers. *Controlled release of bioactive materials*. Academic Press New York.
- HIGUCHI, T. 1961. Rate of release of medicaments from ointment bases containing drugs in suspension. *Journal of pharmaceutical sciences*, 50, 874-875.
- HOLY, C. E., DANG, S. M., DAVIES, J. E. & SHOICHET, M. S. 1999. In vitro degradation of a novel poly (lactide-co-glycolide) 75/25 foam. *Biomaterials*, 20, 1177-1185.
- HOSSAINY, S. & PRABHU, S. 2008. A mathematical model for predicting drug release from a biodurable drug-eluting stent coating. *J Biomed Mater Res A*, 87, 487-93.
- HUANG, M.-H., LI, S. & VERT, M. 2004. Synthesis and degradation of PLA-PCL-PLA triblock copolymer prepared by successive polymerization of  $\epsilon$ -caprolactone and dl-lactide. *Polymer*, 45, 8675-8681.
- HUANG, X. & BRAZEL, C. S. 2001. On the importance and mechanisms of burst release in matrix-controlled drug delivery systems. *Journal of Controlled Release*, 73, 121-136.
- HUSMANN, M., SCHENDERLEIN, S., LÜCK, M., LINDNER, H. & KLEINEBUDDE, P. 2002. Polymer erosion in PLGA microparticles produced by phase separation method. *International Journal of Pharmaceutics*, 242, 277-280.
- IKADA, Y. & TSUJI, H. 2000. Biodegradable polyesters for medical and ecological applications. *Macromolecular rapid communications*, 21, 117-132.
- JIANG, W., HAN, X. & PAN, J. 2008. Effective diffusion coefficient of biodegradation polymers and its role in degradation. *University of Leicester Research Report*.
- JOSHI, A. & HIMMELSTEIN, K. J. 1991. Dynamics of Controlled Release from Bioerodible Matrices. *Journal of Controlled Release*, 15, 95-104.

- 
- KAMALY, N., YAMEEN, B., WU, J. & FAROKHZAD, O. C. 2016. Degradable controlled-release polymers and polymeric nanoparticles: mechanisms of controlling drug release. *Chemical reviews*, 116, 2602-2663.
- KLOSE, D., SIEPMANN, F., ELKHARRAZ, K. & SIEPMANN, J. 2008. PLGA-based drug delivery systems: Importance of the type of drug and device geometry. *International Journal of Pharmaceutics*, 354, 95-103.
- KULKARNI, A., REICHE, J. & LENDLEIN, A. 2007. Hydrolytic degradation of poly(rac-lactide) and poly[(rac-lactide)-co-glycolide] at the air-water interface. *Surface and Interface Analysis*, 39, 740-746.
- LANGER, R. 1980. Invited review polymeric delivery systems for controlled drug release. *Chemical Engineering Communications*, 6, 1-48.
- LEE, W. K., LOSITO, I., GARDELLA, J. A. & HICKS, W. L. 2001. Synthesis and surface properties of fluorocarbon end-capped biodegradable polyesters. *Macromolecules*, 34, 3000-3006.
- LI, S. 1999. Hydrolytic degradation characteristics of aliphatic polyesters derived from lactic and glycolic acids. *Journal of biomedical materials research*, 48, 342-353.
- LI, S., GARREAU, H. & VERT, M. 1990a. Structure-property relationships in the case of the degradation of massive poly ( $\alpha$ -hydroxy acids) in aqueous media. *Journal of Materials Science: Materials in Medicine*, 1, 198-206.
- LI, S., GIROD-HOLLAND, S. & VERT, M. 1996. Hydrolytic degradation of poly(dl-lactic acid) in the presence of caffeine base. *Journal of Controlled Release*, 40, 41-53.
- LI, S. & MCCARTHY, S. 1999. Influence of crystallinity and stereochemistry on the enzymatic degradation of poly (lactide) s. *Macromolecules*, 32, 4454-4456.
- LI, S. M., GARREAU, H. & VERT, M. Structure-property relationships in the case of the degradation of massive aliphatic poly-( $\alpha$ -hydroxy acids) in aqueous media. *Journal of Materials Science: Materials in Medicine*, 1, 123-130.

- 
- LI, S. M., GARREAU, H. & VERT, M. 1990b. Structure-property relationships in the case of the degradation of massive aliphatic poly-( $\alpha$ -hydroxy acids) in aqueous media. *Journal of Materials Science: Materials in Medicine*, 1, 123-130.
- LI, S. M., GARREAU, H. & VERT, M. 1990c. Structure-property relationships in the case of the degradation of massive poly( $\alpha$ -hydroxy acids) in aqueous media. *Journal of Materials Science: Materials in Medicine*, 1, 131-139.
- LOFTSSON, T. & BREWSTER, M. E. 1996. Pharmaceutical applications of cyclodextrins. 1. Drug solubilization and stabilization. *Journal of pharmaceutical sciences*, 85, 1017-1025.
- LYU, S., SCHLEY, J., LOY, B., LIND, D., HOBOT, C., SPARER, R. & UNTEREKER, D. 2007. Kinetics and time-temperature equivalence of polymer degradation. *Biomacromolecules*, 8, 2301-2310.
- LYU, S. & UNTEREKER, D. 2009. Degradability of Polymers for Implantable Biomedical Devices. *International Journal of Molecular Sciences*, 10, 4033.
- MAKADIA, H. K. & SIEGEL, S. J. 2011. Poly lactic-co-glycolic acid (PLGA) as biodegradable controlled drug delivery carrier. *Polymers*, 3, 1377-1397.
- MALHOTRA, R. 2016. *Empirical research in software engineering: concepts, analysis, and applications*, CRC Press.
- MARK, H. 2004. *Encyclopedia of Polymer Science and Technology, 12 Volume Set*, Wiley-Interscience, New York.
- MATHIOWITZ, E., JACOB, J. S., JONG, Y. S., CARINO, G. P., CHICKERING, D. E., CHATURVEDI, P., SANTOS, C. A., VIJAYARAGHAVAN, K., MONTGOMERY, S. & BASSETT, M. 1997. Biologically erodable microspheres as potential oral drug delivery systems. *Nature*, 386, 410-414.
- MAUDUIT, J., BUKH, N. & VERT, M. 1993a. Gentamycin/poly (lactic acid) blends aimed at sustained release local antibiotic therapy administered per-operatively. III. The case of gentamycin sulfate in films prepared from high and low molecular weight poly (DL-lactic acids). *Journal of Controlled Release*, 25, 43-49.

- 
- MAUDUIT, J., BUKH, N. & VERT, M. 1993b. Gentamycin/poly(lactic acid) blends aimed at sustained release local antibiotic therapy administered per-operatively. I. The case of gentamycin base and gentamycin sulfate in poly(dl-lactic acid) oligomers. *Journal of Controlled Release*, 23, 209-220.
- MIDDLETON, J. C. & TIPTON, A. J. 2000. Synthetic biodegradable polymers as orthopedic devices. *Biomaterials*, 21, 2335-2346.
- MIGLIAVACCA, F., PETRINI, L., MASSAROTTI, P., SCHIEVANO, S., AURICCHIO, F. & DUBINI, G. 2004. Stainless and shape memory alloy coronary stents: a computational study on the interaction with the vascular wall. *Biomechanics and Modeling in Mechanobiology*, 2, 205-217.
- MIYAJIMA, M., KOSHIKA, A., OKADA, J. I. & IKEDA, M. 1999. Effect of polymer/basic drug interactions on the two-stage diffusion-controlled release from a poly(l-lactic acid) matrix. *Journal of Controlled Release*, 61, 295-304.
- MIYAJIMA, M., KOSHIKA, A., OKADA, J. I., KUSAI, A. & IKEDA, M. 1998. Factors influencing the diffusion-controlled release of papaverine from poly (l-lactic acid) matrix. *Journal of Controlled Release*, 56, 85-94.
- MOHAMMADI, Y. & JABBARI, E. 2006. Monte Carlo simulation of degradation of porous poly (lactide) scaffolds, 1. *Macromolecular theory and simulations*, 15, 643-653.
- MONTAUDO, G. & RIZZARELLI, P. 2000. Synthesis and enzymatic degradation of aliphatic copolyesters. *Polymer Degradation and Stability*, 70, 305-314.
- NAIR, L. S. & LAURENCIN, C. T. 2007. Biodegradable polymers as biomaterials. *Progress in Polymer Science*, 32, 762-798.
- NARAYANI, R. & PANDURANGA RAO, K. 1996. Gelatin microsphere cocktails of different sizes for the controlled release of anticancer drugs. *International Journal of Pharmaceutics*, 143, 255-258.
- OKADA, H., DOKEN, Y., OGAWA, Y. & TOGUCHI, H. 1994. Preparation of three-month depot injectable microspheres of leuprorelin acetate using biodegradable polymers. *Pharmaceutical research*, 11, 1143-1147.

- PAN, J. 2014. *Modelling degradation of bioresorbable polymeric medical devices*, Elsevier.
- PAN, J. & CHEN, X. 2015. 2 - Modelling degradation of amorphous biodegradable polyesters: basic model. In: PAN, J. (ed.) *Modelling Degradation of Bioresorbable Polymeric Medical Devices*. Woodhead Publishing.
- PAN, J., HAN, X., NIU, W. & CAMERON, R. E. 2011. A model for biodegradation of composite materials made of polyesters and tricalcium phosphates. *Biomaterials*, 32, 2248-2255.
- PARK, T. G. 1994. Degradation of poly (D, L-lactic acid) microspheres: effect of molecular weight. *Journal of Controlled Release*, 30, 161-173.
- PARK, T. G. 1995. Degradation of poly (lactic-co-glycolic acid) microspheres: effect of copolymer composition. *Biomaterials*, 16, 1123-1130.
- PAUL, D. R. & HARRIS, F. W. 1976. *Controlled Release Polymeric Formulations*, AMERICAN CHEMICAL SOCIETY.
- PERALE, G., AROSIO, P., MOSCATELLI, D., BARRI, V., MÜLLER, M., MACCAGNAN, S. & MASI, M. 2009. A new model of resorbable device degradation and drug release: Transient 1-dimension diffusional model. *Journal of Controlled Release*, 136, 196-205.
- PHILIP, S., KESHAVARZ, T. & ROY, I. 2007. Polyhydroxyalkanoates: biodegradable polymers with a range of applications. *Journal of Chemical Technology and Biotechnology*, 82, 233-247.
- PILLAI, O. & PANCHAGNULA, R. 2001. Polymers in drug delivery. *Current Opinion in Chemical Biology*, 5, 447-451.
- PITT, C. G. & GU, Z.-W. 1987. Modification of the rates of chain cleavage of poly( $\epsilon$ -caprolactone) and related polyesters in the solid state. *Journal of Controlled Release*, 4, 283-292.
- PONTRELLI, G. & DE MONTE, F. 2010. A multi-layer porous wall model for coronary drug-eluting stents. *International Journal of Heat and Mass Transfer*, 53, 3629-3637.

- 
- POSPÍŠIL, J., HORÁK, Z., KRULIŠ, Z., NEŠPŮREK, S. & KURODA, S.-I. 1999. Degradation and aging of polymer blends I. Thermomechanical and thermal degradation. *Polymer Degradation and Stability*, 65, 405-414.
- PROIKAKIS, C. S., MAMOUZELOS, N. J., TARANTILI, P. A. & ANDREOPOULOS, A. G. 2006. Swelling and hydrolytic degradation of poly(d,l-lactic acid) in aqueous solutions. *Polymer Degradation and Stability*, 91, 614-619.
- RAMAN, C., BERKLAND, C., KIM, K. & PACK, D. W. 2005. Modeling small-molecule release from PLG microspheres: effects of polymer degradation and nonuniform drug distribution. *Journal of Controlled Release*, 103, 149-158.
- RAMTEKE, K., JADHAV, V. & DHOLE, S. 2012. Microspheres: As carriers used for novel drug delivery system. *IOSRPHR*, 2, 44-48.
- RANGA RAO, K. V. & PADMALATHA DEVI, K. 1988. Swelling controlled-release systems: recent developments and applications. *International Journal of Pharmaceutics*, 48, 1-13.
- RATNER, B. D., HOFFMAN, A. S., SCHOEN, F. J. & LEMONS, J. E. 2004. *Biomaterials science: an introduction to materials in medicine*, Academic press.
- REZAIIE, H. R., BAKHTIARI, L. & ÖCHSNER, A. 2015. *Biomaterials and Their Applications*, Springer.
- SAHA, N. R., SARKAR, G., ROY, I., BHATTACHARYYA, A., RANA, D., DHANARAJAN, G., BANERJEE, R., SEN, R., MISHRA, R. & CHATTOPADHYAY, D. 2016. Nanocomposite films based on cellulose acetate/polyethylene glycol/modified montmorillonite as nontoxic active packaging material. *RSC Advances*, 6, 92569-92578.
- SAMAMI, H. 2016. *Solid Mechanics of Degrading Bioresorbable Polymers*. Department of Engineering.
- SCOTT, G. 2002. *Degradable polymers: principles and applications*, Springer Science & Business Media.
- SEVIM, K. & PAN, J. 2016. A Mechanistic Model for Acidic Drug Release Using Microspheres Made of PLGA 50: 50. *Molecular Pharmaceutics*, 13, 2729-2735.

- SHAIKH, H. K., KSHIRSAGAR, R. & PATIL, S. 2015. Mathematical models for drug release characterization: a review. *WJPPS*, 4, 324-338.
- SIEGEL, R. A. & RATHBONE, M. J. 2012. Overview of controlled release mechanisms. *Fundamentals and Applications of Controlled Release Drug Delivery*. Springer.
- SIEGEL, S. J., KAHN, J. B., METZGER, K., WINEY, K. I., WERNER, K. & DAN, N. 2006. Effect of drug type on the degradation rate of PLGA matrices. *European Journal of Pharmaceutics and Biopharmaceutics*, 64, 287-293.
- SIEPMANN, J., ELKHARRAZ, K., SIEPMANN, F. & KLOSE, D. 2005. How autocatalysis accelerates drug release from PLGA-based microparticles: a quantitative treatment. *Biomacromolecules*, 6, 2312-9.
- SIEPMANN, J., FAISANT, N. & BENOIT, J. P. 2002. A new mathematical model quantifying drug release from bioerodible microparticles using Monte Carlo simulations. *Pharmaceutical Research*, 19, 1885-1893.
- SIEPMANN, J., SIEGEL, R. A. & RATHBONE, M. J. 2011. *Fundamentals and applications of controlled release drug delivery*, Springer Science & Business Media.
- SIEPMANN, J. & SIEPMANN, F. 2012. Swelling Controlled Drug Delivery Systems. In: SIEPMANN, J., SIEGEL, R. A. & RATHBONE, M. J. (eds.) *Fundamentals and Applications of Controlled Release Drug Delivery*. Boston, MA: Springer US.
- SIPARSKY, G. L., VOORHEES, K. J. & MIAO, F. 1998. Hydrolysis of Polylactic Acid (PLA) and Polycaprolactone (PCL) in Aqueous Acetonitrile Solutions: Autocatalysis. *Journal of environmental polymer degradation*, 6, 31-41.
- SMITH, G. D. 1965. *Numerical solutions of partial differential equations*, Oxford University Press London.
- SPENLEHAUER, G., VERT, M., BENOIT, J. & BODDAERT, A. 1989. In vitro and in vivo degradation of poly (D, L lactide/glycolide) type microspheres made by solvent evaporation method. *Biomaterials*, 10, 557-563.
- STEWART, P. S. 2003. Diffusion in Biofilms. *Journal of Bacteriology*, 185, 1485-1491.

- 
- TAMADA, J. & LANGER, R. 1993. Erosion kinetics of hydrolytically degradable polymers. *Proceedings of the National Academy of Sciences*, 90, 552-556.
- TANG, Y. & SINGH, J. 2008. Controlled delivery of aspirin: Effect of aspirin on polymer degradation and in vitro release from PLGA based phase sensitive systems. *International Journal of Pharmaceutics*, 357, 119-125.
- TESTA, B. & MAYER, J. M. 2003. *Hydrolysis in drug and prodrug metabolism*, John Wiley & Sons.
- THOMBRE, A. & HIMMELSTEIN, K. 1985a. A simultaneous transport-reaction model for controlled drug delivery from catalyzed bioerodible polymer matrices. *AIChE Journal*, 31, 759-766.
- THOMBRE, A. G. & HIMMELSTEIN, K. J. 1984. Modelling of drug release kinetics from a laminated device having an erodible drug reservoir. *Biomaterials*, 5, 250-254.
- THOMBRE, A. G. & HIMMELSTEIN, K. J. 1985b. SIMULTANEOUS TRANSPORT-REACTION MODEL FOR CONTROLLED DRUG DELIVERY FROM CATALYZED BIOERODIBLE POLYMER MATRICES. *AIChE Journal*, 31, 759-766.
- TSUJI, H. & IKADA, Y. 2000. Properties and morphology of poly(l-lactide) 4. Effects of structural parameters on long-term hydrolysis of poly(l-lactide) in phosphate-buffered solution. *Polymer Degradation and Stability*, 67, 179-189.
- UHRICH, K. E., CANNIZZARO, S. M., LANGER, R. S. & SHAKESHEFF, K. M. 1999. Polymeric systems for controlled drug release. *Chemical reviews*, 99, 3181-3198.
- ULTRA, C. 2001. 6.0 and Chem3D Ultra. *Cambridge Soft Corporation, Cambridge, USA*.
- VAN NOSTRUM, C. F., VELDHUIS, T. F., BOS, G. W. & HENNINK, W. E. 2004. Hydrolytic degradation of oligo (lactic acid): a kinetic and mechanistic study. *Polymer*, 45, 6779-6787.
- VENUGOPAL, J. & RAMAKRISHNA, S. 2005. Applications of polymer nanofibers in biomedicine and biotechnology. *Applied biochemistry and biotechnology*, 125, 147-157.

- VERT, M. 2009. Degradable and bioresorbable polymers in surgery and in pharmacology: beliefs and facts. *Journal of Materials Science: Materials in Medicine*, 20, 437-446.
- VERT, M., LI, S., SPENLEHAUER, G. & GUÉRIN, P. 1992. Bioresorbability and biocompatibility of aliphatic polyesters. *Journal of materials science: Materials in medicine*, 3, 432-446.
- VON BURKERSRODA, F., SCHEDL, L. & GOPFERICH, A. 2002. Why degradable polymers undergo surface erosion or bulk erosion. *Biomaterials*, 23, 4221-4231.
- WANG, X., VENKATRAMAN, S. S., BOEY, F. Y., LOO, J. S. & TAN, L. P. 2006. Controlled release of sirolimus from a multilayered PLGA stent matrix. *Biomaterials*, 27, 5588-5595.
- WANG, Y. 2009. *Modelling degradation of bioresorbable polymeric devices*. University of Leicester.
- WANG, Y., PAN, J., HAN, X., SINKA, C. & DING, L. 2008. A phenomenological model for the degradation of biodegradable polymers. *Biomaterials*, 29, 3393-3401.
- WARD, M. A. & GEORGIU, T. K. 2011. Thermoresponsive Polymers for Biomedical Applications. *Polymers*, 3, 1215.
- WILSON, C. G. & CROWLEY, P. J. 2011. *Controlled release in oral drug delivery*, New York, Springer.
- WISE, D. L. 2000. *Handbook of pharmaceutical controlled release technology*, New York, Marcel Dekker.
- WISHART, D. S., KNOX, C., GUO, A. C., SHRIVASTAVA, S., HASSANALI, M., STOTHARD, P., CHANG, Z. & WOOLSEY, J. 2006. DrugBank: a comprehensive resource for in silico drug discovery and exploration. *Nucleic Acids Res*, 34, D668-72.
- XIANG, A. & MCHUGH, A. J. 2011. A generalized diffusion–dissolution model for drug release from rigid polymer membrane matrices. *Journal of Membrane Science*, 366, 104-115.

- YOU, S., YANG, Z. & WANG, C.-H. 2016. Toward Understanding Drug Release From Biodegradable Polymer Microspheres of Different Erosion Kinetics Modes. *Journal of pharmaceutical sciences*, 105, 1934-1946.
- ZHANG, M. P., YANG, Z. C., CHOW, L. L. & WANG, C. H. 2003. Simulation of drug release from biodegradable polymeric microspheres with bulk and surface erosions. *Journal of Pharmaceutical Sciences*, 92, 2040-2056.
- ZHAO, A., HUNTER, S. K. & RODGERS, V. 2010. Theoretical prediction of induction period from transient pore evolution in polyester-based microparticles. *Journal of pharmaceutical sciences*, 99, 4477-4487.
- ZHU, X. & BRAATZ, R. D. 2015. A mechanistic model for drug release in PLGA biodegradable stent coatings coupled with polymer degradation and erosion. *Journal of Biomedical Materials Research Part A*, 103, 2269-2279.
- ZHU, X., PACK, D. W. & BRAATZ, R. D. 2014. Modelling intravascular delivery from drug-eluting stents with biodurable coating: investigation of anisotropic vascular drug diffusivity and arterial drug distribution. *Computer methods in biomechanics and biomedical engineering*, 17, 187-198.
- ZILBERMAN, M. & MALKA, A. 2009. Drug controlled release from structured bioresorbable films used in medical devices—a mathematical model. *Journal of Biomedical Materials Research Part B: Applied Biomaterials*, 89, 155-164.
- ZUNINO, P., D'ANGELO, C., PETRINI, L., VERGARA, C., CAPELLI, C. & MIGLIAVACCA, F. 2009. Numerical simulation of drug eluting coronary stents: mechanics, fluid dynamics and drug release. *Computer Methods in Applied Mechanics and Engineering*, 198, 3633-3644.
- ZYGOURAKIS, K. 1990. Development and temporal evolution of erosion fronts in bioerodible controlled release devices. *Chemical Engineering Science*, 45, 2359-2366.

# Appendices

## **Appendix A**

### **FORTRAN codes for the mechanistic model for acidic drug release using microspheres made of PLGA**

In this appendix we present the FORTRAN codes developed for the study in Chapter 3.

```

! PROGRAM: Polymer hydrolytic degradation in the presence of acidic drugs
! PURPOSE: This program computes polymer hydrolytic degradation with respect
to the time and location
! in the presence of acidic drugs
! Author
! Kevser Sevim
! Ph.D. Dissertation 2017
! Department of Engineering
! University of Leicester
! DETAILS:
! ** Finite difference method has been used for numerical solution of chain
scission equations and diffusion equations
! ** Drug dissolution is instantaneous
! *****

module variables
implicit none
integer, parameter:: z=1000
real*8, dimension(z) :: Rs !total number of chainscission
real*8, dimension(z) :: dRs_dt !time derivative of chain scission
real*8, dimension(z) :: Rol !number of ester chains of oligomers
real*8, dimension(z) :: Mn !number averaged molecular weight
real*8, dimension(z) :: Ce !concentration of ester bonds
real*8, dimension(z) :: dCol_dt !time derivative of oligomer concentration
real*8, dimension(z) :: Col ! oligomer concentration
real*8, dimension(z) :: Jr ! oligomer flux
real*8, dimension(z) :: dCdrug_dt !time derivative of drug concentration
real*8, dimension(z) :: dRol_dt !time derivative of number of ester chains
real*8, dimension(z) :: Jdrug ! drug flux and concentration
real*8, dimension(z) :: Cdrug !drug concentration
real*8, dimension(z) :: Rs_b ! normalised value of Rs with Ce0
real*8, dimension(z) :: r ! current radius
real*8, dimension(z):: Vpore !total porosity as a result of oligomer and drug
depletion
real*8, dimension(z):: Vpore_drug !porosity as a result of drug depletion
real*8, dimension(z):: Vpore_poly !porosity as a result of oligomer
real*8, dimension(z):: D !effective oligomer diffusivity
real*8, dimension(z):: Ddrug !effective drug diffusivity
real*8, dimension(z):: C1 !Ka*Col(i)/4.0
real*8, dimension(z):: C2 !Ka_drug*Cdrug(i)
real*8, dimension(z):: cf !factor of quadratic equation
real*8, dimension(z):: deltaaaa !discrimant of the quadratic equation
real*8, dimension(z):: X2_2, X2_1 !dummy roots of the quadratic equation
real*8, dimension(z):: X2 ! root of the quadratic equation
real*8::Vshell !volume of microsphere shell
real*8:: Col0 ! initial oligomer concentration in the polymer before chain
scission
real*8:: A1,A2 !area of the shells
real*8:: af, bf ! factors of quadratic equation
real*8:: Ho ! intial H+ from PBS
real*8:: k1 ! rate constant for non-catalysed hydrolysis
real*8:: k2 ! rate constant for acid catalysed hydrolysis

```

```

real*8:: Ka ! acid dissociation constant
real*8:: Cdrug_ent ! summation of the drug concentration at entire
real*8:: Cdrug_ave ! average drug concentration within the polymer
real*8:: Av_Mn ! average molecular weight
real*8:: CH_ave ! average proton concentration
real*8:: CH_ent ! summation of the drug concentration at entire polymer
real*8:: D_ent ! summation of the oligomer diffusivity at entire polymer
real*8:: Deff_ave ! average effective diffusivity
real*8:: Mn_ent ! summation of the oligomer molecular weight at entire polymer
real*8:: Ce0 ! initial ester concentration
real*8:: delta ! Cs, the saturation solubility of drug in the matrix, mol/m3
real*8:: Mn0 ! initial number average molecular weight
real*8:: Munit ! number average molecular weight of a polymer unit
real*8:: alpha, beta ! empirical parameters of the reaction
real*8:: Ndp0 !initial average degree of polymerisation
real*8:: m ! average polymerization degree of short chains
real*8:: b ! particle radius
real*8:: Ka_drug ! acid dissociation constant of drug
real*8:: Release !drug release
integer:: k ! number of mesh points in x direction
real*8 :: del_r ! spatial discretization size
integer:: nt ! total number of total time steps
integer:: it,i,Icount,Noutput,j !counters
real*8 :: del_t1 ! time step, week
real*8 :: t1 !time
real*8:: Dpoly !diffusion coefficient of oligomers in fresh bulk polymer
real*8:: Dpore !diffusion coefficient of oligomers in liquid filled pores
real*8:: Ddrug0 !diffusion coefficient of drug in fresh bulk polymer
real*8:: Cdrug0 !initial drug concentration
real*8:: fdrug0 !the volume ratio of drug to the polymer phase
real*8:: Dpore_drug !diffusion coefficient of drug in liquid filled pores
end module variables

!*****
program Ficks_diffusion
use variables
implicit none
    open (6, file="fitsiepmann51.txt")
    open (8, file="DrugAve51.txt")
    open (10, file="MnAve51.txt")
    open (11, file="Release51.txt")
    open (20, file="pH.txt")
    open (12, file="Effective_diffusivty.txt")
    open (26, file="Cumulative_release.txt")

    nt=1000000
    k=1000

call
Initial_parameters (k1,k2,Ce0,alpha,beta,Mn0,m,Dpoly,Dpore,b,Col0,Ndp0,delta,Dd
rug0,Ka)
call
Initial_parameters_2 (Ka_drug,Cdrug0,fdrug0,Dpore_drug,Ho)

```

```

del_t1=0.0000045
del_r=(b)/(k-1)

! Spatial discretization of the microsphere
r(1)=0.0
do i=2, k
r(i)=r(i-1)+del_r
end do

! Initial conditions of polymer matrix prior to degradation
do i=1,k
Col(i)=Col0
Rs(i)=0.0
Ce(i)=Ce0
Rol(i)=0.0
Vpore(i)=0.0
Vpore_drug(i)=0.0
Vpore_poly(i)=0.0
D(i)=Dpoly
Cdrug(i)=0.0
end do

! Initial condition of drug in polymer matrix prior to degradation
do i=1,k
Cdrug(i)=Cdrug0
end do

!*****
Noutput=120
Icount=0

t1=0.0

do it=1, nt
do i=1,k

! Solution of the second order quadratic equation for calculation of CH+
! Arrangement of Eq. 3.1, 3.3 and 3.4 leads to
!  $X_2^2 - H_o X_2 - (C_1(i) + C_2(i)) = 0$  (1)
! Here, (CH+)=X2; Ho refers to proton donated by the surrounding medium, CHo,
constant
C1(i)=Ka*Col(i)/4.0
C2(i)=Ka_drug*Cdrug(i)
! The root of the Equation (1) gives the proton coconcentration
! the details are provided in Section 3.2.1
! The solution of the quadratic equation:
af=1
bf=-Ho
cf(i)=-(C1(i)+C2(i))
deltaaaa(i)=(bf*bf)-(4.0*af*cf(i))
if(deltaaaa(i).GT.0.0D0) then
X2_1(i)=(-bf-(sqrt(deltaaaa(i))))/(2.0*af)

```

```

X2_2(i)=(-bf+(sqrt(deltaaa(i))))/(2.0*af)
if ((X2_2(i).LT.0.0D0).AND.(X2_1(i).LT.0.0D0)) then
print*,"The roots are complex"
else if ((X2_1(i).GT.0.0D0) then
X2(i)=X2_1(i)
else if ((X2_2(i).GT.0.0D0) then
X2(i)=X2_2(i)
else
Print*,"There are two positive roots"
end if
else
end if

      dRs_dt(i)=k1*Ce(i)+k2*Ce(i)*X2(i)
      Rs(i)=Rs(i)+dRs_dt(i)*del_t1
      dRol_dt(i)=alpha*beta*(Rs(i)/Ce0)**(beta-1)*dRs_dt(i)
      Rol(i)=Rol(i)+dRol_dt(i)*del_t1
      Ce(i)=Ce0-Rol(i)
      Vpore_poly(i)=1-(Ce(i)/Ce0)-(Col(i)/Ce0)
      Vpore_drug(i)=1-(Cdrug(i)/Cdrug0)
      Vpore(i)=Vpore_poly(i)*(1-fdrug0)+Vpore_drug(i)*fdrug0
      D(i)=Dpoly+(1.3*Vpore(i)**2-0.3*Vpore(i)**3)*(Dpore-Dpoly)
      Ddrug(i)=Ddrug0+(1.3*Vpore(i)**2-0.3*Vpore(i)**3)*(Dpore_drug-
Ddrug0)
end do

! Update oligomer concentration
call oligomer_flux(k,Col,D,r, &      ! input
                  Jr)                ! output
call calculate_dCol_dt(k,r,Jr, &    ! input
                  dCol_dt)          ! output
      do i=1,k-1
      Col(i)=Col(i)+dCol_dt(i)*del_t1+dRol_dt(i)*del_t1
      end do
      Col(k)=0.0    ! boundry condition

! Update drug concentration
call drug_flux(k,Cdrug,Ddrug,r &    ! input
              ,                      ! output
              Jdrug)
call calculate_dCdrug_dt(k,r,Jdrug, & ! input
                  dCdrug_dt)        ! output
      ! Update for drug concentration
      do i=1, k-1
      Cdrug(i)=Cdrug(i)+dCdrug_dt(i)*del_t1
      end do
      Cdrug(k)=0.0    ! boundry condition

! Calculate drug release
      Cdrug_ent=0.0
      do i=1, k-1

```

```

        Cdrug_ent=Cdrug_ent+(4/3*4*atan(1.)*(r(i+1)**3-
r(i)**3)*((Cdrug(i+1)+Cdrug(i))/2))
        end do

        Cdrug_ave=Cdrug_ent/(4/3*4*atan(1.)*b**3)
        Release=(Cdrug0-Cdrug_ave)/Cdrug0*100

Icount=Icount+1
if(Icount>(nt/Noutput)) then

! Write output into files
write(6,7)"time ", t1
7 format(a,5x,f10.6)
write(6,8) "i", " r(i)", "
Mn", "Col(i)", "Ce(i)", "Ndp0", "Rs", "Cdrug", "Rol(i)", "D(i)", "Vpore",
"X2(C_H)", "deltaaa"
8 format(3x,a,10x,a,15x,a,13x,a,10x,a,10x,a,10x,a,10x,a,13x,a,10x,a,20x,a,
20x,a, 20x,a)
write(8,11)"time ", t1
11 format(a,5x,f5.2)
write(8,12) "Cdrug_ave"
12 format(a)
write(8,15) Cdrug_ave
15 format(f10.5)
write(11,*) Release
47 format (f10.5)

do i=1,k
Rs_b(i)=Rs(i)/Ce0
Mn(i)=Mn0*(1.0-alpha*(Rs_b(i))**beta)/(1.0+Ndp0*(Rs_b(i)-
alpha*Rs_b(i)**beta/m))
write(6,10) i, r(i), Mn(i), Col(i), Ce(i), Ndp0, Rs(i), Cdrug(i), Rol(i),
Ddrug(i), Vpore(i)
10 format(i3,10x,f10.8,10x,f9.1,5x,f10.4, 5x, f10.4,5x, f10.4, 5x, f10.4,
5x,f10.4, 5x, f10.4, 5x, f20.15, 5x,f20.15)
end do

! Calculate average molecular weight, Av_Mn
Mn_ent=0.0
do i=1,k-1
        Mn_ent=Mn_ent+(4/3*4*atan(1.)*(r(i+1)**3-r(i)**3)*((Mn(i+1)+Mn(i))/2))
! total Mn of entire nodes
end do
        Av_Mn=Mn_ent/(4/3*4*atan(1.)*b**3)
write(10,33) Av_Mn !
33 FORMAT(f10.4,5x)

!Calculate the acidity, pH, log(CH+)
CH_ent=0.0
do i=1, k-1
        CH_ent=CH_ent+(4/3*4*atan(1.)*(r(i+1)**3-r(i)**3)*((X2(i+1)+X2(i))/2))
end do
        CH_ave=CH_ent/(4/3*4*atan(1.)*b**3)

```

```

write(20,44) -LOG(CH_ave) !
44 FORMAT(f10.4,5x)

! Calculate average effective diffusivity
D_ent=0.0
do i=1, k-1
    D_ent=D_ent+(4/3*4*atan(1.)*(r(i+1)**3-
r(i)**3)*((Ddrug(i+1)+Ddrug(i))/2))
end do
    Deff_ave=D_ent/(4/3*4*atan(1.)*b**3)
write(12,22) Deff_ave !
22 FORMAT(f20.15)
!*****

Icount=0
end if
t1=t1+del_t1
end do
stop

!SUBROUTINES
Contains

Subroutine
Initial_parameters(k1,k2,Ce0,alpha,beta,Mn0,m,a,b,Col0,Ndp0,delta,Dd
rug0,Ka)
implicit none
real*8:: Ce0,alpha,beta,Ka,Mn0,m,a,b,Col0,Ndp0,delta
real*8:: Dpoly,Dpore,Ddrug0,k1,k2

k1=8.D-4          !1/week
k2=0.1            !m3/mol.week
alpha=0.4         !constant
beta=1.           !constant
m=4.              !constant
Dpoly=1.D-12      !m2/week;
Dpore=1000D0*Dpoly
Ddrug0=1.5D-10    !m2/week
Ka=1.35D-4
b=75.D-6          !m; radius of the microsphere
Mn0=35640.5D0     !g/mol for microsphere
Munit=65.0D0      !g/mol
Ce0=20615.D0      !mol/m3
Col0=0.0*Ce0
Ndp0=Mn0/Munit
delta=9.7D0

End subroutine

Subroutine Initial_parameters_2(Ka_drug,Cdrug0,fdrug0,Dpore_drug,Ho)
implicit none

```

```

    real*8:: Ka_drug, Ho, Cdrug0, fdrug0, Dpore_drug
    Cdrug0=223.D0          !mol/m3
    fdrug0=0.0524D0       !m3drug/m3unit
    Dpore_drug=1000D0*Ddrug0 !m2/week
    Ka_drug=6.31D-6       !acid dissociation constant
    Ho=3.98D-8            !Initial H+ concentration in PBS
End subroutine

!*****
! Subroutines quantifying transport of drugs and oligomers

Subroutine oligomer_flux(k,Col,D,r & ! input
, Jr) ! output
    Implicit none
    integer, parameter:: z=1000
    real*8, dimension(z):: r
    real*8, dimension(z):: Jr
    real*8, dimension(z):: Col
    real*8, dimension(z):: D
    integer:: k,i

    Do i=1, k-1
        Jr(i)=-D(i)*(Col(i+1)-Col(i))/(r(i+1)-r(i))
    End do

End subroutine

!*****

Subroutine calculate_dCol_dt(k,r,Jr, & ! input
dCol_dt) ! output

    Implicit none
    integer, parameter:: z=1000
    real*8, dimension(z):: dCol_dt
    real*8, dimension(z):: Jr
    real*8, dimension(z):: r
    real*8::Vshell, A1,A2
    integer:: k,i

    dCol_dt(1)=-3*(Jr(1))/(r(2)/2.0)
    Do i=2, k-1
        del_r=(r(i+1)-r(i))/2+(r(i)-r(i-1))/2
        A1=4* 4.*atan(1.)*(r(i-1)**2)
        A2=4* 4.*atan(1.)*(r(i)**2)
        Vshell=4/3* 4.*atan(1.)*((r(i)**3)-(r(i-1)**3))
        dCol_dt(i)=(Jr(i-1)*A1-Jr(i)*A2)/Vshell
    End do

End subroutine

!! DRUG DIFFUSION-
!! This two subroutine considers drug diffusion by Fick's law and matter
conversation

```

```

Subroutine drug_flux(k,Cdrug,Ddrug,r &          ! input
,          Jdrug)          ! output
implicit none
real*8, dimension(z):: r
real*8, dimension(z):: Cdrug
real*8, dimension(z):: Jdrug
real*8, dimension(z):: Ddrug          !m2/week
integer:: k, i

do i=1, k-1
    Jdrug(i)=-Ddrug(i)*(Cdrug(i+1)-Cdrug(i))/(r(i+1)-r(i))
end do

End subroutine

Subroutine calculate_dCdrug_dt(k,r,Jdrug, &          ! input
dCdrug_dt)          ! output

Implicit none
integer, parameter:: z=1000
real*8, dimension(z):: dCdrug_dt
real*8, dimension(z):: Jdrug
real*8, dimension(z):: r
real*8:: Vshell, A1,A2
integer:: k,i

dCdrug_dt(1)=-3*(Jdrug(1))/(r(2)/2.0)
do i=2, k-1
    del_r=(r(i+1)-r(i))/2+(r(i)-r(i-1))/2
    A1=4* 4.*atan(1.)*(r(i-1)**2)
    A2=4* 4.*atan(1.)*(r(i)**2)
    Vshell=4/3* 4.*atan(1.)*((r(i)**3)-(r(i-1)**3))
    dCdrug_dt(i)=(Jdrug(i-1)*A1-Jdrug(i)*A2)/Vshell
End do

End subroutine

End program

```

## **Appendix B**

### **FORTRAN codes for the mechanistic model for acidic drug release using microspheres made of PLGA**

In this appendix we present the FORTRAN codes developed for the study in Chapter 4.

```
! PROGRAM: Polymer hydrolytic degradation in the presence of basic drugs
! PURPOSE: This program computes polymer hydrolytic degradation with respect
to the time and location
! in the presence of basic drugs
! Author
! Kevser Sevim
! Ph.D. Dissertation 2017
! Department of Engineering
! University of Leicester
! DETAILS:
! ** Finite difference method has been used for numerical solution of chain
scission equations and diffusion equations
! ** Drug dissolution is instantaneous
! *****

module variables
implicit none
integer, parameter:: z=1000
real*16, dimension(z) :: Rs !total number of chain scission
real*16, dimension(z) :: dRs_dt !time derivative of chain scission
real*16, dimension(z) :: Rol !number of ester chains of oligomers
real*16, dimension(z) :: C_COOH_short !concentration of short chains
real*16, dimension(z) :: C_pro !concentration of proton
real*16, dimension(z) :: Coh !concentration of hydroxide ions
real*16, dimension(z) :: Rs_b ! normalised value of Rs with Ce0
real*16, dimension(z) :: Mn !number averaged molecular weight
real*16, dimension(z) :: Ce !concentration of ester bonds
real*16, dimension(z) :: dCol_dt !time derivative of oligomer concentration
real*16, dimension(z) :: Col ! oligomer concentration
real*16, dimension(z) :: Jr ! oligomer flux
real*16, dimension(z) :: dCdrug_dt !time derivative of drug concentration
real*16, dimension(z):: dRol_dt !time derivative of number of ester chains
real*16, dimension(z) :: Cdrug ! drug concentration
real*16, dimension(z) :: Jdrug !drug flux
real*16, dimension(z):: Vpore !total porosity as a result of oligomer and drug
depletion
real*16, dimension(z):: Vpore_drug !porosity as a result of drug depletion
real*16, dimension(z):: Vpore_poly !porosity as a result of oligomer
real*16, dimension(z):: D !effective oligomer diffusivity
real*16, dimension(z):: Ddrug !effective drug diffusivity
real*16, dimension(z) :: r ! current radius
real*16:: Col0 ! initial oligomer concentration in the polymer before chain
scission
real*16:: Kp ! partition parameter
real*16:: k1 !non-catalysed reaction constant
real*16:: k2 !acid-catalysed reaction constant
real*16:: k3 !base-catalysed reaction constant
real*16:: Ka !acid dissociation constant
real*16:: Cdrug_ent ! summation of the drug concentration at entire
real*16:: Cdrug_ave ! average drug concentration within the polymer
real*16:: Av_Mn ! average molecular weight
real*16:: CH_ave ! average proton concentration
real*16:: CH_ent ! summation of the drug concentration at entire polymer
```

```

real*16:: D_ent ! summation of the oligomer diffusivity at entire polymer
real*16:: Deff_ave ! average effective diffusivity
real*16:: Mn_ent ! summation of the oligomer molecular weight at entire
polymer
real*16:: Ce0 ! initial ester concentration
real*16:: delta ! Cs, the saturation solubility of drug in the matrix, mol/m3
real*16:: Mn0 ! initial number average molecular weight
real*16:: Munit ! number average molecular weight of a polymer unit
real*16:: alpha, beta ! emprical parameters of the reaction
real*16:: Ndp0 ! initial average degree of polymerisation
real*16:: m ! average polymerization degree of short chains
real*16:: Kb_drug ! base dissociation constant
real*16:: Release !drug release
real*16:: Col_ent ! summation of the oligomer concentration at entire polymer
real*16:: Col_ave ! average oligomer concentration
real*16:: Rol_ent ! summation of the oligomer production rate at entire
polymer
real*16:: Rol_ave ! average oligomer production rate
real*16 :: del_t1 ! time step, week
real*16 :: t1 !time
real*16:: Dpoly !diffusion coefficient of oligomers in fresh bulk polymer
real*16:: Dpore !diffusion coefficient of oligomers in liquid filled pores
real*16:: Ddrug0 !diffusion coefficient of drug in fresh bulk polymer
real*16:: Cdrug0 !initial drug concentration
real*16:: fdrug0 !the volume ratio of drug to the polymer phase
real*16:: Dpore_drug !diffusion coefficient of drug in liquid filled pores
real*16:: Cdrug_loading !initial drug loading
real*16:: Cchain0 !number of polymer chains per unit volume at the beginning
of the degradation
real*16 :: del_r !space step
real*16:: b !radius of the microsphere
integer:: k ! number of grids
integer:: nt ! total number of time steps
integer:: it,i,Icount,Noutput,j !counters
end module variables

program Loaded
use variables
implicit none
    open (6, file="fitsiepmann_basic.txt")
    open (8, file="DrugAve_basic.txt")
    open (10, file="MnAve_basic.txt")
    open (11, file="Release_basic.txt")
    open (20, file="pH.txt")
    open (12, file="Effective_diffusivity_basic.txt")
    open (26, file="Cumulative_release_basic.txt")
    open (27, file="weight_loss.txt")
nt=400000
k=1000

call
Initial_parameters (k1,k2,Ce0,alpha,beta,Mn0,m,Dpoly,Dpore,b,Col0,Ndp0,delta,Dd
rug0,Ka)

```

```

call Initial_parameters_2(Kb_drug,Cdrug_loading,fdrug0,Dpore_drug,k3)

del_t1=0.0000045
del_r=(b)/(k-1)
Cchain0=1.34D+6/Mn0
Cdrug0=Cdrug_loading
Kp=0.75

! Spatial discretization of the microsphere
r(1)=0.0
do i=2, k
r(i)=r(i-1)+del_r
end do

! Initial conditions of polymer matrix prior to degradation
do i=1,k
Col(i)=Col0
Rs(i)=0.0
Ce(i)=Ce0
Rol(i)=0.0
Vpore(i)=0.0
Vpore_drug(i)=0.0
Vpore_poly(i)=0.0
end do

! Initial condition of drug in polymer matrix prior to degradation
do i=1,k
Cdrug(i)=Cdrug0
end do

!*****
Noutput=120
Icount=0

t1=0.0
do it=1, nt
do i=1,k-1
C_COOH_short(i)=Col(i)/m
C_pro(i)=(C_COOH_short(i)*Ka)**0.5
Coh(i)=(Kb_drug*Cdrug(i))**0.5
! Update Coh and Cpro considering the attachement
Coh(i)=Coh(i)*(1-Kp)
C_pro(i)=(1.D-14)/Coh(i)
dRs_dt(i)=k1*Ce(i)+k2*Ce(i)*(C_pro(i))+k3*Ce(i)*(Coh(i))

Rs(i)=Rs(i)+dRs_dt(i)*del_t1
dRol_dt(i)=alpha*beta*(Rs(i)/Ce0)**(beta-1)*dRs_dt(i)
Rol(i)=Rol(i)+dRol_dt(i)*del_t1
Ce(i)=Ce0-Rol(i)
Vpore_poly(i)=1-(Ce(i)/Ce0)-(Col(i)/Ce0)
Vpore_drug(i)=1-(Cdrug(i)/(Cdrug0))
Vpore(i)=Vpore_poly(i)*(1-fdrug0)+Vpore_drug(i)*fdrug0
D(i)=Dpoly+(1.3*Vpore(i)**2-0.3*Vpore(i)**3)*(Dpore-Dpoly)

```

```

                Ddrug(i)=Ddrug0+(1.3*Vpore(i)**2-
0.3*Vpore(i)**3)*(Dpore_drug-Ddrug0)
                end do

! Update oligomer concentration
call oligomer_flux(k,Col,D,r, &          ! input
&                Jr)                    ! output
call calculate_dCol_dt(k,r,Jr, &       ! input
&                dCol_dt)              ! output

do i=1,k-1
    Col(i)=Col(i)+dCol_dt(i)*del_t1+dRol_dt(i)*del_t1
end do
Col(k)=0.0

call drug_flux(k,Cdrug,Ddrug,r &      ! input
,                Jdrug)                ! output
call calculate_dCdrug_dt(k,r,Jdrug, & !input
                dCdrug_dt)            ! output

! Update for drug concentration
do i=1, k-1
    Cdrug(i)=(Cdrug(i)+dCdrug_dt(i)*del_t1) !control it
end do
Cdrug(k)=0.0

! Calculate drug release
Cdrug_ent=0.0
do i=1, k-1
    Cdrug_ent=Cdrug_ent+(4/3*4*atan(1.)*(r(i+1)**3-
r(i)**3)*((Cdrug(i+1)+Cdrug(i))/2))
end do
Cdrug_ave=Cdrug_ent/(4/3*4*atan(1.)*b**3)
Release=(Cdrug_loading-Cdrug_ave)/Cdrug_loading
!*****
    Icount=Icount+1
    if(Icount>(nt/Noutput)) then
        write (6,7) "time ", t1
7 format(a,5x,f10.6)
        write (6,8) "i", "
r(i)", "Mn", "Col(i)", "Ce(i)", "Ndp0", "Rs", "Cdrug", "Rol(i)", "D(i)", "Vpore", "pH"
8
format(3x,a,10x,a,15x,a,13x,a,10x,a,10x,a,10x,a,10x,a,13x,a,10x,a,20x,a,
20x,a, 20x,a)

!
    write (8,*) 7*24*t1
    write (11,*) Release

    do i=1,k
        Rs_b(i)=Rs(i)/Ce0
        Mn(i)=Mn0*(1.0-alpha*(Rs_b(i))**beta)/(1.0+Ndp0*(Rs_b(i)-
alpha*Rs_b(i)**beta/m))

```

```

        write(6,10) i, r(i), Mn(i), Col(i), Ce(i), Ndp0, Rs(i), Cdrug(i),
        Rol(i), C_pro(i),Coh(i)
        10 format(i3,10x,f10.8,10x,f9.1,5x,f10.4, 5x, f10.4,5x, f10.4, 5x,
        f10.4, 5x,f10.4, 5x, f10.4, 5x, f20.15, 5x,f20.15)
        end do

! Calculate average molecular weight, Av_Mn
        Mn_ent=0.0
        do i=1,k-1
            Mn_ent=Mn_ent+(4/3*4*atan(1.)*(r(i+1)**3-r(i)**3)*((Mn(i+1)+Mn(i))/2))
!total Mn of entire nodes
        end do
        Av_Mn=Mn_ent/(4/3*4*atan(1.)*b**3)
        write(10,33) Av_Mn
33      FORMAT(f10.4,5x)

! Calculate average effective diffusivity, Deff
        D_ent=0.0
        do i=1, k-1
            D_ent=D_ent+(4/3*4*atan(1.)*(r(i+1)**3-r(i)**3)*((Ddrug(i+1)+Ddrug(i))/2))
        end do
        Deff_ave=D_ent/(4/3*4*atan(1.)*b**3)
        write(12,22) Deff_ave ! , AAA1, BBB1
22      FORMAT(f20.15)
        Col_ent=0.0
        do i=1, k-1
            Col_ent=Col_ent+(4/3*4*atan(1.)*(r(i+1)**3-
        r(i)**3)*((Col(i+1)+Col(i))/2))
        end do
        Col_ave=Col_ent/(4/3*4*atan(1.)*b**3)
        Rol_ent=0.0
        do i=1, k-1
            Rol_ent=Rol_ent+(4/3*4*atan(1.)*(r(i+1)**3-
        r(i)**3)*((Rol(i+1)+Rol(i))/2))
        end do
        Rol_ave=Rol_ent/(4/3*4*atan(1.)*b**3)

        write(27,16) 1.0-((Rol_ave-Col_ave)/Ce0)
16      FORMAT(f10.4,5x,f10.4,5x,f10.4,5x) !,f10.4,5x,f10.4,5x,f20.10,5x,f20.10)

        Icount=0
        end if
        t1=t1+del_t1
        end do
        stop
!SUBROUTINES
!*****
Contains

Subroutine
Initial_parameters(k1,k2,Ce0,alpha,beta,Mn0,m,Dpoly,Dpore,b,Col0,Ndp0,delta,Dd
rug0,Ka)
implicit none

```

```

real*16:: Ce0,alpha,beta,Ka,Mn0,m,a,b,Col0,Ndp0,delta
real*16:: Dpoly,Dpore, Ddrug0, k1, k2

k1=0.00005                !1/week
k2=0.1                    !m3/mol.week
alpha=0.4
beta=1.
m=4.
Dpoly=5.D-12
Dpore=1000.D0*Dpoly
Ka=1.35D-4
b=170.D-6                !m; radius of microspheres
Mn0=12577.6D0            !g/mol for microsphere (Siepmann, PDI is assumed as 1)
Munit=65.0D0             !g/mol
Ce0=20615.D0            !mol/m3
Col0=0.0*Ce0
Ndp0=Mn0/Munit
delta=9.7D0              !Cs, the saturation solubility of drug in the matrix,
mol/m3
Ddrug0=6.D-10           !m2/week
End subroutine

Subroutine Initial_parameters_2(Kb_drug,Cdrug_loading,fdrug0,Dpore_drug,k3)
implicit none
real*16:: Kb_drug,k3
real*16:: Cdrug_loading, fdrug0, Dpore_drug

Cdrug_loading=153.0D0
fdrug0=0.024D0
Dpore_drug=1000D0*Ddrug0
Kb_drug=1.D-6
k3=3.0!
End subroutine

!!*****
!!OLIGOMER DIFFUSION- OLIGOMER DIFFUSION- OLIGOMER DIFFUSION
!!These two subroutines considers drug diffusion by Fick's law and matter
conversation

Subroutine oligomer_flux(k,Col,D,r &    ! input
, Jr)                                ! output
  Implicit none
  integer, parameter:: z=1000
  real*16, dimension(z):: r
  real*16, dimension(z):: Jr
  real*16, dimension(z):: Col
  real*16, dimension(z):: D
  integer:: k,i

  Do i=1, k-1
    Jr(i)=-D(i)*((Col(i+1))-(Col(i)))/(r(i+1)-r(i))
  End do

```

```

End subroutine

!*****

Subroutine calculate_dCol_dt(k,r,Jr, &      ! input
                        dCol_dt)          ! output

  Implicit none
  integer, parameter:: z=1000
  real*16, dimension(z):: dCol_dt
  real*16, dimension(z):: Jr
  real*16, dimension(z):: r
  real*16::Vshell, A1,A2
  integer:: k,i

  dCol_dt(1)=-3*(Jr(1))/(r(2)/2.0)
  Do i=2, k-1
    del_r=(r(i+1)-r(i))/2+(r(i)-r(i-1))/2
    A1=4* 4.*atan(1.)*(r(i-1)**2)
    A2=4* 4.*atan(1.)*(r(i)**2)
    Vshell=4/3* 4.*atan(1.)*((r(i)**3)-(r(i-1)**3))
    dCol_dt(i)=(Jr(i-1)*A1-Jr(i)*A2)/Vshell
  End do

End subroutine

Subroutine drug_flux(k,Cdrug,Ddrug,r &      ! input
,                        Jdrug)          ! output
  implicit none
  real*16, dimension(z):: r
  real*16, dimension(z):: Cdrug
  real*16, dimension(z):: Jdrug
  real*16, dimension(z):: Ddrug           !m2/week
  integer:: k, i

  do i=1, k-1
    Jdrug(i)=-Ddrug(i)*((Cdrug(i+1))-(Cdrug(i)))/(r(i+1)-r(i))
  end do
End subroutine

!*****

Subroutine calculate_dCdrug_dt(k,r,Jdrug, &      ! input
                        dCdrug_dt)          ! output

  Implicit none
  integer, parameter:: z=1000
  real*16, dimension(z):: dCdrug_dt
  real*16, dimension(z):: Jdrug
  real*16, dimension(z):: r
  real*16:: Vshell, A1,A2
  integer:: k,i

  dCdrug_dt(1)=-3*(Jdrug(1))/(r(2)/2.0)
  do i=2, k-1

```

```
del_r=(r(i+1)-r(i))/2+(r(i)-r(i-1))/2
A1=4* 4.*atan(1.)*(r(i-1)**2)
A2=4* 4.*atan(1.)*(r(i)**2)
Vshell=4/3* 4.*atan(1.)*((r(i)**3)-(r(i-1)**3))
dCdrug_dt(i)=(Jdrug(i-1)*A1-Jdrug(i)*A2)/Vshell
End do
End subroutine

End program
```

## **Appendix C**

### **FORTRAN codes for the mechanistic model for acidic drug release using microspheres made of PLGA**

In this appendix we present the FORTRAN codes developed for the study in Chapter 5.

```

! PROGRAM: A combined hydrolytic degradation and erosion model which involves
all the mechanisms including degradation, diffusion, surface erosion,
! interior erosion with constant delay. The codes are taken from the model
given in Chapter 5.
! PURPOSE: This program computes polymer hydrolytic degradation, surface
erosion and interior erosion with respect to time and location
! Author
! Kevser Sevim
! Ph.D Dissertation 2017
! Department of Engineering
! University of Leicester
! DETAILS:
! ** Finite difference method and Monte-Carlo sampling technique used for
numerical solution
! ** Drug dissolution is instantaneous
!*****
module variables
implicit none
integer, parameter:: z=1000
integer, parameter:: ny_range=3, nx_range=3
integer, dimension (1) :: seed = (821838)! Fortran random number generator has
a "seed" value which it uses to start its sequence from
integer,parameter:: nx=250, ny=1000 !number of grids in x and y direction
double precision:: nx_r,ny_r !real number counterparts of nx and ny
double precision :: num1, num2, num3, num4, num5 !random numbers
double precision, dimension(z,z):: rand2 !!Box-Muller transform from uniform
distribution to normal distribution
double precision, dimension(z):: x, y !current width and length
integer:: S_total !total count of eroded pixels
integer:: NEXT_to_hole !decides if whether a pixel is next to hole
double precision, dimension(z,z):: Rol !number of ester chains of oligomers
double precision, dimension(z,z):: C_COOH !concentration of carboxylic acid
end groups
double precision, dimension(z,z):: C_pro !concentration of H+
double precision, dimension(z,z):: Mn !number averaged molecular weight
double precision, dimension(z,z):: Ce !concentration of ester bonds
double precision, dimension(z,z):: dCol_dt !time derivative of oligomer
concentration
double precision, dimension(z,z):: Col !oligomer concentration
double precision, dimension(z,z):: dRol_dt !time derivative of number of ester
chains of oligomers
double precision, dimension(z,z):: Life ! delay time for interior erosion,
weeks
double precision, dimension(z,z):: t_delay !counter for delay time
double precision, dimension(z,z):: Dol_x,Dol_y ! effective diffusivities in x
and y directions
double precision, dimension(z,z):: Mn_crt ! critical molecular weight
double precision, dimension(z,z):: Rs !total number of chain scission
double precision, dimension(z,z):: Vpore !total porosity as a result of
oligomer and drug depletion
double precision, dimension(z,z):: Vpore_drug !porosity as a result of drug
depletion
double precision, dimension(z,z):: Vpore_poly !porosity as a result of
oligomer depletion
double precision, dimension(z,z):: dRs_dt !time derivative of chain scission
double precision, dimension(z,z):: Jol !oligomer flux

```

```
double precision, dimension(z,z):: POROSITY_x,POROSITY_y !porosities in x and
y axis
double precision, dimension(z,z):: Mn0 !initial number average molecular
weight
double precision, dimension(z,z):: Cdrug !drug concentration
double precision, dimension(z,z):: Ddrug !effective drug diffusivity
double precision, dimension(z,z):: Jdrug !drug flux
double precision, dimension(z,z):: dCdrug_dt !time derivative of drug
concentration
double precision :: Ndp0 !initial average degree of polymerisation of polymers
double precision :: Initial_Av_Mn !initial average molecular weight
double precision :: k1 !rate constant for non-catalysed hydrolysis
double precision :: r_nyrange,r_stotal ! 1/week
double precision :: k2 !rate constant for acid catalysed hydrolysis
double precision :: Ka !acid dissociation constant of oligomers
double precision :: Cdrug_ent ! summation of the drug concentration at entire
polymer
double precision :: Cdrug_ave ! average drug concentration within the polymer
double precision :: Av_Mn !average molecular weight
double precision :: mass_loss !mass loss
double precision :: Mn_Y_ent ! entire molecular weight at y direction
double precision :: Av_Mn_Y !average molecular weight at y direction
double precision :: Mn_ent ! summation of the molecular weight at entire
polymer
double precision :: mean !mean value for number average molecular weight
double precision :: stdev !standart deviation of number average molecular
weight
double precision :: Ce0 !initial ester bond concentration
double precision :: Rs_b !number of chain scission divided by total number of
initial ester bonds
double precision :: Col0 !initial number of oligomer concentration
double precision :: Munit ! number average molecular weight of a polymer unit
double precision :: alpha, beta !emprical parameters
double precision :: m ! average polymerization degree of short chains
double precision :: Kb_drug !base dissociation constant of basic drug
double precision :: Release !drug release
double precision :: Col_ent ! summation of the oligomer concentration at
entire polymer
double precision :: Col_ave ! average oligomer concentration withing the
polymer
double precision :: Rol_ent ! summation of the oligomer production rate at
entire polymer
double precision :: Rol_ave ! average oligomer production within polymer
double precision :: del_t1 ! time step, week
double precision :: t1 !time
double precision:: Dpoly !diffusion coefficient of oligomers in fresh bulk
polymer
double precision:: Dpore !diffusion coefficient of oligomers in liquid filled
pores
double precision:: Ddrug0 !diffusion coefficient of drug in fresh bulk polymer
double precision:: Cdrug0 !initial mole concentration of drug
double precision:: fdrug0 !the volume ratio of drug to the polymer phase
double precision:: Dpore_drug !diffusion coefficient of drug in liquid filled
pores
double precision:: Cdrug_loading !initial drug loading
double precision :: del_x, del_y ! mesh size
```

```

double precision :: a,b ! width and leght of the plate
double precision ::r_nxrange ! reel value of nxrange
integer,dimension(z,z):: S,S_m,S_k ! states of pixels
integer:: count, count2 ! counters
integer::nt !total number of time steps
integer:: it,Icount !counters
integer::Noutput_time !total number of output
integer:: i,j,k !counters
end module variables

PROGRAM Loaded
USE variables
IMPLICIT NONE
OPEN (6, file="fitsiepmann51.txt")
OPEN (8, file="Release.txt")
OPEN (10,file="Average_Mn.txt")
OPEN (11,file="Svalues_25x25.txt")
OPEN (12,file="Initial_Mn.txt")
OPEN (13,file="S_total.txt")
OPEN (17,file="Mass_losss.txt")
OPEN (18,file="Porosity.txt")
OPEN (19,file="S_totall.txt")
OPEN (20,file="Count.txt")
OPEN (21,file="Time.txt")
OPEN (23,file="Initial_ave_mn.txt")
OPEN (24,file="Diffusivity.txt")
OPEN (25,file="Col.txt")
OPEN (26,file="MN_Y_average.txt")
OPEN (27,file="Col_initial.txt")
OPEN (28,file="dCol_dt.txt")
OPEN (29,file="Mn.dist.txt")
OPEN (30,file="num2.txt")
OPEN (40,file="t1.txt")
OPEN (41,file="t2.txt")
OPEN (42,file="t3.txt")
OPEN (44,file="t5.txt")

nt=35D+6 !total number of time step
a=80.0D-6 ! width of the sample, m
b=320.0D-6 ! lenght of the sample, m
nx_r=nx
ny_r=ny
mean=75000.
stdev=20000.

CALL Initial_parameters(k1,k2,Ce0,alpha,beta,m,Dpoly,Dpore,a,b,Ddrug0,Ka)
del_t1=9.D-7 !time step
del_x=(a)/(nx_r -1.0)
del_y=(b)/(ny_r-1.0)

! Spatial discretization of the plate
x(1)=0.0
y(1)=0.0
DO i=2, nx
DO j=2,ny
x(i)=(i-1)*del_x

```

```

        y(j)=(j-1)*del_y
    END DO
END DO

CALL RANDOM_SEED (PUT=seed)
! Initial conditions of polymer matrix prior to degradation
DO i=1,nx
    DO j=1,ny
        Rs(i,j)=0.0
        dRs_dt=0.0
        dCol_dt=0.0
        Ce(i,j)=Ce0
        Rol(i,j)=0.0
        dRol_dt(i,j)=0.0
        C_COOH(i,j)=0.0
        Jol(i,j)=0.0
        Dol_x(i,j)=Dpoly
        Dol_y(i,j)=Dpoly
        C_pro(i,j)=0.0
        Jol(i,j)=0.0
        CALL RANDOM_NUMBER(num1)
        CALL RANDOM_NUMBER(num2)
        CALL RANDOM_NUMBER(num3)
        CALL RANDOM_NUMBER(num4)
        Col(i,j)=0.0
        rand2=sqrt(-2*log(num3))*sin(2*3.14*num4)    !Box-Muller transform
from uniform distribution to normal distribution
        Mn0(i,j)=mean+stdev*rand2
        Mn_crt(i,j)=27000.
        Life(i,j)=0.5
        t_delay(i,j)=0.0
        POROSITY_x(i,j)=0.0
        POROSITY_y(i,j)=0.0
        Write(12,*) Mn_crt(i,j)
        Write(27,*) Col(i,j)
    END DO
END DO

! Assign the initial conditions of the pixels: surface pixels eroded at t=0
! All interior pixels are non-eroded at t=0
DO i=1,nx
    DO j=1,ny
        IF (i.EQ.nx .OR. i.EQ.nx-1) then
            S(i,j)=0
            S_m(i,j)=0
        ELSE IF (j.EQ.ny .OR. j.EQ.ny-1) then
            S(i,j)=0
            S_m(i,j)=0
        ELSE
            S(i,j)=1
            S_m(i,j)=1
        END IF
    END DO
END DO

```

```

!*****
Ndp0=Initial_Av_Mn/72.
Noutput_time=60
Icount=0

t1=0.0
DO it=1, nt

!*****
CALL calculate_dCol_dt(z,nx,ny,del_x,del_y,Jol,Dol_x,Dol_y,      & ! input
&                      dCol_dt)                                & ! output

      DO i=1, nx-1
        DO j=1,ny-1
          Col(i,j)=Col(i,j)+dCol_dt(i,j)*del_t1+dRol_dt(i,j)*del_t1
        END DO
      END DO
Col(nx,:)=0.0
Col(:,ny)=0.0

!*****
      DO i=1,nx
        DO j=1,ny
          C_COOH(i,j)=Col(i,j)/m
          C_pro(i,j)=(C_COOH(i,j)*Ka)**0.5
          dRs_dt(i,j)=k1*Ce(i,j)+k2*Ce(i,j)*C_pro(i,j)
          Rs(i,j)=Rs(i,j)+dRs_dt(i,j)*del_t1
          dRol_dt(i,j)=alpha*beta*(Rs(i,j)/Ce0)**(beta-
1.)*dRs_dt(i,j)
          Rol(i,j)=Rol(i,j)+dRol_dt(i,j)*del_t1
          Ce(i,j)=Ce0-Rol(i,j)
        END DO
      END DO
!*****
!Calculate Molecular weight, Mn
      DO i=1,nx
        DO j=1,ny
          Rs_b=Rs(i,j)/Ce0
          Mn(i,j)=Mn0(i,j)*(1.0-alpha*(Rs_b)**beta)/(1.0+Ndp0*(Rs_b-
alpha*Rs_b**beta/m))
        END DO
      END DO

!Interior erosion with constant delay
      DO i=1,nx
        DO j=1,ny
          IF (Mn(i,j).LT.Mn_crt(i,j)) THEN
            S_m(i,j)=0
          ENDIF
        END DO
      END DO

      DO i=2,nx-2
        DO j=2,ny-2
          IF(S_m(i,j).EQ.0) Then
            NEXT_to_hole = S(i+1,j)*S(i-1,j)*S(i,j+1)*S(i,j-1)

```

```

        IF(NEXT_to_hole.EQ.0) THEN
            t_delay(i,j)=t_delay(i,j)+del_t1
        ENDIF
    ENDIF
END DO
END DO

DO i=2,nx-2
    DO j=2,ny-2
        IF(S_m(i,j).EQ.0) Then
            IF(t_delay(i,j).GT.Life(i,j)) THEN
                S(i,j)=0
            ENDIF
        ENDIF
    END DO
END DO

!*****
!Count the number of eroded pixels
nx_r=nx
ny_r=ny
Count=0.0
DO i=1,nx-2
    DO j=1,ny-2
        If(S(i,j).EQ.0) THEN
            Count=Count+1.0
        End If
    END DO
END DO

!Calculate the local porosity
CALL porosity_diffusivity_x(ny,ny_range,S,Dpore,Dpoly, & !input
                             Dol_x,POROSITY_x)
!output

CALL porosity_diffusivity_y(nx,nx_range,S,Dpore,Dpoly, & !input
                             Dol_y,POROSITY_y)
!output

!*****
Icount=Icount+1
IF(Icount>(nt/Noutput_time)) then
!*****
Mn_ent=0.0
DO i=1,nx
    DO j=1,ny
        Mn_ent=Mn_ent+Mn(i,j)
    END DO
END DO

Av_Mn=Mn_ent/(nx*ny)
write(10,33) Av_Mn
33 FORMAT(f12.4,5x)

! Calculate the average molecular weight
DO i=1,nx

```

```

        Mn_Y_ent=0.0
        DO j=1,ny
            Mn_Y_ent=Mn_Y_ent+Mn(i,j)
        END DO
        Av_Mn_Y=Mn_Y_ent/ny
        Write(26,*) Av_Mn_Y
    END DO

! Calcolare mass losses
    Col_ent=0.0
    DO i=1,nx
        DO j=1,ny
            Col_ent=Col_ent+Col(i,j)
        END DO
    END DO
    Col_ave=Col_ent/(nx*ny)
    Rol_ent=0.0
    DO i=1,nx
        DO j=1,ny
            Rol_ent=Rol_ent+Rol(i,j)
        END DO
    END DO
    Rol_ave=Rol_ent/(nx*ny)

    Mass_loss=((Count/(nx_r*ny_r))*100.
    write(17,71) mass_loss
71    FORMAT(f10.4,5x,f10.3,5x)
    Write(20,*) Count

!*****
    Icount=0
    END IF
t1=t1+del_t1
!*****
!Write to file at specified times

    If (it==1200000) then
        Do i=1,nx
            Do j=1,ny
                Write(40,*) i,j,S(i,j),Mn(i,j)
            End do
        End do
    End if
    If (it==12800000) then
        Do i=1,nx
            Do j=1,ny
                Write(41,*) i,j,S(i,j),Mn(i,j)
            End do
        End do
    End if
    If (it==15000000) then
        Do i=1,nx
            Do j=1,ny
                Write(42,*) i,j,S(i,j),Mn(i,j)
            End do
        End do
    End if

```

```

        End do
    End if
    If (it==22000000) then
        Do i=1,nx
            Do j=1,ny
                Write(43,*) i,j,S(i,j),Mn(i,j)
            End do
        End do
    End if
    If (it==35000000) then
        Do i=1,nx
            Do j=1,ny
                Write(44,*) i,j,S(i,j),S_m(i,j),Mn(i,j)
            End do
        End do
    End if
!*****

End Do
Stop

Contains
Subroutine
Initial_parameters(k1,k2,Ce0,alpha,beta,m,Dpoly,Dpore,a,b,Ddrug0,Ka)
implicit none
double precision:: Ce0,alpha,beta,m,a,b
double precision:: Dpoly,Dpore, Ddrug0, k1, k2, Ka

k1=0.5D-5           !1/week
k2=0.02            !m3/mol.week
Ka=1.35D-4
alpha=0.4
beta=1.
m=4.
Dpoly=5.0D-15      !m2/week;
Dpore=1.0D-8       !100.D-9
Ddrug0=0.0         !m2/week
a=80.0D-6          !m
b=320.0D-6         !m;
Munit=65.0D0       !g/mol
Ce0=20615.D0       !mol/m3
End subroutine

!*****
Subroutine calculate_dCol_dt(z,nx,ny,del_x,del_y,Joll,Doll_x,Doll_y,      &
! input
&                               dColl_dt)                               ! output

Implicit none
integer:: z
integer:: i,j,nx,ny
double precision, dimension(z,z):: dColl_dt,Joll,Doll_x,Doll_y
double precision::del_x,del_y

do i=2, nx-1
do j=2, ny-1

```

```

                dColl_dt(i,j)=((Doll_x(i,j)/(del_x**2))*(Col(i+1,j)-
2*Col(i,j)+Col(i-1,j)))+&
                ((Doll_y(i,j)/(del_y**2))*(Col(i,j+1)-2*Col(i,j)+Col(i,j-1)))
        end do
    end do

End subroutine

!*****
!This subroutine calculates local porosities and diffusivities in x direction
Subroutine porosity_diffusivity_x(ny,ny_range,S,Dpore,Dpoly, &
!input
                Doll_x,POROSITYY_x)

!output
integer:: ny,S_total,i,j,k
integer:: ny_range
integer,dimension(z,z):: S
double precision, dimension(z,z)::POROSITYY_x
double precision::r_nyrange,r_stotal,Dpore,Dpoly
double precision, dimension(z,z) :: Doll_x

    DO i=1,nx
        DO j=ny_range+1,ny-ny_range
            S_total=0.0
            DO k=j-ny_range,j+ny_range
                IF (S(i,k).EQ.0) THEN
                    S_total=S_total+1.0
                ENDIF
            END DO
            r_nyrange= ny_range
            r_stotal= S_total
            POROSITYY_x(i,j)=((1.0/(2.0*r_nyrange+1.0))*r_stotal)
        END DO

        DO j=1,ny_range
            POROSITYY_x(i,j)=POROSITYY_x(i,ny_range+1)
        END DO

        DO j=ny-ny_range+1,ny
            POROSITYY_x(i,j)=POROSITYY_x(i,ny-ny_range)
        END DO
    END DO

    DO i=1,nx
        DO j=1,ny
            Doll_x(i,j)=Dpoly+(1.3*POROSITYY_x(i,j)**2-
0.3*POROSITYY_x(i,j)**3)*(Dpore-Dpoly)
        END DO
    END DO
End subroutine

!*****
!This subroutine calculates local porosities and diffusivities in y direction
Subroutine porosity_diffusivity_y(nx,nx_range,S, Dpore,Dpoly, &
!input

```

```

                                Doll_y,POROSITYY_y)
!output
integer::nx,S_total,i,j,k
integer:: nx_range
integer,dimension(z,z):: S
double precision, dimension(z,z)::POROSITYY_y
double precision:: r_stotal,Dpore,Dpoly
double precision, dimension(z,z):: Doll_y

    DO j=1,ny
        DO i=nx_range+1,nx-nx_range
            S_total=0.0
            DO k=i-nx_range,i+nx_range
                IF (S(k,j).EQ.0) THEN
                    S_total=S_total+1.0
                ENDIF
            END DO
            r_nxrange= nx_range
            r_stotal= S_total
            POROSITYY_y(i,j)=((1.0/(2.0*r_nxrange+1.0))*r_stotal)
        END DO

        DO i=1,nx_range
            POROSITYY_y(i,j)=POROSITYY_y(nx_range+1,j)
        END DO

        DO i=nx-nx_range+1,nx
            POROSITYY_y(i,j)=POROSITYY_y(nx-nx_range,j)
        END DO
    END DO

    DO i=1,nx
        DO j=1,ny
            Doll_y(i,j)=Dpoly+(1.3*POROSITYY_y(i,j)**2-
0.3*POROSITYY_y(i,j)**3)*(Dpore-Dpoly)
        END DO
    END DO
End subroutine

END PROGRAM

```